Final Report

Project Title:	Sensing and arresting metal corrosion in molten chloride salts at 800 degrees Celsius
Project Period:	04/01/2019 – 01/05/21
Project Budget:	$440,072.00
Submission Date:	04/03/21
Recipient:	Arizona Board of Regents/University of Arizona
Address:	1133 E. James Rogers Way**,** Tucson, Arizona 85721
Award Number:	DE- EE0008539
Principal Investigator:	Dominic Gervasio, Associate Professor Phone: 267- 230-5563 Email: gervasio@email.arizona.edu
Business Contact:	Jennifer Dukes for Paul Sandoval Title: Manager, Post award Team 4, Sponsored Projects & Contracting Services | University of Arizona Email address: porterj@email.arizona.edu Phone number: 520-626-6110; 520-626-6000
Technology Manager:	Levi Irwin
Project Officer:	Carter, Christine
Grant Specialist:	Parrish, Elizabeth Phone: 720-356-1431 E-Mail: Elizabeth.Parrish@EE.DOE.Gov
Contracting Officer:	Brodie, Pamela Phone: 720-356-1449 E-Mail: pamela.brodie@ee.doe.gov

Executive Summary:

Originally this was planned as a 5 task, 3 year project, starting in May 2019,
Task 1 Detecting oxidants and metal corrosion in molten chloride salt at 800˚C
Task 2 Effectiveness of Zr getter using head gas sensors of inlet and outlet gases
Task 3 Cathodic protection of metal in molten salt at reducing potential
Task 4 Find reduction potential of metals in molten chloride salts & quantum modeling
Task 5 Develop corrosion test sections integrated into molten salt flow loop
After Q4, the project was scaled back and the reorganized SOPO was reduced to 3 tasks to be completed at the end of Q7 on 01/05/2021. The 3 SOPO tasks are:
Task 1 Sense oxidants and the metal corrosion in molten Na-K-Mg-Cl salt at 800°C
Task 3 Cathodically protect H230 alloy in molten Na-K-Mg-Cl salt at 800C by making H230 alloy the cathode of a power supply with a chromium-rich-metal as the anode
Task 4 Find the reduction potential of Cr metal in molten Na-K-Mg-Cl salt at 800°C.
The total timeline was reduced from 12 to 7 quarters with the end date being, January 5, 2021. This amounted to task 1,3 and 4 being done in Q5,6 and 7 of an extended year 1, ending on January 5, 2021.
Task 1, 3 and 4 were completed. For task1) the increase of oxidants in molten salt is detected by two things: i) a positive shift of the electrode potential for a Haynes 230 alloy (H230) metal coupon versus a silver/silver-chloride reference electrode (SSE) and ii) an increase in the corrosion rate of a H230 electrode at 800C. For task 3) applying a cathodic potential (negative overpotential) to a H230 electrode versus SSE arrested the corrosion of the cathodically protected H230 compared to an unprotected “spectator H230 electrode” in the same molten chloride salt. Lastly, for task 4) the reduction potential of chrome and chrome rich, and nickel metal electrodes were measured.

The most valuable outcome of this work is that a power supply can arrest metal corrosion for metal in molten chloride salt when the power supply applies a cathodic potential to bare metal, like H230, in molten chloride salts, like ternary Mg-K-Na-chloride salt. H230 is a high strength metal for containing molten chloride salt and ternary Mg-K-Na-chloride salt is used as heat transfer fluids in concentrating solar power plants. When to use cathodic protection for protecting metal in molten chloride salts? Two scenarios are envisioned: 1) for protecting high-valued components, like solar collectors and heat exchangers and 2) for protecting the bare surface in holidays (point defects) of corrosion inhibitors that are to intended to cover the entire surface of metal.

The results of this project provides power utilities with tools for bringing a clean, reliable and economic solar thermal electrical converter technology, as an clean and sustainable alternative electrical power supply to the for the American public.

Table of Contents Page

Acknowledgement: "This material is based upon work supported by the Department of Energy, Office of Energy Efficiency and Renewable Energy, Solar Energy Technologies Office, under Award Number DE-EE0008539.

Background:

The work in this project is similar to corrosion protection in the gas and oil pipelines, but there are some differences. Instead of protecting the exterior of pipes from ambient water and oxygen with trace chloride, in CSP systems the interior of the metal pipe is being protected from corrosion where chloride is abundant and water and oxygen are trace contaminants. Accordingly, new strategies and methods for protecting metal from corrosion for inside CSP systems where there is much higher and more uniform ionic-electrical conductivity of molten salts and where no “passive” layers spontaneously form on the metal surface. The cathodic protection of the metal uses a cathodic potential imposed by a power supply. Evidence is given to show CP is a practical, effective and economic way to arrest corrosion of bare metal surfaces by trace oxidants in molten chloride salt at high temperatures. The choice of the anode (counter electrode) is an important feature for maintaining the metallic static of structural metal that under cathodic protection. A sacrificial anode (like magnesium or chromium) shorted to the cathode (e.g. H230 structural metal alloy) maintains the metallic state of the metal, because the potential of this metal cathode is the reduction potential of the sacrificial anode. Effective reducing electrons are given by proper choice of sacrificial anode metal which emits metal-ion residue into the molten salt when the anode metal oxidizes during cathodic protection. Shorting a sacrificial anode directly to metal protects the metal two ways: 1) by removing oxidants and 2) by holding the metal in the metallic state. However, this approach gives no signal that corrosive oxidants (water, oxygen) are in the molten salt and the sacrificial anode is being consumed to protect the structural metal. So there is no way to know if oxidants are invading the system and corrective action is needed, like sealing a leak and replacing the sacrificial anode. Cathodic protection *with a power supply* gives 2 signals showing that oxidant is invading the molten salt 1) the positive shift of structural metal potential metal versus a reference electrode (e.g., silver/silver-chloride electrode, SSE) in the presence of oxidant and 2) a reduction current of the oxidant by the metal biased at a cathodic potential. In addition, cathodic protection of metal with a power supply allows the reducing potential of the metal to be electrically set different than the reduction potential of the sacrificial anode. The cathodic potential is not set just by the choice of the anode. Different anodes can be set to the same reducing potential, by adding electric power. So the anode ionic residue is can be set by choice of any convenient anode material. The anode should be chosen to oxidize to anode metal-ions and not polarize. If the anode polarizes too much then chloride in the molten salt oxidizes to chlorine, an aggressive oxidant.

This report is about arresting the corrosion of metal surfaces of test coupons immersed in molten chloride salt to model the INSIDE surface of a metal container filled with molten salt with and without added oxidants. The original intention was to demonstrate this arresting of corrosion on an actual pipeline (University of Arizona test loop), but this project ended prematurely so this pipeline protection was not done.

To date there has been one degree granted, a Master of Science of Chemical Engineering and another, a Ph. D. of Chemical Engineering is expected in the summer after this report. Two manuscript are in preparation to peer-reviewed journals. Two patents are being sought from the work undertaken in the project i) on simplified reference electrodes and ii) applying the cathodic protection to metal in molten salts.

Project Objectives:

The overall objective is to detect and arrest the corrosion of structural metal used to contain molten chloride salt by making the metal the cathode of a power supply. This is being done to preserve heat transfer and heat storage units using molten chloride salts as heat transfer fluids in concentrating solar power (CSP) systems.

Cathodic protection (CP) of metal housings of molten salt (such as, pipes, heat exchangers, solar collectors and storage containers) has been developed to preserve power and energy sources using molten salt heat transfer (such as concentrating solar power (CSP) and nuclear power (NP) sources). CSP systems for providing electrical power and energy storage that are longer-lived, economical, clean and sustainable to ensure National energy security, independence and leadership in the U. S. A.

Cathodic protection has long been used in the gas and oil pipeline industries to protect the outside of pipes from uneven ambient environmental conditions where the outside of pipe is in soil exposed to air. Wet aerated soil is conductive and corrosive and dry soil is relatively insulating and benign to the pipe metal.

On the outside of pipelines, where water and oxygen are abundant and chloride is typically a trace material, chrome containing alloys form insulating chrome oxide on the surface, arresting corrosion. The situation is inverted for CSP systems using molten chloride salt heat transfer fluids inside the pipe. The metal surface inside the pipe is stable and does not corrode in the presence of molten chloride salt, but contaminant water and oxygen from air will corrode the metal surface and surface oxide will exchange with chloride to sustain more corrosion as long as water and oxygen are in the molten salt.

During this project, CP has been designed to protect the inside surface of metal containers of molten chloride salt with oxidants from air leaks. The design of the CP is based on the higher and more uniform ionic-electrical conductivity of molten salts and the absence of “passive” layers spontaneously on the inside metal surface. Here cathodic protection (CP) has a cathodic potential (E^C) imposed by a power supply on the inside surface of the metal housing molten chloride salt. During this project the sensing and arresting of corrosion has been demonstrated for bare metal coupon surfaces immersed in molten chloride salt at high temperatures (800^{o}C), This is done to model the interior surface of pipe holding molten chloride salt. Mostly the sensing and arresting corrosion of metal surfaces has been demonstrated for H230 test coupons immersed in ternary Mg-K-Na-chloride salt with and without added water as oxidant. Applying cathodic potential (E^C) for the CP of metal in molten chloride salt is envisioned mainly for two scenarios: 1) for protecting high-valued components, like solar collectors and heat exchangers and 2) for protecting point defects on the surface of metal otherwise covered with corrosion inhibitors.

The original intention was to demonstrate CP on an actual pipeline, University of Arizona test loop, but it was decided to cease this pipeline effort and limit efforts to studying metal coupons in molten salt. Nonetheless, the results from this project show how to make a CSP system using metal to contain molten chloride salt that is reliable longer-lived and more economical in order to provide power utilities with tools for bringing clean, reliable and economical solar thermal electrical converter technology to the electrical power grid.

Originally this was planned as a 5 task, 3 year project, starting in May 2019,

Task 1 Detecting oxidants and metal corrosion in molten chloride salt at 800˚C
Task 2 Effectiveness of Zr getter using head gas sensors of inlet and outlet gases
Task 3 Cathodic protection of metal in molten salt at reducing potential
Task 4 Find reduction potential of metals in molten chloride salts & quantum modeling
Task 5 Develop corrosion test sections integrated into molten salt flow loop
After Q4, the project was scaled back and the reorganized SOPO was reduced to 3 tasks to end in 3 quarters, that is, after Q7. The 3 tasks are:
Task 1.0.: Sense oxidant and metal corrosion in molten Na-K-Mg-Cl salt at 800°C
Task 3.0. Cathodically protect H230 alloy in molten Na-K-Mg-Cl salt at 800C by making the H230 the cathode of a power supply using a chromium-rich-metal as the anode
Task 4.0 Find the reduction potential of Cr metal in molten Na-K-Mg-Cl salt at 800°C.
The total timeline was starting in April 2019, but reduced from 12 to 7 quarters with the end-date being, January 5, 2021.

Project Results and Discussion

Major Goals & Objectives[1]: Two goals are to 1) detect and 2) arrest corrosion of metal surfaces inside vessels containing molten chloride salt.
Metal alloy is stable in contact with molten $MgCl_2$-2KCl chloride salt at 800ºC free of oxidants (like water, O_2, CO_2 and metal-ions more noble than structural metal for containing the molten chloride salt). Left unchecked, oxidants (e. g., from air) leaking into molten salt inside metal vessels induce corrosion of the inside metal surface. Applying a cathodic potential to the inside metal surface using a power supply does 2 things: 1) detects oxidants in molten salt using electrical current signals and 2) arrests metal corrosion using electrical power. This detection warns of a leak and arresting corrosion buys more time to do maintenance to plug the air leak in the system before damage leads to catastrophic failure of the CSP hardware. The original SOPO called for 5 tasks, which were addressed for 4 quarters. The results are reported for this work on the original 5 tasks starting in May 2019 are:
Task 1 Detecting oxidants and metal corrosion in molten chloride salt at 800˚C
Task 2 Effectiveness of Zr getter using head gas sensors of inlet and outlet gases
Task 3 Cathodic protection of metal in molten salt at reducing potential
Task 4 Find reduction potential of metals in molten chloride salts & quantum modeling
Task 5 Develop corrosion test sections integrated into molten salt flow loop
The work for Task 1, 2, 3 is the set up of equipment for: measuring current to sense corrosion, getters (Zr, Cr, Al, etc.) to act as an anode for a H230 cathode (which is a typical CSP structural metal) and a power supply to electrically arrest corrosion. A getter metal has 2 functions: 1) to chemical react with oxidants to directly remove oxidants 2) act as the anode for the power supply. Tasks 1, 2, 3, 4 have been done in model salt NaCl-KCl to compare to sodium supplemented carnallite salt (MgCl2-NaCl-KCl). Tasks 2, 3 test cathodic protection done for H230 in molten chloride salts. Task 4 gives a measure of reduction potentials of pure metal in model salt NaCl-KCl and synthetic carnallite (MgCl2-NaCl-KCl). Quantum Mechanical modeling helps explain ordering of reduction potentials; Ultra dry gases (CO2, Argon, air) are prepared using water–removing filters to lower concentration of trace water in Argon used to sparge molten

salts for baseline electrochemical response; then. molten salt is back fill with controlled amounts of water for studies of metal corrosion in wet molten salt. While working on Task 1-4, in parallel, the molten salt flow loop was refurbished and set up in the lab of Prof. Peiwen Li of the Mechanical Engineering (ASME) department at the University of Arizona; Task 5 is to incorporate the sensing and cathodic protection technology of Task 1 and 3 respectively, as supported by results learning doingTasks 2 and 4.
At Q4 the work was restructured to a 3 task SOPO which was Task 1,3 and 4 of the original SOPO. The 3 tasks defined in the reorganized SOPO are:
Task 1 Sense oxidant and metal corrosion in molten Na-K-Mg-Cl salt at 800°C
Task 3 Cathodically protect H230 alloy in molten Na-K-Mg-Cl salt at 800C by making the H230 the cathode of a power supply using a chromium-rich-metal as the anode
Task 4 Find the reduction potential of Cr rich metal in molten Na-K-Mg-Cl salt at 800°C.
Task 1, 3 and 4 were completed by the end date being, January 5, 2021.
Non-volatile MgClOH oxidant has been found to form and remain in wet Mg-Na-K-Cl salt when removing most molecular water from salt during its sparging with inert gas, like Argon at high temperatures (200 to 800^{o}C). This MgClOH causes high corrosion rates of the metal surface in molten chloride salt. After Q4, three steps were used to remove oxidants from Na-K-Mg-Cl eutectic molten chloride salt.

1. Chloride salt is dried at 150°C with a stream of Dry Argon (ultra-pure Argon passed through Drierite and an organometallic filter) for 2 hours. The filters drop the moisture in tank Argon from 3500PPB as supplied to < 10PPB.
2. The Dry Argon is sparged for 5 hours into the molten salt in a sealed quartz at 800°C cell to remove the dipole-bound water. DryArgon enters; moist Argon leaves.
3. Pure Magnesium foil or rod is inserted at 600C for an hour to remove non-volatile oxidant, MgClOH.

Mg foil is put in the salt for 1 hour at 600C (below Mg melting point) with dry Argon sparging into the salt to stir so MgClOH is exposed to and removed by the pure Mg metal. After 1 hour, the Mg foil is removed. These 3 salt treatment steps are to make the salt as dry and oxidant free as possible.

Project tasks and go/no-go milestones/deliverables and metrics

At Q4 U of Arizona did not meet its cost share so the DOE management decided to wind down this project at the end of Q7. All 3 remaining SOPO tasks were met by January 5, 2021. For **Task 1** oxidant water was sensed as a potential, current and corrosion rate as a function of water in the salt. Increasing water gave a more positive potential, a higher reduction current and higher corrosion rate in molten Na-K-Mg-Cl salt at 800°C **For Task 3, corrosion of** H230 alloy in molten Na-K-Mg-Cl salt at 800C was arrested by imposing a cathodic potential on an H230 cathode of a power supply using a chromium-rich-metal as the anode to show over an order of magnitude lower corrosion rate than a piece of H230 in the same cell but not connected to a power supply so that it under its free corrosion potential instead of a cathodic potential.
For Task 4 the reduction potential of Cr rich metal was measured in molten Na-K-Mg-Cl salt at 800°C. Details of the accomplished works follow and are given by SOPO task.

Task 1 Detecting oxidants and metal corrosion in molten chloride salt at 800˚C

Problem Statement 1 – Sense corrosive environments and metal corrosion at 800ºC

Haynes 230 alloy is a high strength metal at high temperatures used in CSP systems, so a Haynes 230 metal coupon is the working electrode (WE). A 3-electrode electrochemical cell made of: an airtight quartz body allows control of atmosphere in molten salt and is used to test the H230 WE with a H230 counter electrode (CE) and silver/silver-chloride (SSE) reference electrode (RE). The WE in the salt models the inside of a metal pipe filled with molten salt. WE signals give the levels of oxidants in molten salt, such as: 1i) the electrode potential of H230 WE in molten chloride salt versus the RE, 1ii) a current for reducing oxidants at a fixed WE potential 1iii) a Raman optical signal. This cell was also used 2) to measure the low corrosion rate (CR) of metal in molten salt without oxidants (Argon sparged) and high corrosion rate with oxidants (air sparged) in the molten salt.

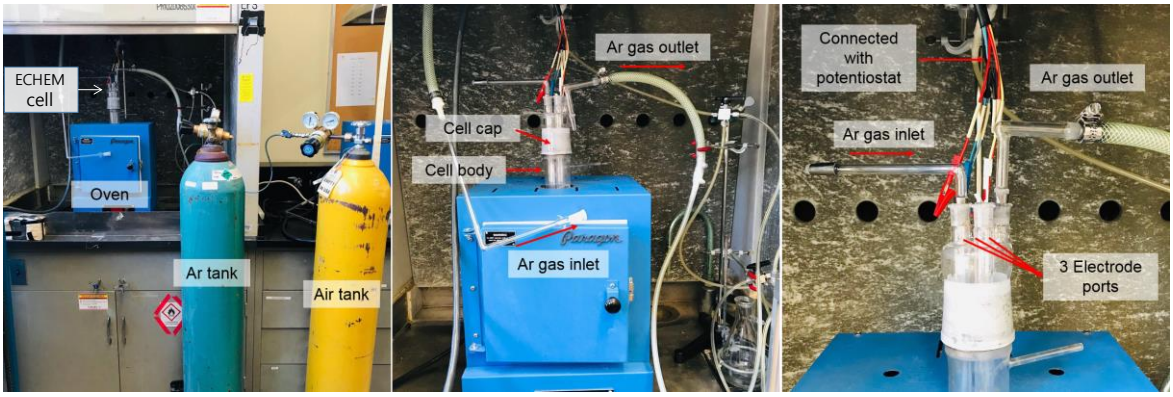

Electrochemical setup to measure metal corrosion in molten salt with controlled atmosphere and high temperature.

Quartz cell with molten salt under controlled atmosphere . Cell temperature can range from room temperature to 900˚C.

The 3 ports for 3 electrodes: WE; CE; RE sealed gas-tight into cell using ground glass joints.

Figure 1-1. Apparatus for electrochemical test under controlled atmosphere.

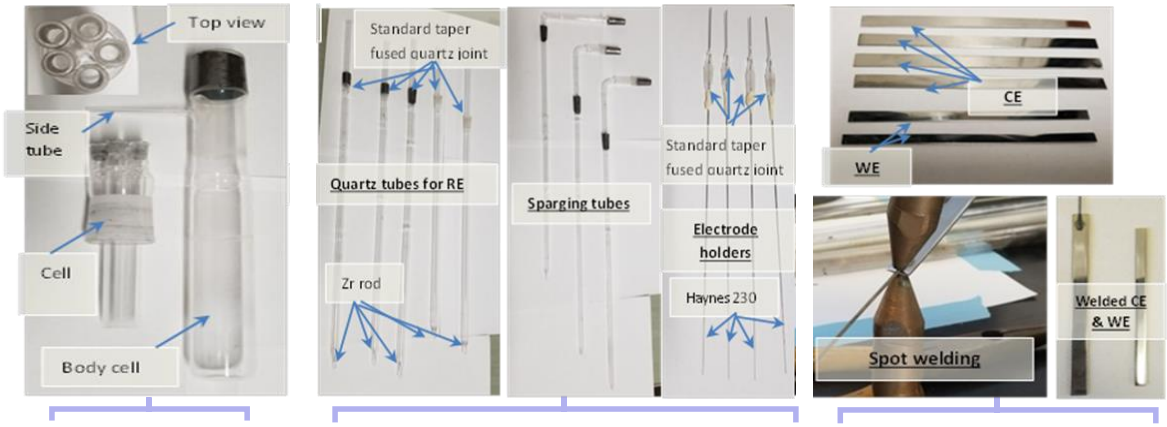

Quartz cell for measuring corrosion rate of metal in molten salt up to 900˚C Cell cap has 3 ports for 3 electrodes 2 ports for gas in and out.

Ancillaries for plumbing for gas-tight controlling either Argon, Air or CO_2. atmosphere

Electrode prepared by welding a rod to plate. Only bottom of plate is immersed in salt.

Figure 1-2. The parts for in-situ electrochemical detection of oxidants in molten salt at temperatures up to 900 ºC.

Task 1: Detecting oxidants and metal corrosion in molten chloride salt at 800˚C
Task 1.1 Sensing nominally anerobic (non-corrosive) and aerobic (corrosive) molten salt.
Detection of oxidants in corrosive molten salt is explored three ways, by:

i. measuring WE potential versus SSE in molten salt to find at which corrective action is needed.
ii. measuring the mass-transport-limited current for reduction of oxidant at high overpotential.
iii. fiber optic Raman absorption.

Experimental Methods

Signal i.i. Detection of oxidants in molten salt, OCV of WE in Argon versus air atmosphere
A H230 metal electrode (WE) placed in a cell sparged with argon gas gives an open circuit voltage, OCV, the potential difference between the WE and RE (Ag/AgCl), which is recorded in time shown in Fig. 1-3.

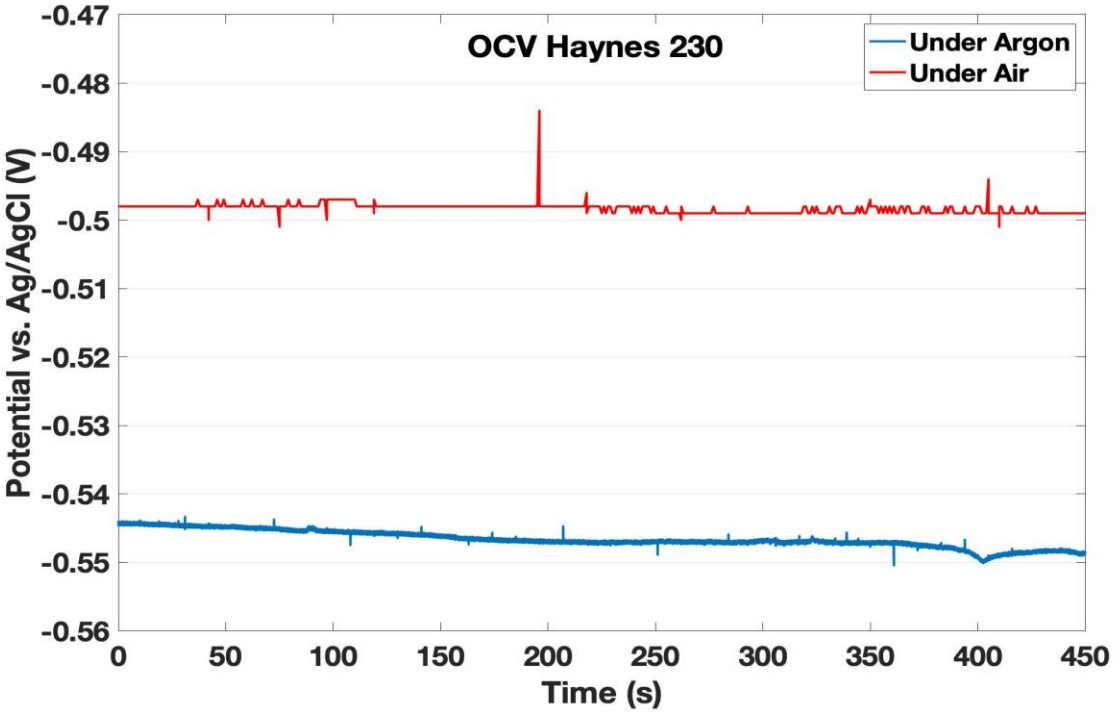

Figure 1-3. Open circuit voltage, $E_{OCV,}$ of H230 vs SSE in molten NaCl-KCl under argon (blue line) and in air (red line) at 800°C.

The molten NaCl-KCl salt was dried by bubbling with argon at 800°C then the electrodes immersed. The open circuit voltage under Argon reached steady state at -0.545V vs SSE (blue line in **Fig. 1-3)**. Then the WE was removed and the salt was equilibrated with air by bubbling air into the salt at 240 sccm at 800°C. The electrode is removed when exchanging stmosphere over salt in order to prevent salt splashing on the top of the working electrode (WE) during the bubbling, which would change the active WE area. The measured steady state OCV in air is ~ -440mV vs SSE *The more positive OCV for the metal in air indicates higher levels of oxidants in molten salt equilibrated with air (water and oxygen) compared to equilibrated with Argon (trace water).*

Removing oxidants from molten salt

The structural metal under test is Haynes230 alloy unless stated otherwise. The positive shift of H230 potential versus a SSE reference electrode in molten chloride salt indicates the level of the oxidant water in salt at 800°C. The H230 anode is also used when measure the current for reduction of oxidant in the molten salt. Various treatments have been developed to dry NaCl-KCl, $MgCl_2$-KCl and Na-K-Mg-Cl molten

chloride salt mixtures, and electrochemical experiments and to sense oxidants that corrode H230 metal in molten chloride salts. Non-volatile MgClOH oxidant forms and remains in Mg-Na-K-Cl salt when removing the water by heating and sparging the aerated salt with inert gas, like Argon. The proton on the MgClOH is an oxidant that causes high corrosion rates of the structural metal surface in contact with the molten chloride salt. Three steps are done to remove all oxidants from Na-K-Mg-Cl eutectic molten chloride salt.

1. Chloride salt is dried at 150°C with a stream of Dry Argon (ultra-pure Argon passed through Drierite and an organometallic filter) for 2 hours. The filters drop the moisture in tank Argon from 3500PPB to < 10 PPB.
2. Dry Argon is sparged into the molten salt in a sealed quartz at 800°C cell for 5 hours to remove the dipole-bound water. Dry Argon enters; moist Argon leaves the cell.
3. Pure Magnesium metal is inserted in the Mg-Na-K-Cl salt at 600C for an hour or more to remove non-volatile oxidant, MgClOH.

Mg foil is put in the salt for 1 hour at 600C (below Mg metal melting point) while dry Argon is sparging into the salt to stir so MgClOH is exposed to Mg surface to remove the proton on MgClOH leaving MgO $MgCl_2$ and H_2.which is carried out of the cell in the Argon stream After 1 hour, the Mg foil is removed. These 3 salt treatment steps make the salt as dry and oxidant free as possible.

Sensing Corrosion

The corrosion potential, E_{corr} , of Haynes 230 alloy is found in molten salt as follows. A Haynes-230-alloy-coupon surface is prepared by wet grinding with 1200 grit SiC paper using water as cutting fluid, cleaned with 2M aqueous HCl, dried and weighed. The open circuit voltage (OCV) between H230 (high) and SSE (low) is measured in molten salt to give the open circuit potential (OCP) of H230 versus the SSE, which is a crude measure of the corrosion potential, E_{corr}, of H230 in the molten salt. Cyclic voltammetry (CV) is then performed in a small potential interval ($\pm$ 30 mV) about this OCP in order to find a robust precise measure of the corrosion potential, E_{corr}, via a Stern-Geary plot (that is, E_{corr} is the potential at minimum of log I in a plot of log I versus E). After the corrosion potential, E_{corr}, of H230 vs SSE is measured in oxidant-free molten salt equilibrated with dry salt oxidant-free salt at 800C, then E_{corr} is found for H230 in molten salt equilibrated with Argon gas of various values of relative humidity. Doing this fulfilled task 1, that is, fulfilled finding the corrosion potential of H230 in the molten salt as a function of added water content.

Subtask 1.1.: Plot corrosion potential, E_{corr}, of H230 alloy in anaerobic oxidant-free (non-corrosive) molten salt and in molten salt equilibrated with Argon of various oxidant water concentrations (by sparging Argon carrier gas at various values of RH.

Subtask Summary: Correlate change of oxidant levels in molten Na-K-Mg-Cl eutectic salt to the change of the corrosion potential, E_{corr}, of a H230 electrode versus SSE. Corrosion potential, E_{corr}, of H230 is measured in molten salt equilibrated with Dry Argon atmosphere (i.e., the corrosion potential will first be determined at “0 relative humidity”). Then the OCP is found for metal in the molten salt equilibrated with “wet Argon” of different RHs by mixing known flows of Argon equilibrated with water at 20°C and dry Argon. The mixed gases have a new “wet Argon” are sparged into salt and OCP is found. The OCP measurements are taken in time, and the time invariance in the potential of H230 vs SSE is the indicator of equilibration of salt with atmosphere over gas. Invariance is defined as when the variation in potential is less than a millivolt per hour. The potential is then checked every 15 minutes for 75 minutes. If the potential is

still not varying, then the salt is confirmed to be equilibrated with the wet Argon atmosphere. *The results are expressed as a plot of corrosion potential, E_{corr}, of H230 vs RH (partial pressure) of water vapor in Argon*. The potential shifts positive with increasing partial pressure of water vapor in the Argon. The potential of the H230 vs SSE at each RH has been measured at least 5 times to give statistical error.

Equipment and methods:

Haynes230 alloy 1mm thick sheet and 1mm in diameter rods have been purchased from Haynes International (https://www.haynesintl.com/). The composition of the alloy is the composition in the Haynes brochure (http://haynesintl.com/docs/default-source/pdfs/new-alloy-brochures/high-temperature-alloys/brochures/230-brochure.pdf).
Sheet is water-jet cut. All metal is polished under a stream of water on a Pace Technologies Grinder-Polisher with 320, 600 and 1200 grit silicon carbide (SiC) paper. The sheet coupons are spot-welded to the rod, and the weld is well above the molten salt gas interface in the cell shown in Fig. 1-2. To make a good conductive connection to the control electronics, a nickel wire (1mm in diameter, Alfa Aesar) is spot-welded to the H230 and the potentiostat clip is connected to the nickel wire. The electrode is submerged in HCl and sonicated for 2-3 minutes to ensure any copper residue from spot welding is removed. The electrode is gas tight sealed into a fused quartz joint using Aremco Ceramabond to glue to a ground glass joint which placed in the electrochemical cell. Rod electrodes are used for experiments which involve the measurement of metal potential in molten salt equilibrated with various oxidizing atmospheres. This is done to minimize welds from the electrode entering the salt, as well as to reduce the cost per experiment. A picture of a H230 rod electrode is shown in Figure 1-4.

Figure 1-4. Haynes230 Working Electrode and Counter Electrode type b)

In the previous work we determined there is no difference in results when using plate coupons electrode and rode electrodes, for sensing and detecting corrosion of H230. The Na-K-Mg-Cl salt mixture used is 29.4%NaCl, 25.8%KCl, 44.7%$MgCl_2$. Alfa Aesar anhydrous salt (NaCl, KCl, $MgCl_2$) are weighted individually, mixed using a mortar and pestle for 2 minutes and then inserted and kept in vacuum under Argon atmosphere at 120°C prior to the experiments. 157.86g total salt was used for Experiments 1 and 2, and 236.85g total salt was used for Exp 3 to 12.
The electrochemical cell has 2 parts, 1) a cap and 2) a bottom. These are custom made of fused quartz by Technical Glass Products (Cleveland, Ohio; https://technicalglass.com/). The cap has 5 feed throughs with ground glass joints and the bottom is the body that contains the molten salt and the coupons and has a gas outlet. To provide a controlled atmosphere, the electrode is inserted into the electrochemical cell and is sealed using a combination of fused quartz joints, graphite tape and high temperature resistant Ceramabond paste. This gives gas-tight seal even when the electrode is inserted and removed many times to and from the

electrochemical cell. The same seal is used to provide a bubbler tube to the cell for controlling the atmosphere over the molten salt. In Figure 1-5, the electrochemical cell with its connections is presented. The experimental setup is similar to the previous work. Heating tape between is used to prevent condensation of water in the transfer line when using Argon with different degrees of humidity. A sketch of the experimental setup is presented in Fig. 1-6.

Atmosphere: Two streams of "Dry Argon" are mixed to control RH of the Argon sparged into the molten salt. One Argon stream is sparged through D.I. water at 25^{o}C at one flow rate and the other Argon stream at another flow rate. The flow rates of these 2 streams are mixed at various ratios to control the RH of the "wet Argon" stream sparged into molten salt. The total Argon flow is 250sccm.

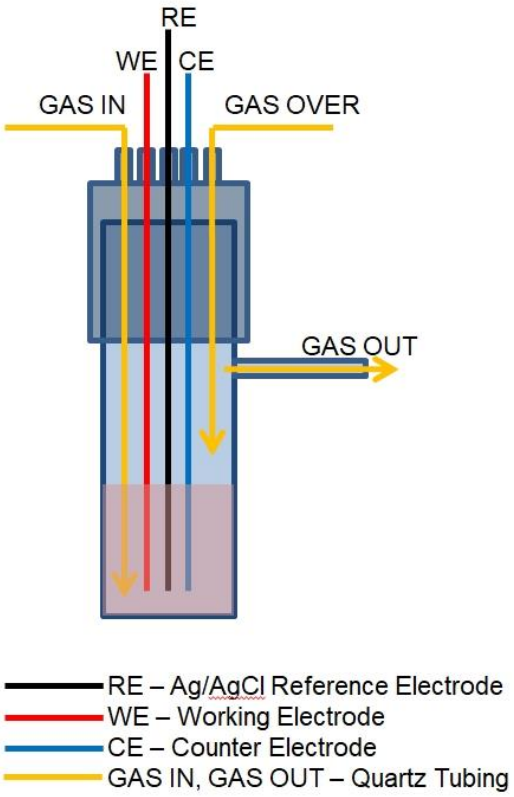

Figure 1-5. Sketch of the all quartz electrochemical cell for use at high temperatures

Silver/silver chloride (SSE) is the reference electrode. The working and counter electrodes are Haynes 230 alloy rods with diameter of 0.15cm polished with 1200 SiC. The total rod length is over 15 inch and a length of 4.1cm is immersed in salt. Volatile oxidants are surface water, dipole-bound water and molecular oxygen. After adding the salt to the electrochemical cell, the oven was kept at 120°C for 2 hours under an Argon flow. Then the temperature was turned up to 800°C, while "Dry Argon" is sparged inside the molten salt to remove volatile impurities (oxygen, water vapor, HCl) for 24 hours (except Exp 2 where it was sparged for 3 hours) Non-volatile oxidant forms when the ternary MgCl2-NaCl-KCl salt is heated to high temperatures. The non-volatile impurity, MgClOH, spontaneously forms and cannot be removed by dry Argon sparging. The proton on MgClOH corrodes Haynes 230 metal alloy in the ternary molten salt. To remove MgClOH, metallic magnesium is added to the salt while sparging Argon stirs the salt at 600^{o}C. This Mg converts MgClOH to MgO and H_2 and Cl^-. The preferred way to introduce Mg is to drop the temperature of the salt to 600C, which is above the

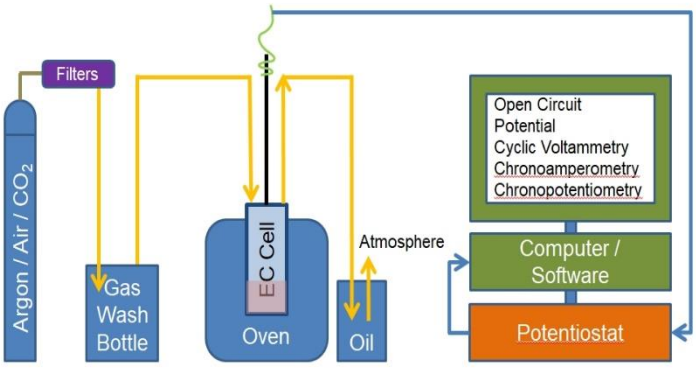

Figure 1-6. Sketch of setup for OCV determinations as a function of RH over salt.

melting temperature of the salt, but below the melting temperature of the Mg; and then insert area Mg foils in the molten salt for a period of time, then pull out the Mg foil.

Table 1-1 : OCP of H230 in 158g (experiment 1 and 2) and 237g (exp. 3, 4, 5) grams of Mg-K-Na Cl molten salt equilibrated with Dry Argon (column 1) and Dry Argon + magnesium metal (col. 2 and col. 3)

Experiment (Na-K-Mg Cl) #	Time Dry Argon sparged (h)	Column 1 OCP in Dry Argon vs SSE** (V) /(no Mg added)	Column 2 OCP in Dry Argon after Magnesium vs SSE (V)/ (Mg added)	Column 3 OCP in Dry Argon after more Magnesium vs SSE (V)/ (Mg added)
1	24*	- 0.342	---	---
2	3	- 0.524	- 0.786 (232mg Mg)	- 0.756 (474mg Mg)
3	22	-0.665	-0.875 (769mg Mg)	---
4	24	-0.783	-0.900 (347mg Mg)	---
5***	23	-0.960	-1.000 (307mg Mg)	---

* Replaced SSE reference which cracked released silver ion into the salt shifting OCP positive.
** Variability in OCP due to variable MgOHCl in salt.
*** Experiment 5 had that connection issue, so -0.960V is questionable
Usually OCP of H230 in oxidant free salt equilibrated with dry argon is around -700 mV vs SSE.

Experiment (Na-K-Mg Cl) #	OCP in Dry Argon* vs SSE (V)	OCP in Dry Argon After Mg (V)	OCP in Dry Argon with 27%RH (V)	OCP in Dry Argon with 40%RH (V)	OCP in Dry Argon with 60%RH (V)
1	- 0.342	---	---	---	---
2	- 0.524	- 0.786	---	---	---
3	-0.665	-0.875	-0.420	---	----
4	-0.783	-0.900	---	-0.350	---
5	-0.960*	-1.000	---	---	-0.530**

* bad connection, questionable result
** sparger clogged after an unknown number of hours, when the salt was NOT YET equilibrated with the 60%RH in Argon flow, value *should be* MORE POSITIVE if truly equilibrated

Three quartz cell bottoms cracked from a solid substance accumulating on bottom. This substance is solid MgO from hydrolysis of $MgCl_2$, as found by XRD of the solid. RH from sparging Argon into water at T >25C then into the molten salt causes clogging due to this solid. Weighed Mg metal put in and removed from molten salt at 600C and re-weighed gives the Mg weight loss and allows estimation of the amount of Mg consumed and water in the salt. Other research groups found adding Magnesium (0.7%mol, 396mg Mg metal per 236.85 grams of our salt mix) removes the non-volatile impurities Our experiments are in agreement with these workers and confirm that to remove non-volatile impurities from 236.85 grams of salt a range of 232mg-769mg of Mg metal (0.4%mol – 1.3%mol) arrests metal corrosion confirmed by corrosion rate and OCP measurements.

Table 1-2: OCP of H230 in 157.86g (for experiment 1 and 2) and 236.85g (for experiment 3, 4, 5) grams of Mg-K-Na Cl molten salt equilibrated with Dry Argon (column 1) and Dry Argon + magnesium metal (column 2 and column 3)

Experiment (Na-K-Mg Cl) #	Column 1 CR in Dry Argon vs SSE micron/y	Column 2 CR in Dry Argon after inserting Mg micron/y	Column 3 CR in Dry Argon with 27%RH micron/y	Column 4 CR in Dry Argon with 40%RH micron/y	Column 5 CR in Dry Argon with 60%RH micron/y
1	30664, 38603		---	---	---
2	7702	2521 & 3324	---	---	---
3	90	43	3000	---	---
4	530	44	---	4115	---
5*	312	49	---	---	2112**

* Mg dropped in salt

** sparger clogged *before atmosphere equilibrated with molten salt*, so the water levels did not go as high as it should have been so CR should be higher.

New experiments checking OCP and CR at several lower water levels and repeating for reproducibility are next.

These above earlier works led to a few conclusions regarding optimizing the experimental setup for detecting oxidant in molten chloride salt: The total gas flow maintained at 250sccm is effective for equilibrating molten salt with the gas atmosphere over the salt. Haynes230 rods are effective for eliminating welds in the salt for electrochemical experiments. Haynes230 rods prepared with water as cutting fluid during wet-polish using 1200 grit of SiC grinding paper followed by cleaning by sonication in 2M aqueous HCl gives a reproducible surface for electrochemical studies of metal in molten chloride salts.

Task 1.0. optimized measurements for sensing oxidants in molten salt
For the optimized experiments, all tubing is FEP giving higher confidence that no oxygen or water from atmosphere diffuses through the tubing into the cell from the gas train. Sparge gas with lower RH in Argon than 100% RH at 25ºC is used to prevent clogging of sparging tube in the molten salt. The RH of the sparge gas was lowered by sparging one stream of Argon into gas-wash bottle with water to make 100% RH water in Argon at 25ºC. Note that: 100% RH water in Argon at 25ºC is a 25mmHg of partial pressure for water out of 760mmHg total pressure of the sparge gas, or 3.3% water vapor in 96.7% Argon gas. A second flow is mixed. Two flow meters are used at different flows to mix 100%RH Argon at 25 ºC with dry Argon in the other stream at 25 ºC to make various RH in Argon atmospheres, The total flow is always 250 sccm. This mixture is used to equilibrate with the molten salt in the electrochemical cell The RHs are 0, 10, 20, 30 and 40% of 100% RH at 25ºC (that is, 0, 10, 20, 30 and 40% where 100% RH at 25ºC is 3.3% water vapor with balance Argon gas). This gives enough variation in RH to see the trend and draw conclusions.

Open Circuit Potential (Open Circuit Voltage, OCP or E_{corr}) determination
Working, Counter and Reference electrode have to be inserted in the salt for 2 hours before taking any measurements to allow the temperature to stabilize. After 2 hours, a

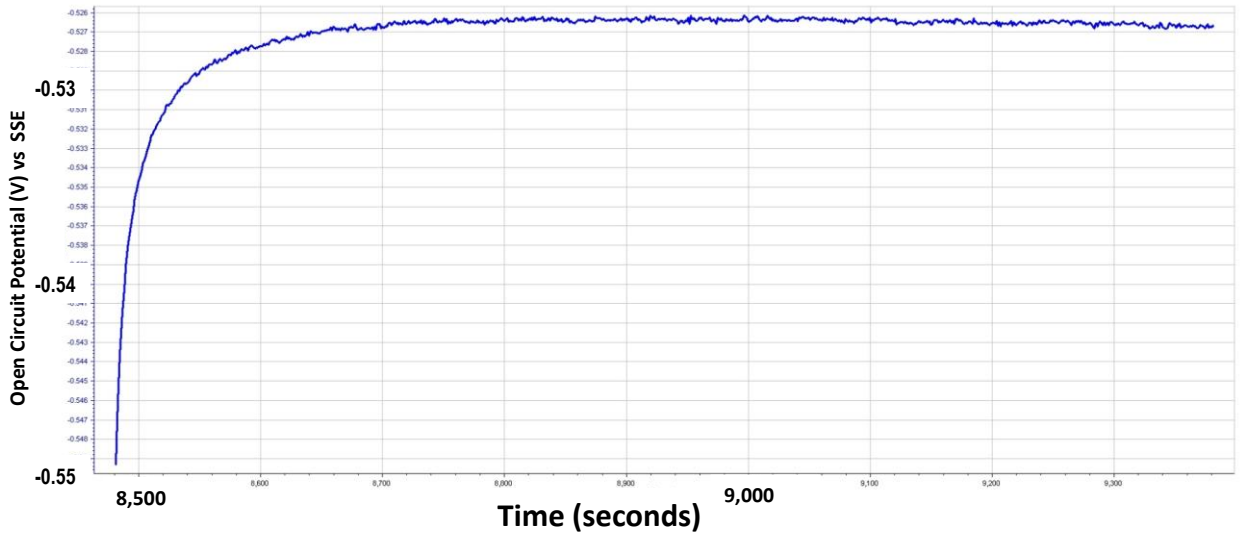

Fig. 1-7. Open Circuit Potential (OCV) vs SCE in time for Experiment 9, for Haynes230 vs SSE in molten salt in Dry Argon. at 800ºC.

measurement of potential versus time of the working electrode and reference electrode is started. This reading continues until the potential does not change more than 1mV/h as shown for Haynes230 vs SSE in molten salt in Dry Argon. at 800ºC in Fig. 1-7. This is possible in Dry Argon equilibrated salt and Dry Argon + Magnesium equilibrated salt. When oxidants like water are equilibrated by sparging and being inserted continuously by blowing over the salt, the potential readings may fluctuate due to various effects like

supersaturation, water condensate and bubble formation and bursting, etc. The Stern Geary method more reliably establishes the open circuit potential, because it is a driven current method and not a passive potential measurement, which fluctuates due to floating potentials, switching noise, bubbles, etc. which fluctuates readings of $\boldsymbol{E_{corr}}$.

Stern-Geary method for OCP (E_{corr}) and Corrosion Rate (CR) determinations

The corrosion potential ($\boldsymbol{E_{corr}}$) is the open circuit potential of the metal under test (WE) vs the reference (SSE) in the molten salt. This is found using the Stern-Geary method, from the current measured during a small 30mV perturbation before and after the OCP. Sample data are shown in Fig. 1-8, below

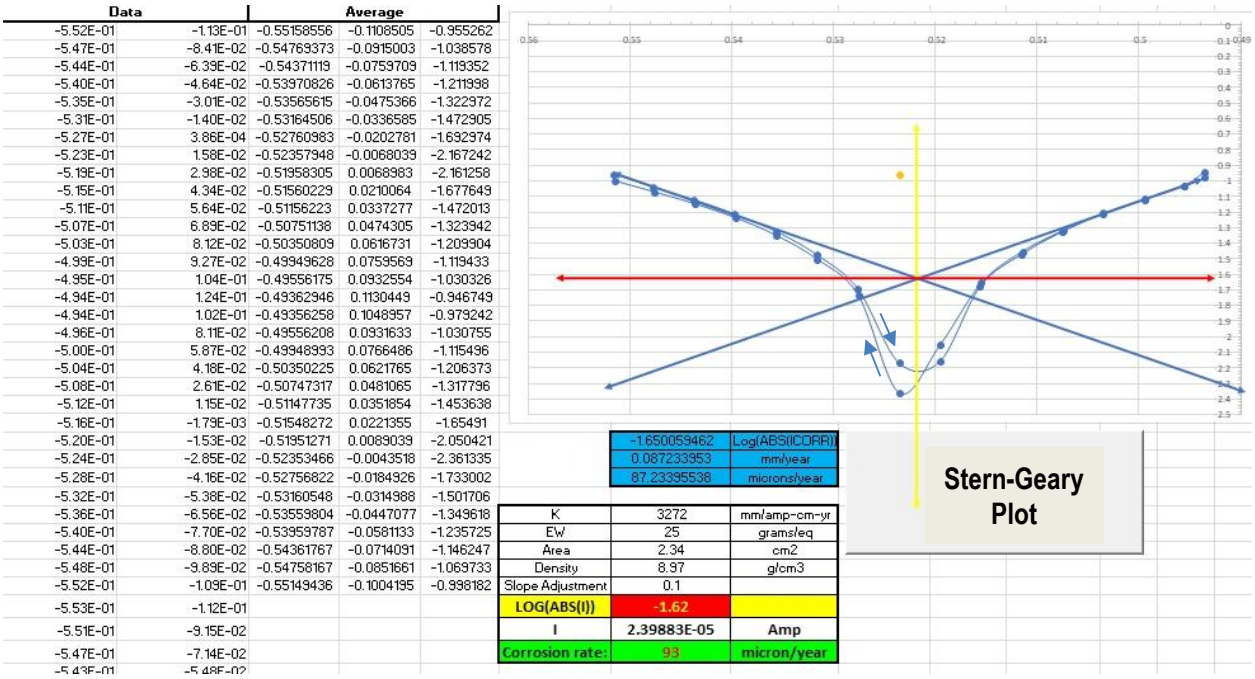

Data		Average		
-5.52E-01	-1.13E-01	-0.55158556	-0.1108505	-0.955262
-5.47E-01	-8.41E-02	-0.54769373	-0.0915003	-1.038578
-5.44E-01	-6.39E-02	-0.54371119	-0.0759709	-1.119352
-5.40E-01	-4.64E-02	-0.53970826	-0.0613765	-1.211938
-5.35E-01	-3.01E-02	-0.53565615	-0.0475366	-1.322972
-5.31E-01	-1.40E-02	-0.53164506	-0.0336585	-1.472905
-5.27E-01	3.86E-04	-0.52760983	-0.0202781	-1.692974
-5.23E-01	1.58E-02	-0.52357948	-0.0068039	-2.167242
-5.19E-01	2.98E-02	-0.51958305	0.0068983	-2.161258
-5.15E-01	4.34E-02	-0.51560229	0.0210064	-1.677649
-5.11E-01	5.64E-02	-0.51156223	0.0337277	-1.472013
-5.07E-01	6.89E-02	-0.50751138	0.0474305	-1.323942
-5.03E-01	8.12E-02	-0.50350809	0.0616731	-1.209304
-4.99E-01	9.27E-02	-0.49949628	0.0759569	-1.119433
-4.95E-01	1.04E-01	-0.49556175	0.0932554	-1.030326
-4.94E-01	1.24E-01	-0.49362946	0.1130449	-0.946749
-4.94E-01	1.02E-01	-0.49356258	0.1048957	-0.979242
-4.96E-01	8.11E-02	-0.49556208	0.0931633	-1.030755
-5.00E-01	5.87E-02	-0.49948933	0.0766486	-1.115496
-5.04E-01	4.18E-02	-0.50350225	0.0621765	-1.206373
-5.08E-01	2.61E-02	-0.50747317	0.0481065	-1.317796
-5.12E-01	1.15E-02	-0.51147735	0.0351854	-1.453638
-5.16E-01	-1.79E-03	-0.51548272	0.0221355	-1.65491
-5.20E-01	-1.53E-02	-0.51951271	0.0089039	-2.050421
-5.24E-01	-2.85E-02	-0.52353466	-0.0043518	-2.361335
-5.28E-01	-4.16E-02	-0.52756822	-0.0184926	-1.733002
-5.32E-01	-5.38E-02	-0.53160548	-0.0314988	-1.501706
-5.36E-01	-6.56E-02	-0.53559804	-0.0447077	-1.349618
-5.40E-01	-7.70E-02	-0.53959787	-0.0581133	-1.235725
-5.44E-01	-8.80E-02	-0.54361767	-0.0714091	-1.146247
-5.48E-01	-9.89E-02	-0.54758167	-0.0851661	-1.069733
-5.52E-01	-1.09E-01	-0.55149436	-0.1004195	-0.998182
-5.53E-01	-1.12E-01			
-5.51E-01	-9.15E-02			
-5.47E-01	-7.14E-02			
-5.43E-01	-5.48E-02			

-1.650059462	Log(ABS(ICORR))	
0.087233953	mm/year	
87.23395538	microns/year	
K	3272	mm/amp-cm-yr
EW	25	grams/eq
Area	2.34	cm2
Density	8.97	g/cm3
Slope Adjustment	0.1	
LOG(ABS(I))	-1.62	
I	2.39883E-05	Amp
Corrosion rate:	93	micron/year

Fig. 1-8. Corrosion Rate Calculation for Exp 9, which is for Haynes230 when in molten salt at 800^{o}C in Dry Argon Atmosphere

The initial positive going and following negative going potential scans are averaged, the absolute value of the average current is plotted on a log scale. The tangent lines of the cathodic and anodic currents intersect the x-axis at the corrosion potential and intercept on the y-axis at the corrosion potential is the corrosion current. which is used to calculate the corrosion rate (CR):

Corrosion Rate = (Current*Equivalent Weight*K(constant))/(Area*Density)

…where…

Corrosion Rate = [mm/year]
Current = [amp]
Equivalent Weight = 25[grams/eq]
K= 3272[mm/amp*cm*year]
Area = [cm^2]
Density = [g/cm^3]

The values of open circuit and corrosion rate from Stern Geary analyses were given previously, but new improved open circuit values and the corrosion rates for H230 in molten chloride salt as a function of RH of Argon gas equilibrated with the salt derived by the Stern Geary method are given next.

Task 1-3. E_{corr} of H230 in molten chloride salt with Argon and wet Argon atmospheres

The conditions of the metal and the salt are given in the table below during optimized experiments done in Q7. The open circuit potentials and the corrosion rates are given as a function of RH in the atmosphere over and equilibrated with the molten Mg-K-Na-Cl eutectic salt.

Table 1-3. Experimental Conditions, such as salt weigh, drying period, electrode area immersed, etc. for the 12 experiments

Date	Exp #	Salt Mix Mass (g)	Drying at 800°C (hours)	Working Electrode Area (cm^2)	Gas flow (sccm)	Mg added (mg)	Reference SSE #	Tubing	Result/Comments
8/17/2020	1	157.86	25	2.4	250	X	1	Vinyl+FEP	DryArgon Extreme Corrosion Rates
8/18/2020	2	157.86	3	2.39	250	232+242.2	1	Vinyl+FEP	DryArgon Extreme Corrosion Rates
8/29/2020	3	236.85	24	2.67	250	74.5+183.2+577.8	1	FEP	Mg increased corrosion?
10/1/2020	4	236.85	24	1.97	250	347.1	1	FEP	60RH Clogged
10/7/2020	5	236.85	24	2.11	250	307	1	FEP	Success
10/22/2020	6	236.85	24	2.34	250	367	1	FEP	Success
10/25/2020	7	236.85	24	X	250	X	1	FEP	Fail - Cracked Reference
11/3/2020	8	236.85	24	2.3	250	517.3	2	FEP	DryArgon Extreme Corrosion Rates, Mg broke off inside salt
11/20/2020	9	236.85	24	2.34	250	528	2	FEP	High RH Clogged
12/7/2020	10	236.85	24	X	250	X	2	FEP	Fail - Cracked Cell / Oven
12/19/2020	11	236.85	24	2.16	250	32.6	2	FEP	Success
12/28/2020	12	236.85	24	X	250	X	2	FEP	Fail - Cracked Cell and Reference

Open circuit potentials (E_{corr}) for H230 in the salt at different RH in the Argon atmosphere are given in Table 1.2 below.

Table 1-4. Open circuit potentials of H230 in molten Mg-K-Na-Cl eutectic salt as a function of RH in the atmosphere equilibrated with the salt performed during Q7

(All data Points)	Dry Argon + Mg	Dry Argon	10% RH	20% RH	30% RH	40% RH Above	40% RH Inside
Replicates	42	49	4	14	7	3	28
OCV	-0.709	-0.604	-0.459	-0.451	-0.416	-0.364	-0.123
OCV STDEV	0.139	0.129	0.001	0.007	0.001	0.001	0.027

The raw data is graphically plotted in **Figure 1-9** below and replotted in Figures 1-10 a through d. Figures 1-10 a and b are OCV versus RH with x-axis linear increasing RH and Figures 8c and d shows OCV versus log of RH on the x-axis. The oxidation reaction for metal oxidation by water is $M + H_2O \rightarrow MO + 2\ H^+$ and the corresponding Nernst Equation is $OCV = E^{o'} + nF \log [M]\,[H_2O]/[MO][H^+]^2$

The change in OCV with RH appears to be non-linear. OCV appears to give a linear fit to the change in the log of water, that is, log RH, as expected if the OCV is under thermodynamic control and governed by the Nernst equation.

.

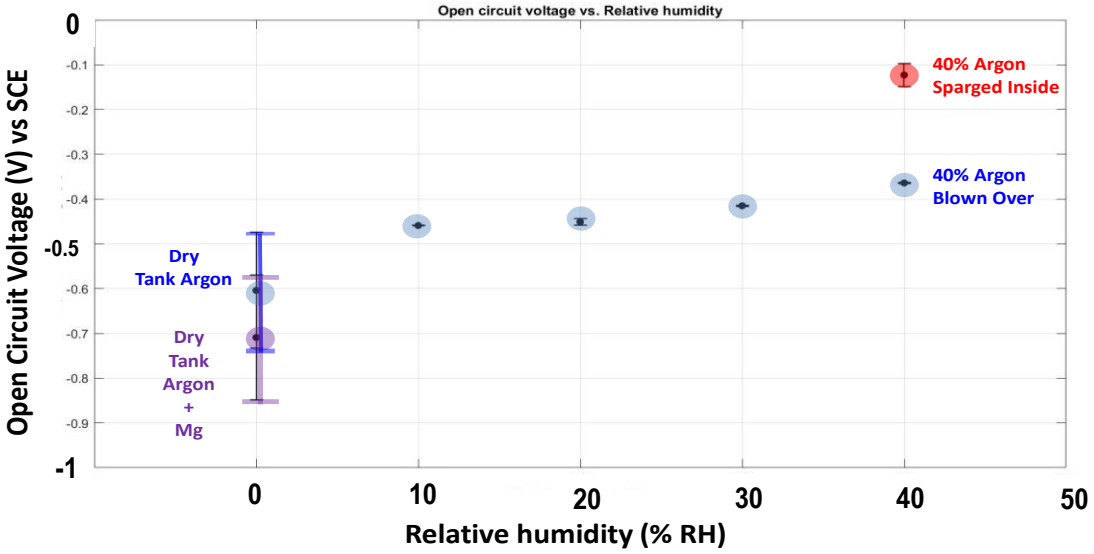

Figure 1-9. Open Circuit Voltage versus Relative Humidity of Haynes230 versus SSE in molten salt at 800*C equilibrated with various atmospheres such as Dry Argon, and Dry Argon + various amounts of water. Dry Argon + 40%RH with sparging at 250 sccm.

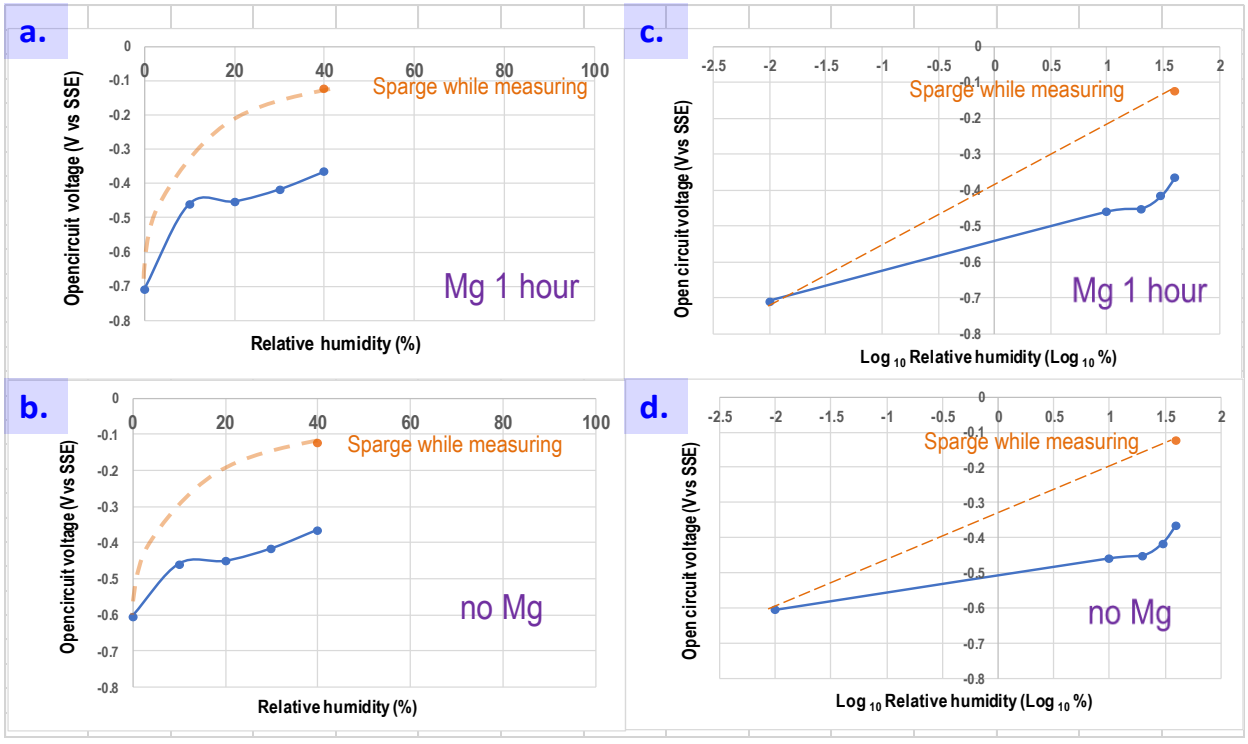

Figure 1-10. Open Circuit Voltage versus Relative Humidity of Haynes230 versus SSE in molten salt at 800*C equilibrated with various atmospheres Dry Argon + various amounts of water. Dry Argon + 40%RH with sparging at 250 sccm.

The corrosion rates for H230 as a function of RH derived from the Stern Geary data is in Table 1.5 and Figure 1-11

Table 1.5 Corrosion rates of H230 in molten Mg-K-Na-Cl eutectic salt at 800°C as a function of RH in the atmosphere equilibrated with the salt performed during Q7

All data Points	Dry Argon + Mg	Dry Argon	10% RH	20% RH	30% RH	40% RH Above	40% RH Inside
Replicates	28	32	4	14	7	3	28
CR	145	194	947	1051	2117	3831	7865
CR STDEV	101	155	267	395	230	846	3583

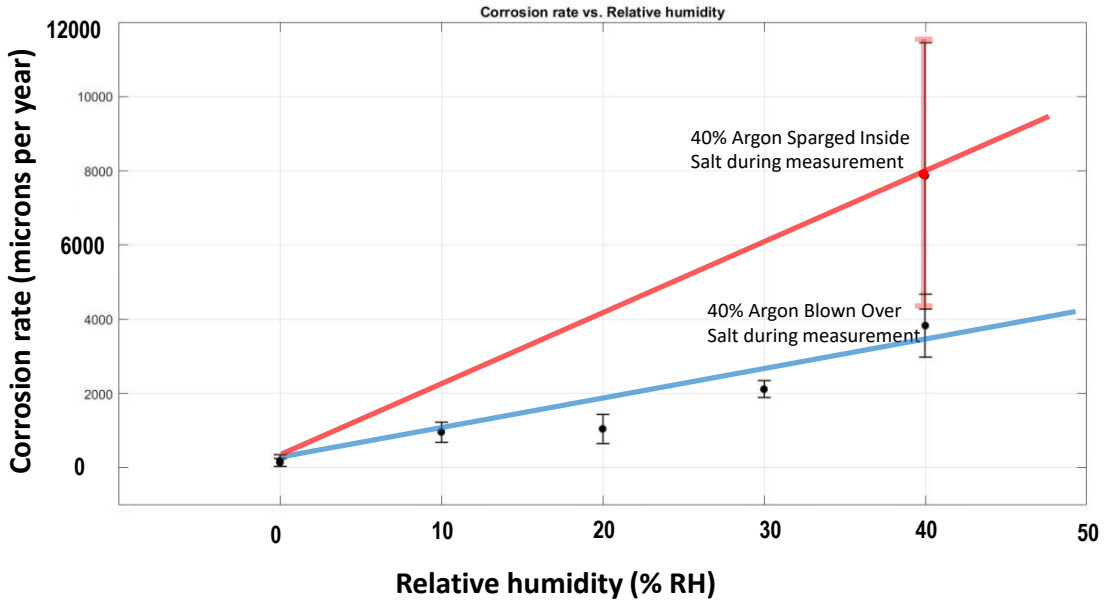

Figure 1-11. Plot of **c**orrosion rates of (CR) Haynes230 at the corrosion potential (E_{corr}) when metal is in molten ternary Mg-K-Na-Cl eutectic chloride salt at 800°C and equilibrated with various atmospheres over the salt including: Dry Argon, and Argon at various RH. Argon Flow rate = 250 sccm. E_{corr} is open circuit potential (OCP) versus SSE. Blown over means salt equilibrated with sparging gas and gas blown over salt during measurement for corrosion rate in wet stagnant molten salt. Sparged inside means salt equilibrated with sparging gas and gas sparged inside salt during measurement to illustrated the effect of convection of molten salt.

Conclusions

This work successfully concludes task 1. Non-volatile oxidants can be removed with magnesium metal and volatile water and oxygen by sparging Argon into the salt. The open circuit potential and the corrosion rates for H230 in molten chloride salt change as expected when the salt is equilibrated with different levels of water, an oxidant to H230. The salt with oxidants has a more positive OCP than salt without oxidants, seemingly following a log trend for OCP and linear trend for CR.

Task 1. ii. Chronoamperometric detection of oxidants leaking into molten salt:

Chronoamperometry (current at fixed WE potential in time) gives the current for oxidant reduction at a fixed voltage between H230 WE and the SSE reference electrode, as shown in firgure 1-12, below.

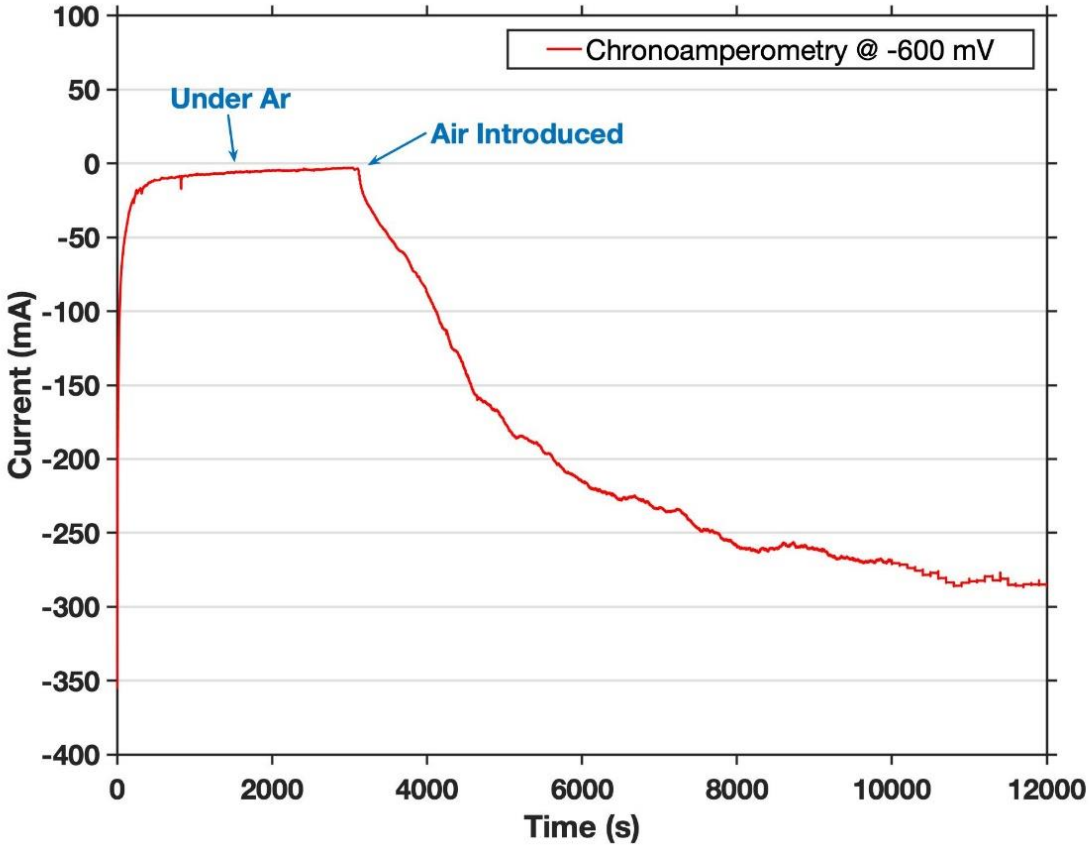

Figure 1-12. Chronoamperometry (i vs t at const E) of H230 coupon in molten NaCl-KCl salt. E set at -600mV vs SSE which is -100 mV versus open circuit of Haynes 230 immersed in NaCl-KCl salt at 800^{o}C. System was held under argon for 1hr followed by air for 2.5 hr.

Molten NaCl-KCl salt was equilibrated with Argon at 800^{o}C to create an inert atmosphere similar to that inside a pipe. The OCV (E_{oc}) of the H230-WE vs SSE-RE was recorded and at steady state, the E_{oc} was -500 mV. H230 metal was then set to -600 mV vs Ag/AgCl reference electrode (that is, -100 mV vs. E_{oc}) to deplete residual oxidants (water, oxygen) from salt solution. When current went from -50 mA to near 0 mA, that indicated depletion complete near the H230 surface. Air was then blown over the molten salt to simulate a leak in the pipe metal. The generation of a large negative current leveling off to -280 mA shows oxidants entered in the system. This current can be correlated to oxidant concentration using the well know Cottrell equation. ***F.G. Cottrell, Z. Phys. Chem. 42 (1903), p. 385***

Controlling and measuring water in gas equilibrated with molten chloride salt

Measuring water levels: The removal of residual water in tank gases and the measuring water in gases is important for evaluating the *INTRINSIC tendency of CO2 to oxidize metal* in molten chloride salt equilibrated with CO2 atmosphere. The effects of residual water in a pressurized CO2 tank may mask the corrosive behavior of CO2 itself. An alternative to a Vaisala meter for measurement of water levels in gases is an optical method developed by Tiger Optics, the MTO-1000-H_2O is a trace water is gas analyzer, and is shown in **Fig. 1-13**, below.

Figure 1-13. Tiger Optics MTO-1000-H2O setup for optically measuring PPM down to sub-PPB levels of water vapor in various (Ar, CO_2, air) tank gases (before and after using water removing filters) that are being equilibrated with molten chloride salts.

The Tiger Optics MTO-1000-H2O complements the Vaisala meter for measuring water in gases in that both meters can read in the 1 to 10 ppm range but the Vaisala meter can read high water levels (10's of thousands of ppm water in gas) while the Tiger Optics can read to sub ppb level of water in gas. Using the Tiger Optics MTO we have confirmed that nominally "Dry" Argon tank gas contains around 3ppm of moisture as shown in **Fig. 1-14.** During a preliminary test, we found out that the Argon contains between 2.8 to 3.5 ppm of water vapor. This Tiger Optics MTO setup is very sensitive for measuring the concentration of water in various gases like Argon, N2, CO2 and air. We are in the process of setting water removing filters to lower the water in tank gases, especially CO2 and Argon so we can compare corrosion rates in truly dry Argon and truly dry CO2.

Fig. 1-14.TigerOptics detected 3.5ppm of water vapor in Argon tank gas.

Controlling water levels: Removal of water from gases is controlled by using gas filters, such as, Drierite dessicant and NuPure reactive getters, shown in **Fig. 1-15**. The Drierite desiccants are made from calcium sulfate ($CaSO_4$) and remove water from gas streams at room temperature down to 0.005 mg of water/liter, that is, 0.005 ppm or 5 ppb water vapor in tank gas, according to the National Institute of Standards and Technology (NIST). Drierite removes most of the water found in pressurized gas tanks. The Drierite tubes shown are effective up to 300 sccm flows, but there are other drierite tubes that can handle higher flow rates. The NuPure Eliminator CAG is a room temperature water remover. Different ones are used to remove water from different gases. NuPure uses catalyst/absorber/getter (CAG) water removal to remove water from gas streams and dries gas to <0.5ppb levels of water vapor at flows up to 300 SLPM. These NuPure filters are used after Drierite as a second filtering step to bring water in dry gas in gas below ppb levels. Tank gases typically have 3 to 10 ppm of water vapor so using these filters can lower water levels in gas by a factor of ~10,000 (~ 5 ppm / 0.0005 ppm). Comparing metal corrosion in molten salt equilibrated with a CO_2 atmosphere with and without water removing filtering of tank CO_2 is useful to make clear the intrinsic metal oxidizing power of CO_2 itself in molten salt as opposed to the water in the CO_2.

(a) Drierite (b) NuPure for CO2 (c) NuPure for Argon

Figure 1-15. Water removing from gas filters. Drierite (left) and NuPure (middle and right).

Task 1iii: Detection of oxidants by in-situ Raman optical method

Oxidants from air are a threat to the stability of metal pipes and containers filled with molten salt. So it is desired to have an accurate measurement of water and oxygen in the molten salt. Clearly sensors are needed for measuring water, oxygen and carbon dioxide content in molten salt. Raman Spectroscopy is a powerful optical method for detecting and monitoring the water content in molten salt. Raman Spectroscopy gives highly specific information for the analysis of chemical compounds, like water, oxygen and carbon dioxide molecules in molten salt. For example, water molecules exhibit peak heights proportional to concentration. A Raman probe with a green laser is ideal for real-time detection of the presence and levels of water in molten salt. The Raman method is preferred because Raman can distinguish oxidants in air, like O_2 , CO_2, and water. Raman is the inelastic scattering of high energy radiation, so interference by the infrared radiation emitted at 900˚C is minimal. A Raman detector for measuring water and oxygen in salt is useful 1) as an on-line Raman sensor of salt in a working metal pipe and 2) during salt pre-treatment before filling the pipe. To make a practical sensor requires a fiber optic probe, as shown in **Fig. 1-16**. The new setup in **Fig. 1.16 to 1-18** have been used to give information about the water content in molten salt. The Argon outlet tube is connected to a glass chamber fitted with a VAISALA HMT 337 humidity probe and thermocouple, then a drying tube of DRIERITE, a Teledyne Analytical Instrument, model 2240 hydrogen sensor, a Teledyne GB-300 oxygen probe, and a VWR, SympHony SP80PI pH meter which are all connected in series. The exit tube and the RH relative humidity (RH) probe chamber

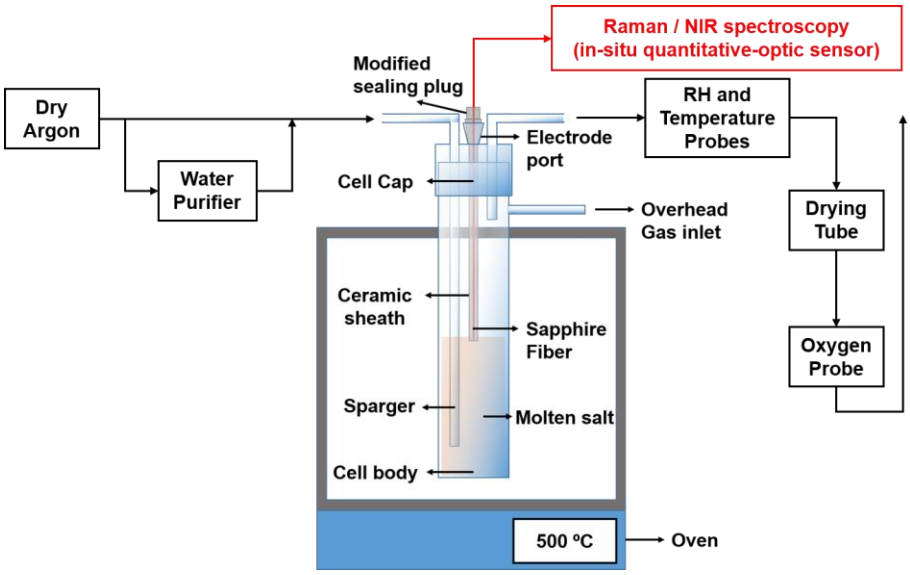

Figure 1-16 Schematic diagram of modified experimental setup for fiber-optics photometer for in-situ sensing of water and oxygen in molten salts at high temperature by Raman spectroscopy.

are heated around 115˚C to prevent the water condensation. The DRIERITE drying tube is used to remove any water before outlet gas reached the hydrogen and oxygen sensor to protect these sensors. A specially designed cell cap has the 2 ports for gas in andout and 1 large port for Raman probe. A quartz sheath is used as like a cover to avoid the probe directly touching the molten salt. The Raman probe has it own Ar gas inlet line, to protect the probe. An anodisc filter is sued to protect the gas sensing probes from salts spray.

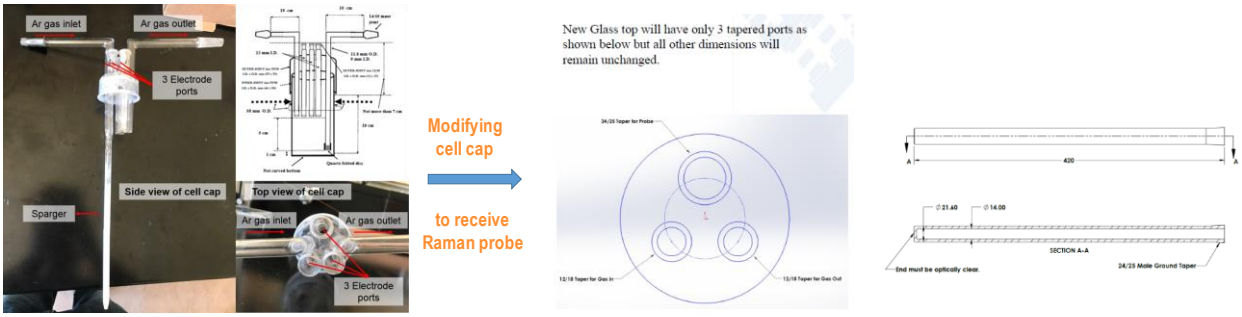

Cell cap for the electrochemical detection of oxidant in molten salt at 800˚C

Cell cap for Raman probe for detecting oxidant in molten salt at 800˚C

Raman probe for detecting oxidant in molten salt at 800˚C

Figure 1-17 Electrochemical (left side) and the modified cell cap for the optical sensing test (middle) and fiber optic probe (right) for sensing oxidants in molten salt.

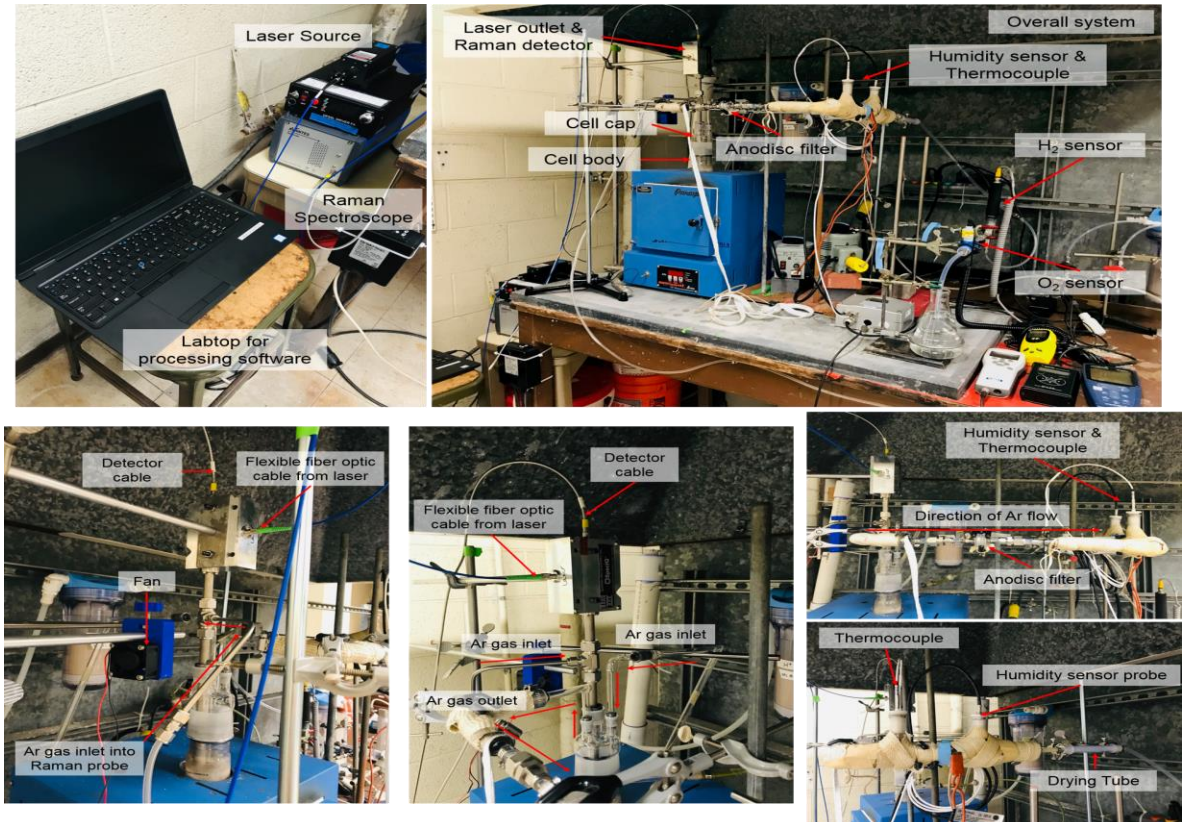

Figure 1.18 Apparatus for the in-situ Raman spectroscope under controlled atmosphere and manifold to monitor gas leaving Raman probe for sensing water, hydrogen, oxygen and pH in outlet gas.

The spectrometer range of 535 – 765 nm is set based on the laser source and expected Raman shift range that should cover both the salt and water peaks. The 532nm excitation source is chosen for a few reasons: 1) it is far from black-body radiation wavelenghts 2) Sporian's prior work on molten salts with 532nm excitation to compare to 3) and 532nm seemed to produce the least amount of background fluorescence in salt mixtures. 4) although lower wavelength excitation produces stronger peaks, the photo-detector efficiency is lower at lower wavelengths. The product of expected signal intensity (per mw of laser power) and photo-detector efficiency, QE, 450 to 550nm is the best range for excitation in general. 5) Most laser sources in the 450 to 550nm range are low power, with too wide spectral bandwidth, and very expensive. In summary, 532nm lasers are cheap. narrow spectral bandwidth, and available in very high power.

Detection of water in NaCl-KCl by in-situ Raman optical method

A Raman signal shows the presence of water in molten salt but disttinct water vibration from Raman scattering has NOT been obtained during this study. The experiment done to date are outlined below.
The Raman spectroscopic probe uses 1) a modified quartz cell and cell cap for mounting the sensing probe 2) conditions, such as temperature and probe location 3) optimizing for operation at high temperature. **Molten s**alt must touch the outside of the quartz sheath after salt is melted. A dark, with the laser off, is taken before every measurement at the prescribed temperature. Fig. 1-19 shows as the temperature increases, the Raman signals was getting wider. At 800˚C, all signals saturated, and are not distingushable. In general, when a materials temperature is increased, the Raman peak will widen and move to the right.

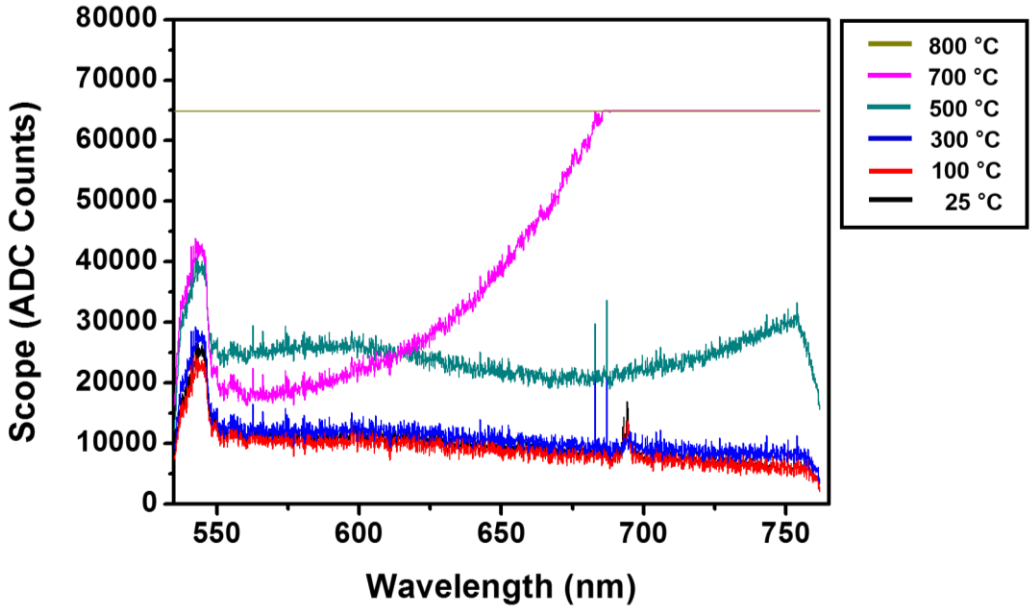

Figure 1.19 Raman spectra of NaCl-KCl salt mixture with various temperature from 25 to 800˚C

To minimize the saturated signal, we checked the effect of the integration time on Raman signals at 800˚C. The integration time was adjusted from 5 sec to 35 sec as shown in **Figure 1.20**. All signals were not distinguishable over 40 sec. Lowering integration time and increasing the number of averages is done to bring the signal out some more. But there no major improvement resuults.

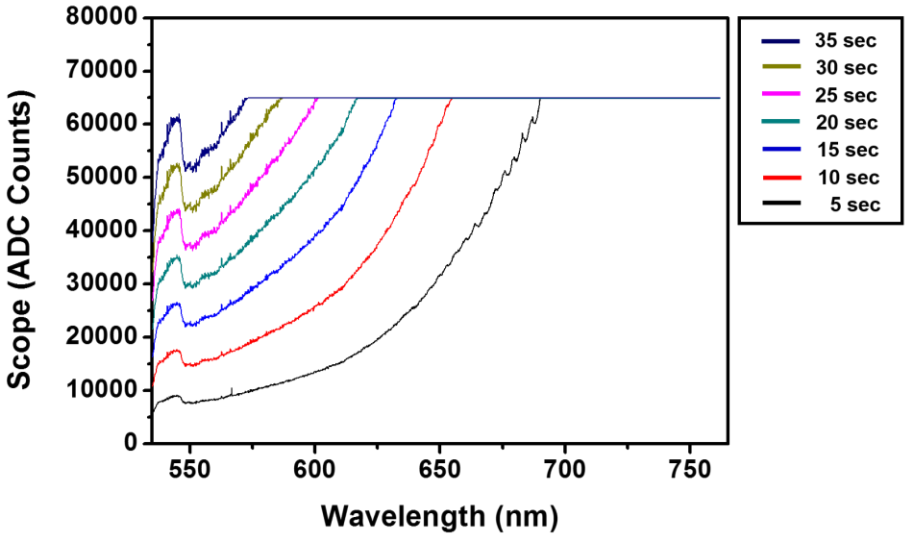

Figure 1.20 Raman spectra of NaCl-KCl salt at 800˚C with various integration times from 5 to 35 sec.

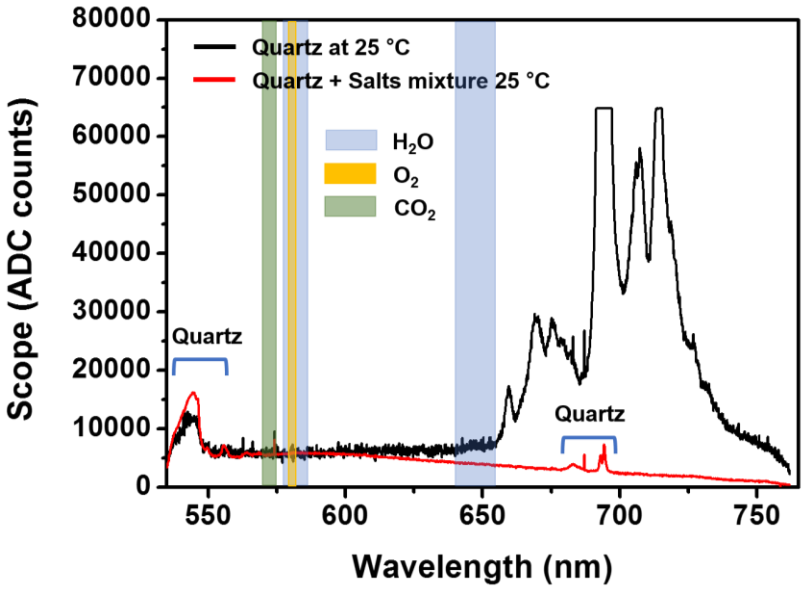

Figure 1.21 Raman spectra of quartz sheath with and without NaCl-KCl salts mixture at 25˚C. Excitation wavelength: 532 nm, Integration time: 60 sec (Quartz + salt) and 35 sec (Quartz only)

The Raman response from 535 to 550 nm is from the quartz sheath not water as determined from Raman spectra of quartz sheath with salt and without salt at 25˚C, indicate. There are reported vibrational peaks from 675 to 690 nm as shown in **Figure 1-21**.

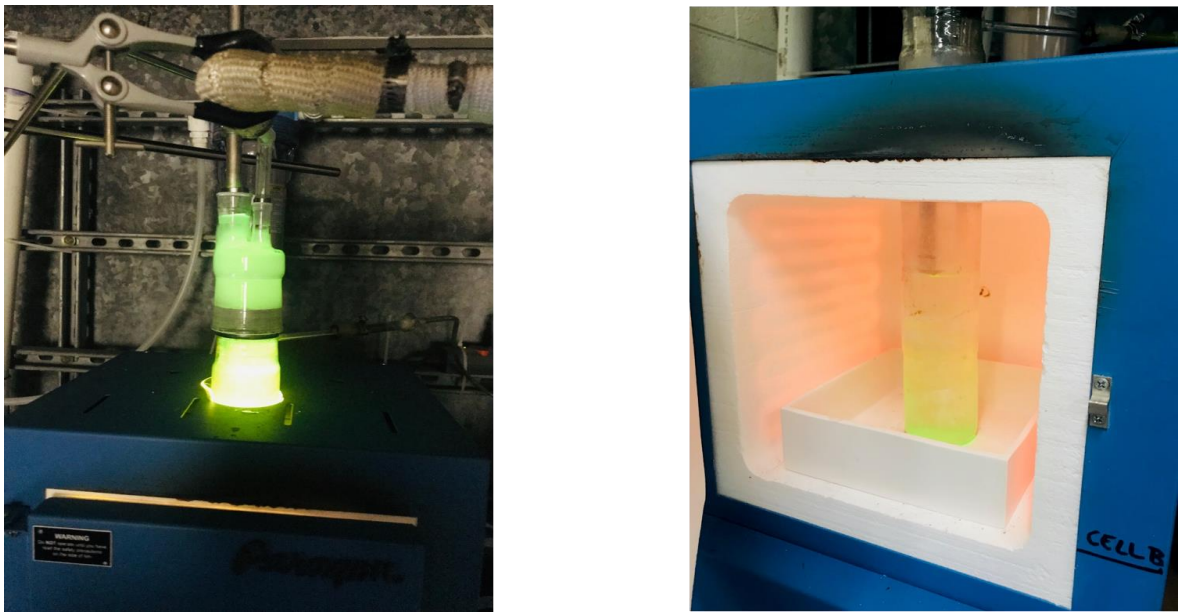

Figure 1.22 Pictures of actual operation of the Raman spectroscope.

Effort was focussed on where the peak noise comes from, especially between 655 and 730 nm, since the major water peaks appear near this noise.

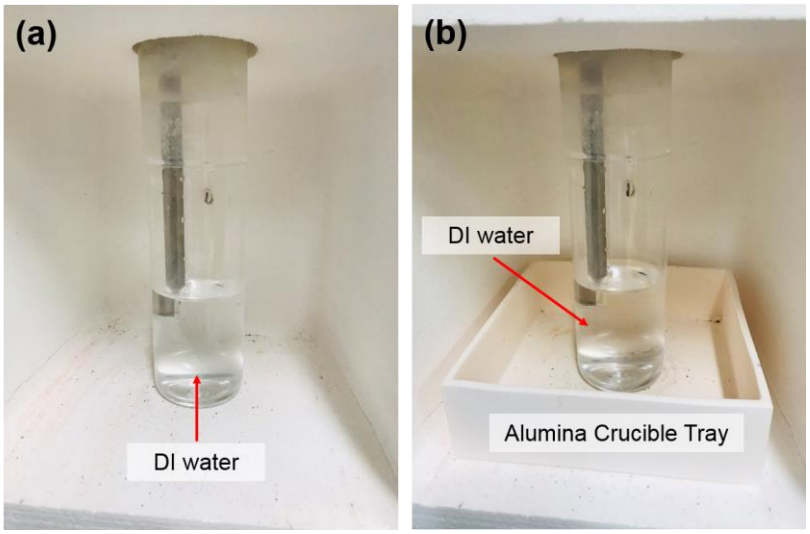

Figure 1.23 (a) Detecting the Raman signals without alumina crucible tray and (b) Detecting the Raman Signals with alumina crucible tray

Fig. 1-23 shows an alumina crucible tray is typically used to protect the oven if the cell is broken and molten salts spills out of the cell. The alumina tray could strongly affect on making the undesiralbe Raman signals because when the experiment is conducted with salts mixture at the room temperature, no peak noise is obseved. In this case, the laser source cannot be reached at the alumina tray. In contrast, when the expriment is run without salts, there were strong peaks as the laser source reaches the surface of the alumina tray. The reason why this is important is that when the salts are melted at high temperature, the laser will be able to pass though the molten salt to the bottom of the cell. To verify peaks from 655 to 730 nm, we investigated how the Raman signal is changed with and with out the alumina crucible tray at 25^{o}C.

Based on experimental observation,tthe strong peak noise are coming from the alumina crucible. More importantly, when the tray was removed, more distinguishable Raman signals are observed.

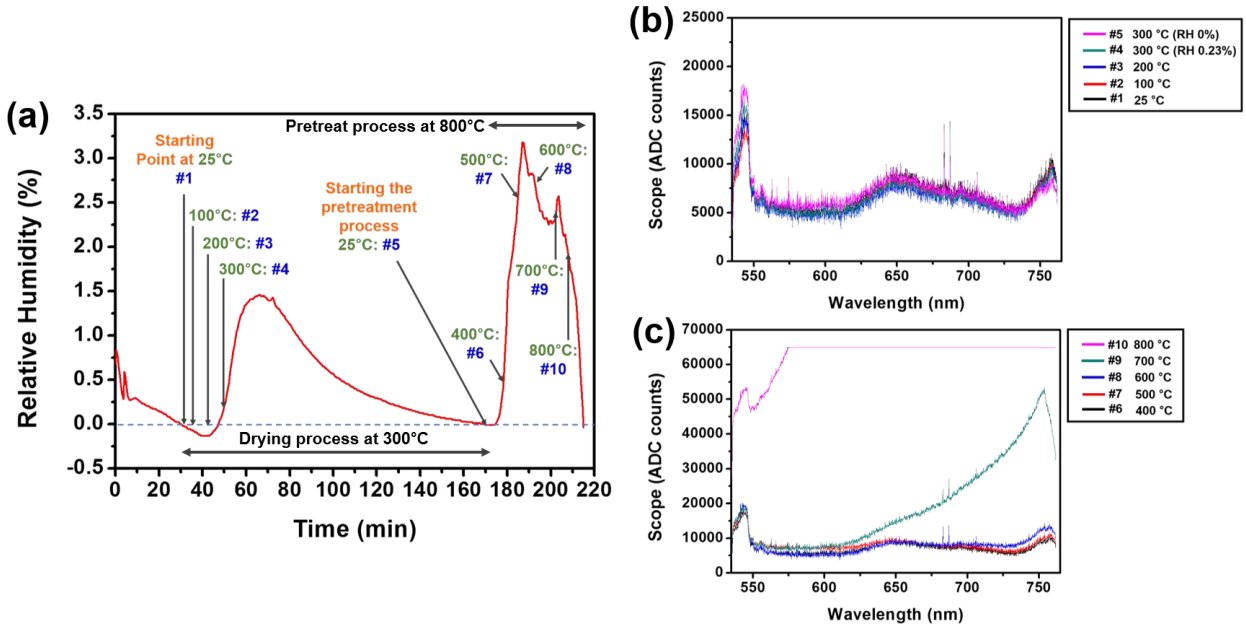

Figure 1.24 (a) H_2O versus time of exiting gas during and after treatment process of NaCl-KCl. The drying and pretreatment processes were conducted at 300 and 800°C. (b) and (c) Raman spectra of NaCl-KCl salt mixture at various temperatures from 25 to 800˚C. Excitation Wavelength: 532 nm, Integration time: 30 sec

Fig. 1-23 shows how the Raman signal evolves from low to high temperature without the alumina crucible tray, NaCl-KCl salt we conducted was dehumidified. As shown in **Figure 1.24(a)**, the drying and pretreatment processes are successfully done at 300 and 800˚C, respectively. The Raman signals are as pointed by numbered arrows. After the drying for removing physi-bound water in **Figure 1-24(b)**, it was hard to detect the change of the water signal (arrow #5) as compared with signal #1 before the drying process. As the temperature increased, the Raman signals saturated. At 800˚C, the signals are saturated, and not distinguishable in **Figure 1.24(c)**. The signals up to 600˚C are relatively stable.
The main problem is the thermal radiation from the oven at the high temperature. The oven starts to emit red light above 600˚C, which interferes with detecting the water signal from molten salts. The U of A team discussed how to block this with the Sporian teamThere are 3 different ways to get rid of the thermal radiation as follows; 1) Covering the inside surface in the oven with graphite foil, 2) Making anodized stainless steel walls to block red light, and 3) Using a lenz filter to remove the thermal radiation. Also using longer integration time increase the water signal. All inside surfaces in the oven were covered with graphite to reduce the effect of the radiation from the heating coil in **Figure 1.25 (top line)**. After covering the surface, the oven was dried for overnight. Then, the thermal stability of the graphite foil was checked as the temperature increased from 25 to 600°C. Although the graphite sheets start o pucker at 300°C, all surfaces are stable up to 500°C **(Figure 1.25 (middle line))**. Although the covering sheet started to be partially detached at 600°C, it maintains its shape even after the end of the test **(Figure 1.25 (bottom line))**. However, the graphite cover on the door completely detached.

Figure 1.25 All inside surface in the oven covered with graphite foils. The graphite foils are stable from 25 to 600°C, so the Raman experiment can be run up to 600°C by covering the oven surface with graphite.

A schematic diagram of improved hardware for Raman probe in molten salt is in Fig. 1.25.

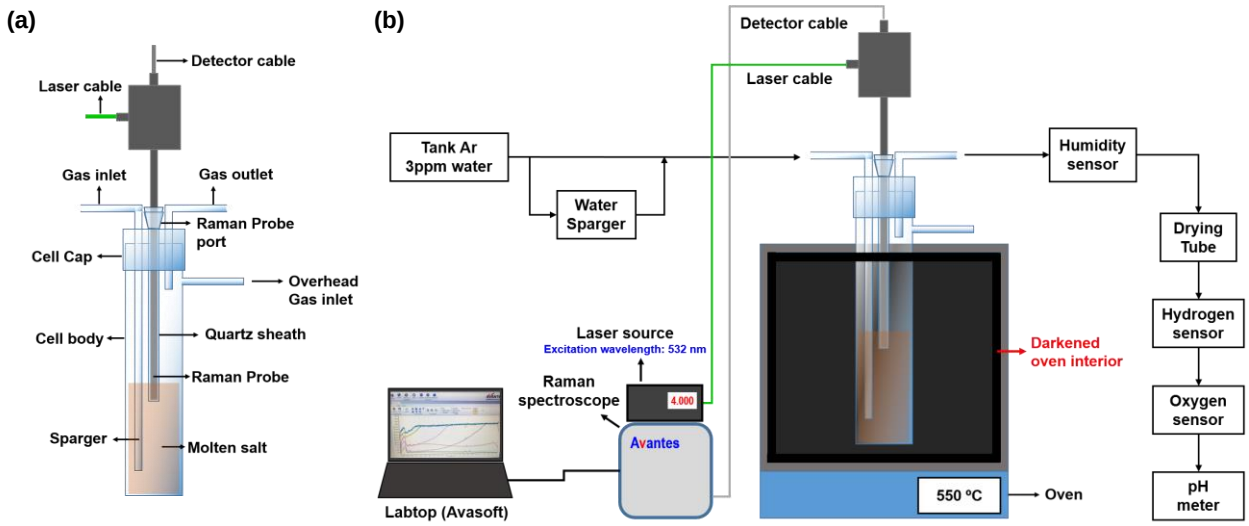

Figure 1.26. Schematic diagram of experimental setup for Raman probe for in-situ sensing the oxidants in molten salts at temperatures up to 800 ˚C. (a) Sketch of the high temperature cell showing how the Raman probe is installed and (b) Sketch of the system shows temperature and atmosphere control and blackened furnace walls. Data acquisition software is '**Avasoft 8**'.

The methodology for presenting data in chemically meaningful way is done using Avasoft 8 software to transform raw wavelength data to wavenumber used in vibrational spectroscopy. The transform equation: wavelength (nm) to wavenumber (cm^{-1}) is

$$Wavenumber(cm^{-1}) = \frac{10000000}{Excitation\ waverlength\ (nm)} - \frac{10000000}{wavelength\ (nm)}$$

and the analysis of data is done 2 ways, by

1. Peak assignments obtained by comparing peaks to those in references in the chemical literature
2. Relationship of peak strength to concentration of analyte,
    a. experiments with controlled analyte concentrations
    b. filter out background fluorescence

The Raman experiments are done first on solids at low temperatures (25°C) and then on solids at higher temperatures (200°C) and finally above melting temperatures (550°C). The temperature was limited to 550°C to avoid saturation by black body radiation.

Low temperature Raman probing of solid chloride salts

The Raman signal of solid $MgCl_2$ was measured before and after exposure to moisture in the air at room temperature Figure 1-27.b shows the Raman spectrum of pure MgCl2 before exposed to moisture in the air. Integration time set to 2 sec since signal saturated when set over 3 seconds. A high intense peak at 241 cm-1 could be assigned to MgCl2. No peaks for water and oxygen were observed.

Before measurement, a pure salt is put into a beaker from a salt storage bottle.

During measurement, the salt is exposed to air.

When getting the Raman signal, the software was set up to automatically scan 10 times. The last one was plotted in order to have a stable signal.

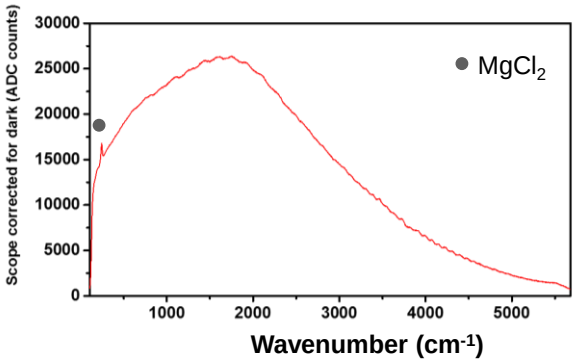

Figure 1-27.a. Raman probe is located very close (1-2 mm) to MgCl2 in an open beaker exposed to moisture from air at room temperature and atmospheric pressure during Raman spectrum sampling.

Figure 1-27.b. Raman spectrum of MgCl2 before exposure to moisture at room temperature and atmospheric pressure. Peak at 241 cm-1 is for MgCl2. Excitation Wavelength: 532 nm, Integration time: 2 sec, Averaging 10, and Current 4 A

Figure **1-28.a.** shows the Raman spectrum of pure MgCl2 after exposed to moisture in the air for 1 day (just put a beaker filled with a salt on the lab table.)Two peaks at around 3400 cm-1 and 1585 cm-1 appeared, which is certainly from absorbed water in the air.

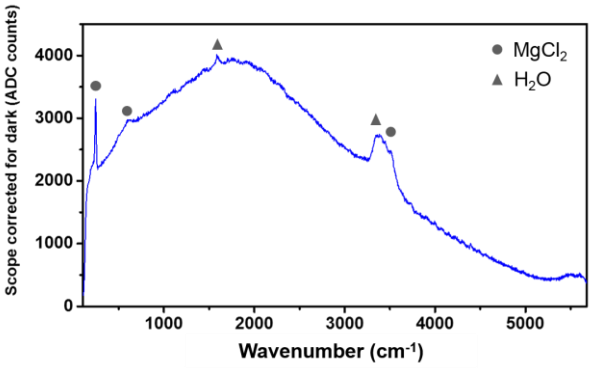

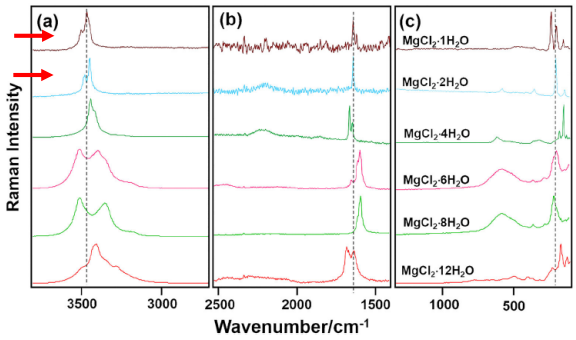

Figure 1-28.a. Raman spectrum of MgCl2 after 1day exposure to moisture at room temperature and atmospheric pressure. (● represents the MgCl2 peaks and ▲ represent the H2O peaks) Excitation Wavelength: 532 nm, Integration time: 2 sec, Averaging 10, and Current 4 A

Figure 1-28.b. The Raman spectra of magnesium chlorides with different hydration states in the range of 100-3,800 cm-1. Erbin Shi *et al*., J Raman Spectrosc. 1-14 (2019)

Some peaks indicated by grey circle, were observed and could be attributed to magnesium hydrates. The peak at around 3475 cm-1 Erbin Shi *et al* attributed to $MgCl_2 \cdot 1H_2O$ and $MgCl_2 \cdot 2H_2O$ as shown in **Figure 1-28.b**. **Figure 1-29.a.** shows the Raman spectrum of pure MgCl2 after exposed to moisture in the air for 2 days.

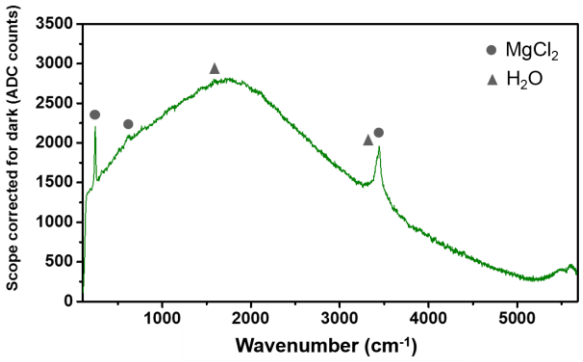

Figure 1-29.a. Raman spectrum of MgCl2 after 2-day exposed to moisture at room temperature and atmospheric pressure. (● represents the MgCl2 peaks and ▲ represent the H2O peaks). Excitation Wavelength: 532 nm, Integration time: 2 sec, Averaging 10, and Current 4 A

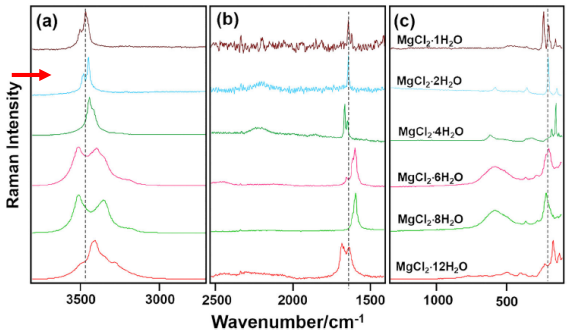

Figure 1-29.b. The Raman spectra of magnesium chlorides with different hydration states in the range of 100-3,800 cm^{-1}. Erbin Shi *et al*., J Raman Spectrosc. 1-14 (2019)

The intensity of peaks at around 3400 cm^{-1} and 1585 cm^{-1} slightly decreased. A shape of peak at around 3475 cm^{-1} changed as compared to 1-day exposure of $MgCl_2$. Now attributed to $MgCl_2 \cdot 4H_2O$.

As exposure time increased, the overall intensity of Raman signal decreased and the intensity of the peak corresponding to $MgCl_2$ decreased as shown in Figure 1.30. Magnesium chloride is very hygroscopic chemical so it can easily absorb moisture from the air. The absorbed water could attenuate the intrinsic property of magnesium chloride, resulting in the decreased intensity. The shape of peak at around 3400 cm-1 changed. Similar behavior is observed with solid KCl, MgC2–KCl before and after exposure to moisture from air at 25°C as is observed for $MgCl_2$ and discussed above. The effect of drying on is that water features disappear as shown in Figure 1-31. In **Figure 1-31.a.** the red, blue, green, orange, and pink lines were taken at 0, 10, 30, 50, and 70 minutes after starting drying process. During drying process at 200°C, two peaks for water were continuously decreased, but other peaks, for $MgCl_2$ and KCl, were well maintained. This entire set of experiments hydrating and dehydrating of MgCl2-KCl salt was repeated and was precisely reproduced. Table 1-6 is Raman peaks in $MgCl_2$ from the literature.

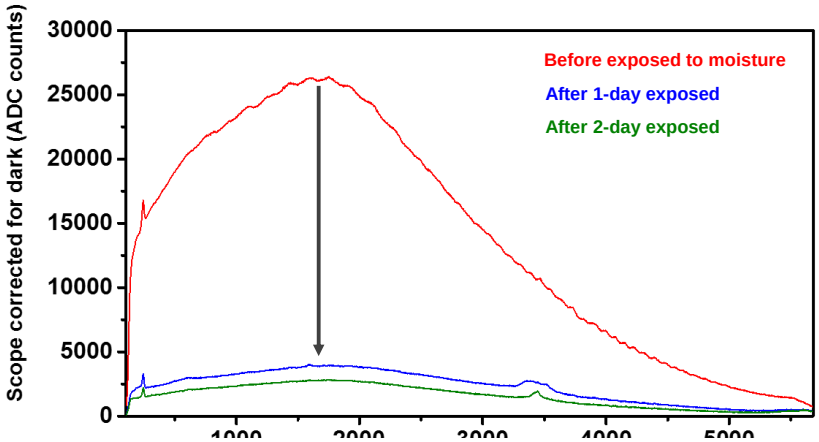

Figure 1-30. Comparison of Raman spectra of MgCl2 with various exposing time at room temperature and atmospheric pressure. (red line: before exposed to moisture, blue line: 1-day exposed, and green line: 2-day exposed) Excitation Wavelength: 532 nm, Integration time: 2 sec, Averaging 10, and Current 4 A

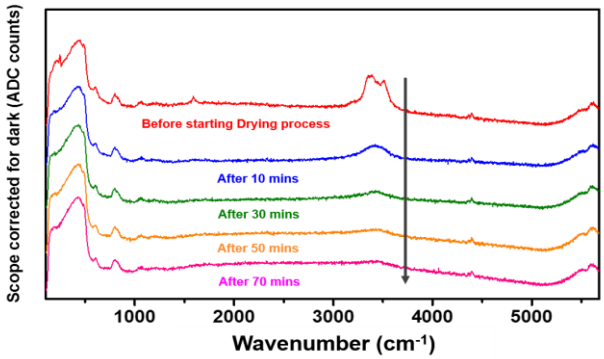

Figure 1-31.a. Raman spectra of 6-day exposed Mg-K (32:68 mole%) during drying process at 200˚C with sparging dry Argon at 240 sccm .Excitation Wavelength: 532 nm, Integration time: 4 sec, Averaging 10, and Current 4 A

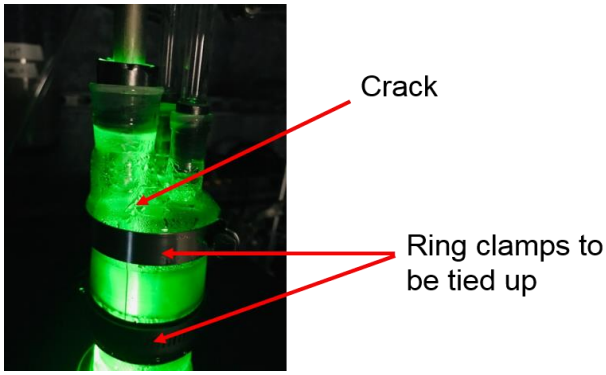

Figure 1-31.b. The cracked cell cap was tied up by ring clamps. Air can go through crack and provide moisture.

Table 1-6. Raman peak positions and the assignments of 6 magnesium chlorides from Erbin Shi *et al*., J Raman Spectrosc. 1-14 (2019)

Sample	H_2O mode										Mg-oxygen stretching		Lattice vibrations	
	Stretching		Bending		Librational		Bending + Rocking		Hydrogen bond					
	cm^{-1}	nm	cm^{-1}	nm	cm^{-1}	nm	cm^{-1}	nm	cm^{-1}	nm	cm^{-1}	nm	cm^{-1}	nm
$MgCl_2$ H_2O	3,247.5	643.1	1,610.4	581.6			2,327.9	607.2			472.8	545.7	119.2	525.4
	3,462.4	652.1	1,632.2	582.6							577.9	548.9	148.2	536.2
	3,502.7	653.8											194.6	537.6
													231.1	538.6
													290.9	540.4
													351.0	542.1
$MgCl_2$ $2H_2O$	3,211.8	641.6	1,632.9	582.6	792.6	555.4	2,328.6	607.2	610.0	549.8	480.1	545.9	133.5	535.8
	3,447.4	651.5									581.0	549.0	141.8	536.1
	3,482.7	653.0											197.5	537.7
													351.4	542.1
													405.1	543.7
$MgCl_2$ $4H_2O$	3,236.6	642.6	1,644.7	583.0	802.5	555.7	2,330.1	607.3	614.3	550.0	548.7	548.0	105.3	535.0
	3,280.2	644.5	1,661.6	583.6									121.2	535.5
	3,413.5	650.1											143.7	536.1
	3,443.4	651.3											173.1	536.9
													191.4	537.5
													215.5	538.2
													312.7	541.0
													358.8	542.4
$MgCl_2$ $6H_2O$	3,211.3	641.6	1,588.4	581.1	799.9	537.7	2,331.0	607.3	665.6	551.5	502.6	546.6	110.0	535.1
	3,353.7	647.5	1,606.6	581.7							589.6	549.2	136.3	535.9
	3,396.4	649.3	1,628.9	582.5									191.0	537.5
	3,434.7	650.9	1,644.3	583.0									216.8	538.2
	3,512.3	654.3											283.9	540.2
													362.0	542.5
$MgCl_2$ $8H_2O$	3,182.9	640.5	1,587.1	581.1	831.6	556.6	2,329.9	607.3			495.4	546.4	109.2	535.1
	3,350.2	647.4	1,606.2	581.7							587.1	549.2	133.3	535.8
	3,414.5	650.1											158.2	536.5
	3,511.5	654.2											189.5	537.4
													215.1	538.2
													279.8	540.0
													359.1	542.4
$MgCl_2$ $12H_2O$	3,228.8	642.3	1,629.5	582.5	773.2	554.8	2,329.4	607.3	678.7	551.9	495.4	546.4	119.8	535.4
	3,275.8	644.3	1,659.5	583.5							565.3	548.5	162.7	536.7
	3,357.1	647.5	1,677.0	584.1									191.8	537.5
	3,402.9	649.6											220.3	538.3
	3,426.5	650.6											243.9	539.0
	3,484.4	653.1											314.3	541.1
	3,516.4	654.4											364.9	542.5
													397.2	543.5

High temperature Raman probing of chloride salt

Figure 1-32-a and 1-32-b show Raman spectra of Mg-K (32:68 mole%) in the sealed cell measured at various times at *room temperature* and atmospheric pressure. When obtaining the Raman signal, the software automatically saves 10 scans. Last one plotted in order to stabilize the signal. In this preliminary test, shown in Figure 1-32-a and -b, there is a need to check when the signal stabilized. So scans were obtained every 30 minutes as shown in Figure 1-32-a. Peaks observed for $MgCl_2$ and a tiny peak for $H2_2O$ was observed. No peaks for KCl appeared. Even though the cell was completely sealed, with no Argon gas flow, the overall intensity of signal decreased. This behavior may be due to water on cell walls being absorbed by the salt. The intensity drop tapering off in time as shown in Fig. 1-32a.

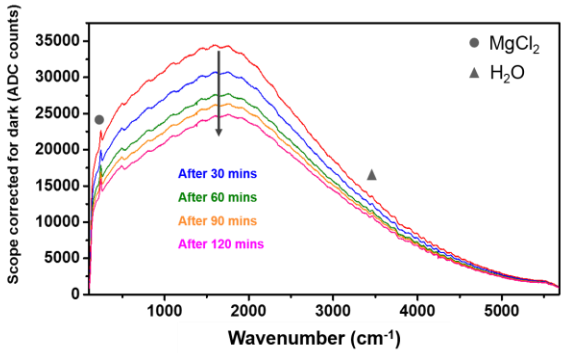

Figure 1-32-2a. Raman spectra of Mg-K (32:68 mole%) in the sealed cell measured at various times at *room temperature* and atmospheric pressure. Red, blue, green, orange, and pink lines were taken at 0, 30, 60, 90, and 120 mins after starting measurement, respectively. (● represents the MgCl2 peaks, ■ represents the KCl peaks, and ▲ represents the H2O peaks) Excitation Wavelength: 532 nm, Integration time: 4 sec, Averaging 10, and Current 4 A / Humidity 15%

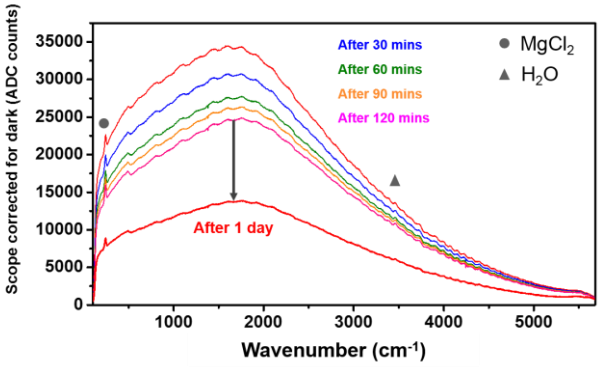

Figure 1-32-b. Raman spectra of Mg-K (32:68 mole%) in the sealed cell with various measured time at *room temperature* and atmospheric pressure. Red, blue, green, orange, pink, and bold red lines were taken at 0, 30, 60, 90, 120 mins, and 1 day after starting measurement, respectively. (● represents the MgCl2 peaks, ■ represents the KCl peaks, and ▲ represents the H2O peaks). Excitation Wavelength: 532 nm, Integration time: 4 sec, Averaging 10, and Current 4 A / Humidity 15%

Figure 1-32-b shows that after 1day, the peak intensity decreased. This is attributed to water on the cell walls being absorbed (desiccated) by the salt after 1 day.

Raman signals of MgCl2-KCl in the cell during Drying process (200°C)

Figure 1-33 shows the Raman spectra of MgCl2-KCl salt(32:68 mole%) in the cell during drying process for 1 hour *at 200˚C with* dry argon was blowing at 240 sccm The bold red line labelled “After 1day” shows the signal before starting drying process. Then, oven was set to 200°C and dry Ar gas was introduced. And the signal checked every 10 minutes for 1 hour. Arrow (1) shows the intensity was reduced when the temperature reached at 200°C. This was expected since the moisture in tubing line could come out with Ar flow and initially get adsorbed on the salt. After that, we could see that the strength Raman intensity gradually increased as seen by following arrows increasing in numerical order.

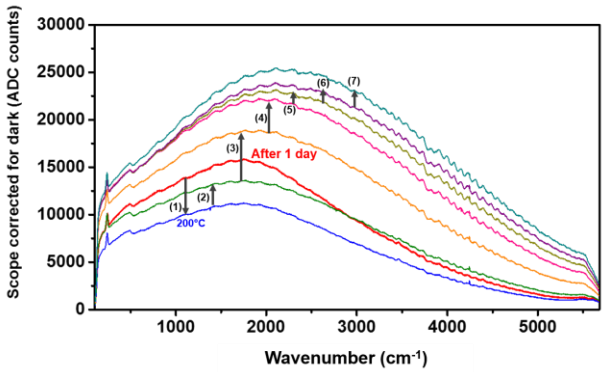

Figure 1-33. Raman spectra of Mg-K (32:68 mole%) in the cell during drying process for 1 hour *at 200˚C* The dry argon was sparged at 240 sccm. The numbers show timeline which has a 10-minute interval for each. Excitation Wavelength: 532 nm, Integration time: 4 sec, Averaging 10, and Current 4 A / Humidity 11%

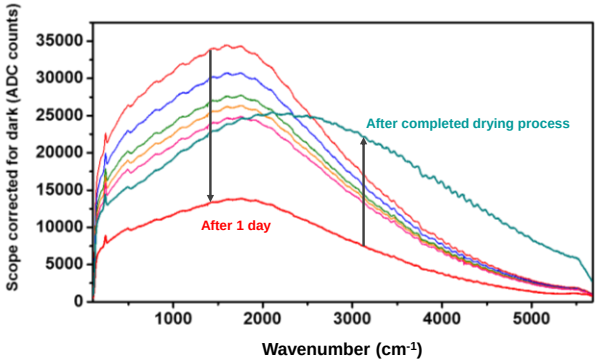

Figure 1-34. Raman spectra of Mg-K (32:68 mole%) in the cell from beginning to end of drying process for 1 hour at 200˚C The dry argon was sparged at 240 sccm. Black down arrow is decrease due to water in MgCl2-KCl salt. Black up arrow is increase due to water removed from MgCl2-KCl salt. Excitation Wavelength: 532 nm, Integration time: 4 sec, Averaging 10, and Current 4 A

The reason this increase in intensity happened is the loss of absorbed water during drying process. The Raman spectrum of dry MgCl2-KCl gradually recovered as the absorbed water was removed.

Figure 1-34 shows how the Raman signals to change from beginning to end of drying process. After drying process was completed, the Raman intensity was recovered to the initial level even though the overall shape was slightly changed. This the overall shape change could be new indicator of water.

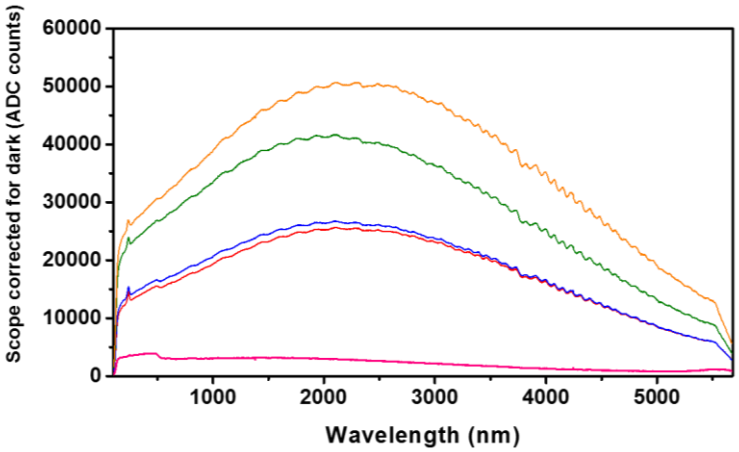

Figure 1-35. Raman spectra of Mg-K (32:68 mole%) in the cell during increasing temperature from 200 to 500˚C. The dry argon was sparged at 240 sccm. Red, blue, green, orange, and pink lines show that the temperature reached at 200, 300, 400, 500, and 550 °C, respectively. Excitation Wavelength: 532 nm, Integration time: 4 sec, Averaging 10, and Current 4 A / Humidity 11%

Figure 1-35 shows the Raman spectra of Mg-K (32:68 mole%) in the cell while increasing temperature from 200 to 500˚C with dry argon sparged at 240 sccm. Red line (1) shows the signal after 1 hour at 200˚C for completed drying process as shown by green line in Figure 1-33. Then, oven was set to 550°C and the signal checked when temperature reached 300, 400, 500, and 550°C. The Raman intensity continuously increased up to 500°C. Figure 1-36 shows a considerable amount of water was on the surface of the cell cap, yet no water signal was detected.

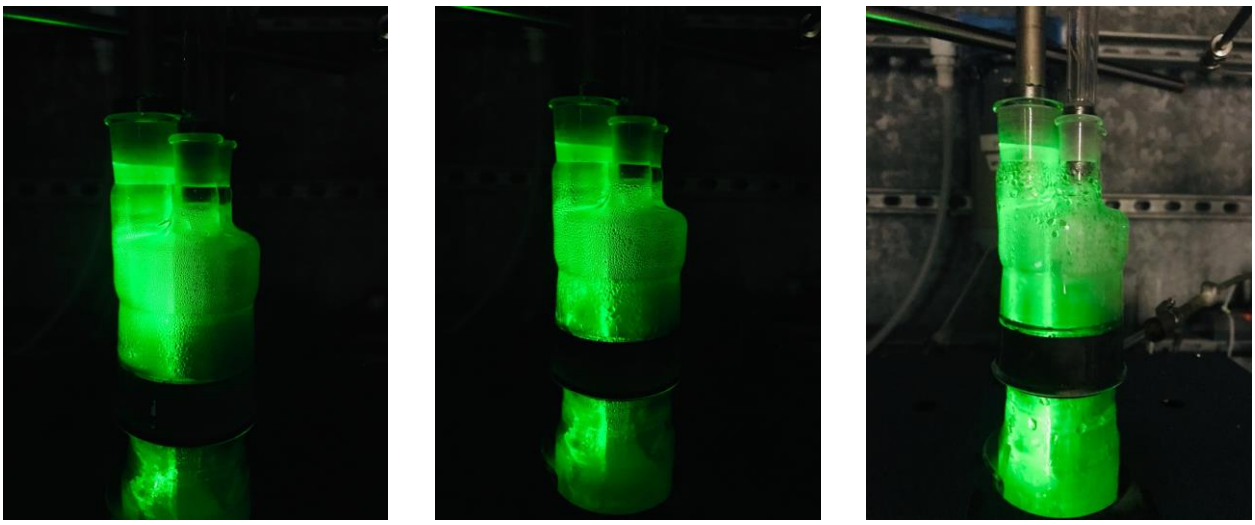

Figure 1-36. Pictures showing large amount of water accumulating on the cell cap with increased temperature.

Apparently, the reason intensity goes up is the loss of dipole bound and physisorbed water. After the salt melted at 550°C, the signal intensity dropped into the bottom. The molten salts had honey-like viscosity noted from the violent release of large bubbles found in viscous liquids.

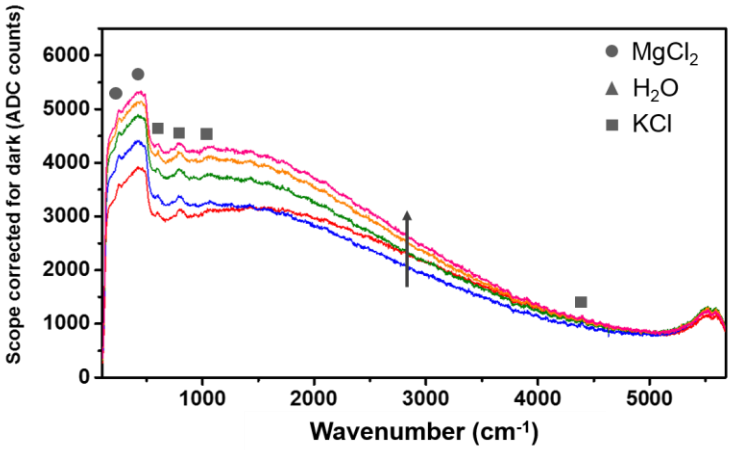

Figure 1-37. Raman spectra of Mg-K (32:68 mole%) during pretreatment process at 550˚C for 40 mins. Red (0), blue (10), green (20), orange (30), and pink (40) lines were taken at 0, 10, 20, 30, and 40 mins after starting pretreatment process, respectively. The dry argon was sparged at 240 sccm. Excitation Wavelength: 532 nm, Integration time: 4 sec, Averaging 10, and Current 4 A / Humidity 15%

Figure 1-37 is the Raman spectra of Mg-K (32:68 mole%) during pretreatment process at 550˚C for 40 mins
The salts amount was enough to immerse the quartz sheath in the molten salts. Then, oven was set to 550°C and dry Ar gas was introduced. The signal was checked every 10 minutes for 40 minutes. The Red line shows the signal after oven reached at 550°C. Peaks for MgCl2 and KCl observed even after MgCl2-KCl salt melted, but no peaks for water were observed. The intensity gradually increased for 40 minutes. Could be due to expansion of salt bringing greater contact to the probe or due to the loss of the dipole bound water.

Figure 1-38 is a picture showing the Raman probe is in contact with salt after it melts.

Figure 1.38. Picture showing that the Raman probe is in contact with the salt after it melts.

Overall conclusion about Raman probe in chloride salt

For the first time, we now have a Raman signature of molten salt with and without water at high and low temperatures. There is a challenge to see the oxidant peaks, e.g., specific OH stretches and vibrations, in the presence of thermal noise. This work was continued in a separate DOE funded SBIR program between the UA team with Sporian microsystems. The above discussion showed that only the broad baseline was changing in the presence versus absence of water. In our hands with the hardware provided, the background was all that could be seen in the presence of thermal noise; specific vibrational features could not be detected at high temperature (800°C).

Task 1.2: Electrochemical metal corrosion rate in molten chloride salt at 800°C

The corrosion rate of metal in molten salt was measured electrochemically shown in **Fig. 1.2-1 and 1.2-2**

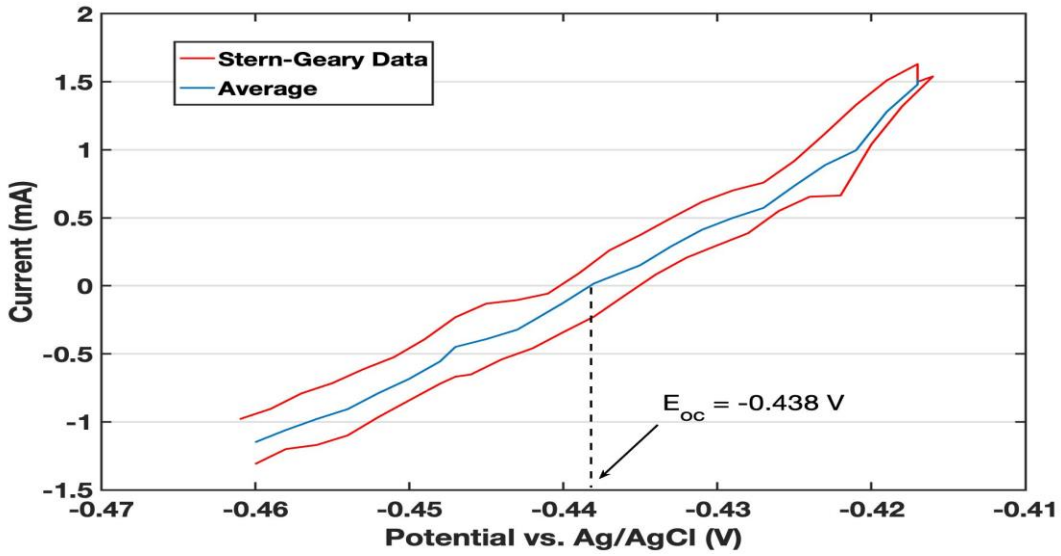

Figure 1.2-1. Potentiodynamic scan of H230 in NaCl-KCl molten salt equilibrated with air at 800°C. The potential was scanned from -30 mV to +30 mV from open circuit vs. SSE. Scan Rate= 0.1 mV $s^{-1.}$ The 1st positive going and the 2nd negative going are shown in red. The average of 2 scans shown in blue.

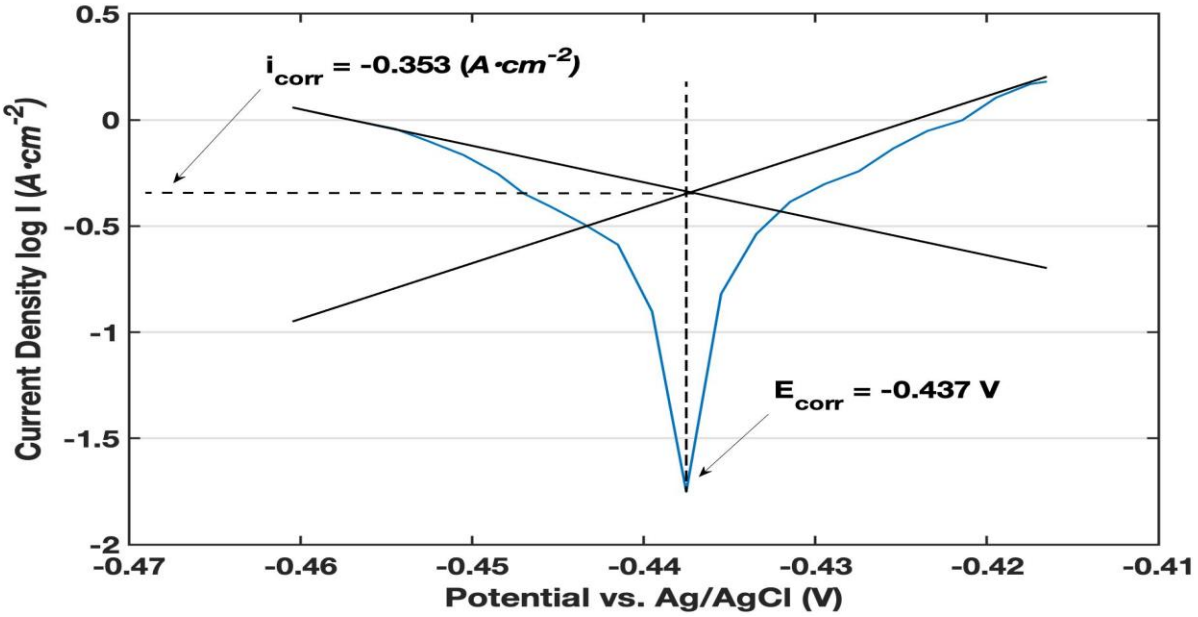

Figure 1.2-2. The potentiodynamic polarization scan of H230 in NaCl-KCl molten salt equilibrated with air at 800°C. The potential was scanned from -30 mV to +30 mV from open circuit -0.44V vs. SSE. The scan Rate= 0.1 mV s^{-1}. *This small signal polarization curve, often called a "Stern-Geary plot".*

This H230 corrosion rate in NaCl-KCl in air at 800°C is done by immersing a Haynes 230 WE electrode in salt equilibrated with air along with a H230 CE and an SSE RE. The current between the H230 WE and CE electrodes is recorded, as the potential is controlled, starting at -30 mV and ending at +30 mV versus the OCV measured to be -0.438 V vs. RE as indicated in **Fig**. **1.2-1**. The scan rate was 0.1 mV s^{-1}, and the OCV The top red scan in **Fig**. **1.2-1** is the positive-going first scan and the bottom red scan is the negative-going second scan. The hysteresis between these two red curves is due to electrode capacitance. To eliminate capacitive contribution to the curve, the 2 red scans are averaged to give the capacitance-free blue curve in **Fig 1.2-1**. The blue curve is then plotted as the base 10 log of the absolute value of average current versus H230 WE electrode potential. This transformed curve is shown in **Figure 1.2-2**. The perturbation to the system during a Stern-Geary plot is only 30 millivolts, so a nondestructive small perturbation of the metal in molten salt system which can be repeated many times. The blue curve in **Figs**. **1.2-1** is an excellent approximation to a steady state polarization curve for the metal corroding in air. The corrosion current is analyzed using first principles to find the corrosion rate (CR) of the H230 metal alloy in molten salt equilibrated with air. to be 722 microns/year. An EXCEL spreadsheet automates the calculation of corrosion rate when data like that in **Fig 1.2-1** is obtained. The CR is calculated using the equation,

$$CR = I_{corr} \cdot K \cdot EW \cdot \rho^{-1} A^{-1},$$

by inserting the values of I_{corr} and the parameters, below:

I_{corr} is corrosion current density in A cm^2 = -0.353 A cm^{-2}
K is a unit constant = 3272 mm A^{-1} cm^{-1} yr^{-1}
A is area in cm^2 = 7.86 cm^2
EW is equivalent weight in g eq^{-1} = 35 g eq^{-1}
ρ is density in g cm^{-2} = 8.97 g cm^{-2}

Task 2 Effectiveness of getters of oxidants

Problem Statement 2 – Getter and counter electrode development

A chemical metal getter of oxidants is an active metal , like Mg and Zr metal, that reduces the oxidant and forms metal ions. This sacrificial anode can directly interaction with oxidant as in **Fig. 2-1a** or be electrically connected to another metal and impress a highly negative potential on that metal and offer cathodic protection as shown in **Figure 2-1b and 2-1c**, below.

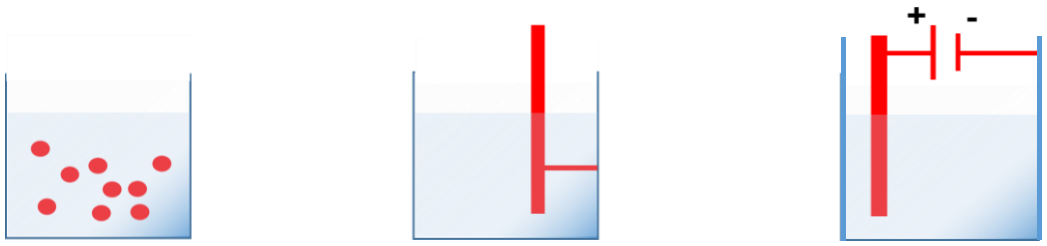

2-1a. Chips of metal in molten salt

201b. Wire between anode and cathode

2-1c. Impressed voltage source inserted between anode (counter electrode) and cathode (pipe)

Figure 2-1 Schematic diagram of experimental setup to determine effectiveness of 2a) chemical getter, 2b)sacrificial anode, and 2c) impressed negative voltage cathodic protection.

Prior Work: Monitoring exhaust gas during dehumifying of molten chloride salts

The dehumidification of molten NaCl-KCl-$ZnCl_2$, $MgCl_2$-KCl , NaCl-KCl and $MgCl_2$- NaCl-KCl has been done in a quartz cell containing a known amount of the molten salt bubbling Argon gas into the salt and measuring the outgas with gas sensors. The cell was placed in an oven and isothermally set at a desired temperature from 500 to 900˚C as shown in **Fig**. **2-2**. The overhead gas inlet and out are sealed such that

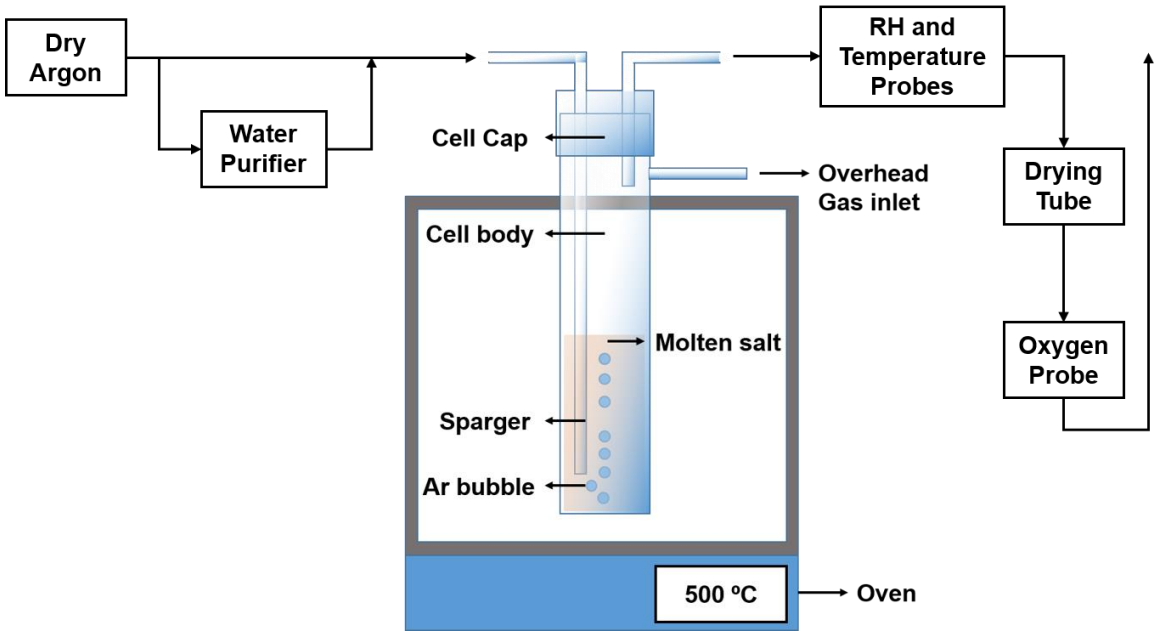

Figure 2-2. Schematic diagram of experimental setup for sparging Argon carrier gas into molten salt for in-situ sensing of oxidants (water, oxygen, etc.) in Argon carrier outgasing from the molten salt at high temperatures (up to 900˚C) to a manifold with gas sensors.

outgas exits from the top of the cell to a glass chamber manifold heated to around 110°C containing sensors to monitor H_2O and O_2 levels in ppm in time. The sensor for oxygen from air is measured in the Argon outgassing from the salt by a Teledyne GB-300 sensor. Although oxygen is a powerful oxidant , it comes out easily and quickly. **Proton derived from water from air is the most harmful oxidant to metal containers of molten chloride salt, because it is so difficult to remove from chloride salt.** Volatile water leaving the dehumifying salt goes out into the outgassing Argon whose RH is measured by a humidity sensor, a VAISALA HMT 337. Integrating the RH in time give the mass of volatile water in the mass of salt. Molten chloride salt is effectively deaerated by heating while sparging with dry argon gas flowing at ≥ 240 sccm. Prior to the monitoring RH the HMT337 probe is calibrated with the HMK15 humidity calibrator, a kit with dessicants over which the atmosphere has known RHs.

Dehumidification of NaCl-KCl-$ZnCl_2$

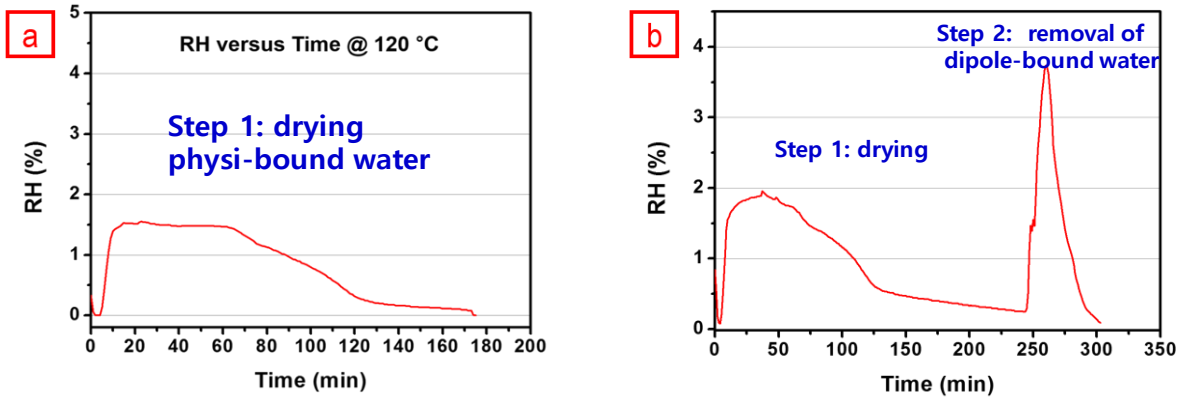

Figure 2-3. 2-step drying of 150 g NaCl-KCl-$ZnCl_2$ salt from 25 to 120 to 500˚C with Argon sparging at 240 sccm. Heating ramp rate 2°C min^{-1}. **a)** RH vs time of gas exiting at 120˚C for physibound surface water and **b)** RH vs time for the 2-steps at 120˚C and removal of dipole-bound water at 500˚C.

The dehumidification of NaCl-KCl-$ZnCl_2$ eutectic salt mixture was done in one step at 500˚C (data not shown). We found that if the salt was melted with high initial water concentration, the treatment time takes longer, requires more energy, and can exceed our expected time to remove corrosive water from the molten salt in metal. The 2-step dehumidification was faster and required less energy.The 2-step process consists of 1) a low temprature pre-dying process at 120˚C to minimize the physisorbed water on the salt surface before melting the salt followed by 2) sparging the argon into the molten salt at 500˚C. The measured RH shown in **Figure 2.3a** is the evaporation of the physisorbed water on the surface of the salt mixture. **Figure 2.3b** shows that once this pre-drying was done at 120°C, the Argon sparging pretreatment processing at 500 ˚C takes about 60 min. After the drying process, at 120 ˚C, there are no more physisorbed water molecules, only dipole bound water. The drying process at 120 ˚C effectively removes the absorbed water molecules on the surface of the salts, which leads to a reproducible 60 minute pretreatment process to remove dipole bound water from the salt at 500˚C for the Na-K-Zn ternary chloride. The 2 step process was used for other eutectic mixtures of chloride salts, such as Mg-K binary, Na-K-Mg ternary of different ratios, etc.

Calculation of water content in molten salt form outgas signals

Figure 2-3 shows the H_2O parts per million (ppm) curves for NaCl-KCl-$ZnCl_2$ salt mixture in time during the 2 step 1)drying and 2) pretreatment processes. This data allows calculation of the water in the salt by integrating the RH versus time curves.The water from test #1 and #2 are 1.936 and 1.258 g, respectively.

Sample #1 has more physisorbed water (1.360 g) than sample #2 (0.713 g) for the initial drying process at 120˚C. Both samples have nearly the same amount of dipole bound water (0.576 and 0.545 g, respectively) removed at 500 ˚C after drying at 120 ˚C. The pre-drying at 120 ˚C effectively removes the absorbed water molecules on the surface of the salts, which is a key factor for ensuring the reproducibility of the pretreatment process done at 500 ˚C. The water in all samples calculated by integration of outgas are given in Tables below.

Table 2.1 NaCl-KCl-$ZnCl_2$ water amount by the integration of Vaisala sensor readings

$NaCl + KCl + ZnCl_2$	Water amount from the integration of Vaisala signals		Total amount
	Pre-drying process (120˚C)	Pretreatment process (500˚C)	
Test 1	1.360 g	0.576 g	1.936 g
Test 2	0.713 g	0.545 g	1.258 g

Table 2.2 $MgCl_2$-KCl) water amount calculated by the integration of Vaisala sensor readings

$MgCl_2 + KCl$	Water amount from the integration of Vaisala signals		Total amount
	Pre-drying process	Pretreatment process	
Test 1	0 g (120˚C)	0.441 g (500˚C)	0.441 g
Test 2	0 g (120˚C)	0.613 g (500˚C)	0.613 g
Test 3	0 g (120˚C)	≈ 1.522 g (700˚C)	≈ 1.522 g
Test 4	0.152 g (200˚C)	Not conducted	Unknown
Test 5	0.302 g (250˚C)	Not conducted	Unknown
Test 6	0.273 g (300˚C)	Not conducted	Unknown
Test 7	0.501 g (350˚C)	Not conducted	Unknown

Table 2.3 NaCl-KCl water amount by the integration of Vaisala sensor readings

NaCl + KCl	Water amount from the integration of Vaisala signals		Total amount
	Pre-drying process	Pretreatment process (800˚C)	
Test 1	0 g (200˚C)	0.351 g	0.351 g
Test 2	0 g (200˚C)	0.313 g	0.313 g
Test 3	0 g (200˚C)	0.292 g	0.292 g
Test 4	0 g (200˚C)	0.259 g	0.259 g
Test 5	0.029 g (250˚C)	0.331 g	0.360 g
Test 6	0.024 g (250˚C)	0.330 g	0.354 g
Test 7	0.029 g (250˚C)	0.313 g	0.342 g
Test 8	0.021 g (250˚C)	0.304 g	0.325 g
Test 9	0.089 g (300˚C)	0.244 g	0.333 g
Test 10	0.088 g (300˚C)	0.207 g	0.295 g
Test 11	0.047 g (300˚C)	0.252 g	0.299 g
Test 12	0.033 g (300˚C)	0.267 g	0.300 g
Test 13	0.041 g (300˚C)	0.240 g	0.281 g
Test 14	0.085 g (300˚C)	0.205 g	0.290 g

Task 2: Effectiveness of Zr as chemical getter using head gas sensors of inlet and outlet gases

Fig. 2-1 showed water can be removed 3 ways: 2a) chemical getter, 2b)sacrificial anode, and 2c) impressed negative voltage cathodic protection. Doing 2a) with a Zr gives water removal due to the reaction of Zr metal with water, $Zr^{o} + 2\,H_2O \rightarrow Zr^{IV}O_2 + 2\,H_2$, All 3 ways give electrons to the protons on water, reducing the protons to molecular hydrogen. So sparging Argon into molten salt treated any of these three ways should generate hydrogen in the Argon carrier gas, if these treatments are effective. **Fig**. **2-4** shows the set up for measuring hydrogen in the Argon carrier gas.

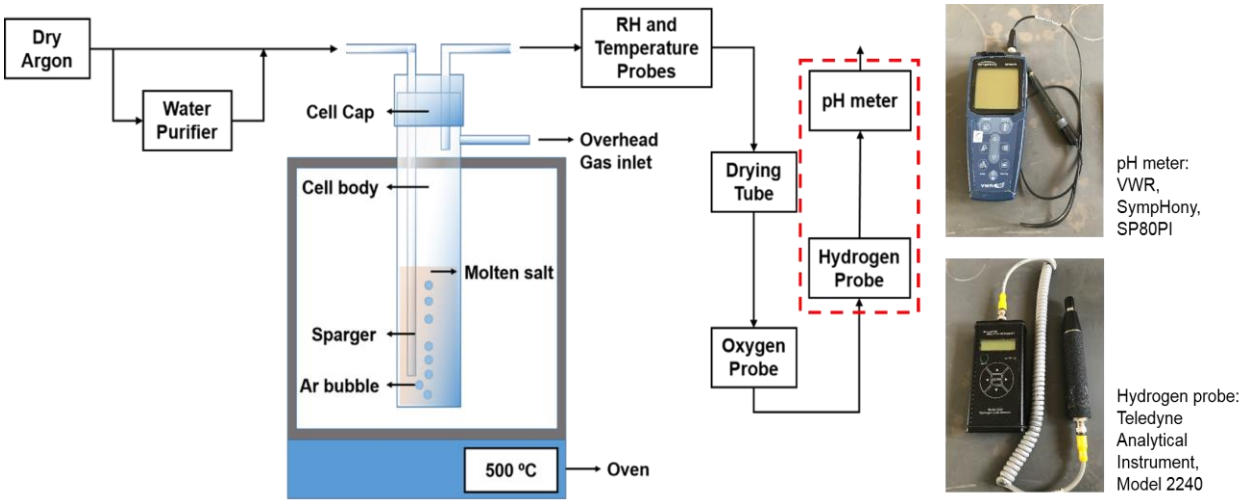

Figure 2-4. Schematic diagram of setup with added hydrogen probe and pH meter to record the hydrogen and acid content in the outgassing Argon.

Figure 2-4 shows the schmatic diagram of the setup for monitoring Argon outgas modified by adding a hydrogen probe and a pH meter in 1 liter of water at the end of the gas stream to determine the time dependence of the hydrogen and acid in the outgas. This new setup in **Fig. 2-4** gives information about formation of corrosive gas like HCl and hydrogen from reduction of proton on water when a getter is added to molten salt. The Argon outlet tube is connected to a glass chamber fitted with a VAISALA HMT 337 humidity probe and thermocouple, then a drying tube of DRIERITE, a Teledyne Analytical Instrument, model 2240 hydrogen sensor, a Teledyne GB-300 oxygen probe, and a VWR, SympHony SP80PI pH meter in 1 liter of DI water is the last place the sparge gas goes for all sensors all connected in series. The exit tube and the RH relative humidity (RH) probe chamber are heated around 115˚C to prevent the water condensation. The DRIERITE drying tube is used to remove any water before outlet gas reached the hydrogen and oxygen sensor to protect and increase accuracy of these sensors. The hydrogen sensor is shown in **Figure 2-5.** Hydrogen readings are displayed on the controller LCD and the probe tip LED bar graph array.The upper line of the controller LCD indicates a numerical value or range for the percent hydrogen concentration or peak hydrogen value. The lower line is used to display the hydrogen meter, a logarithmic bar graph ranging from 0.001 % (10 ppm) to 100 % hydrogen by volume. An open box on the bar indicates the last peak value obtained and a filled boxed indicates the current value. The right side of **Figure 2-5** describes how to interpret the hydrogen meter. The probe tip LED indicator shows an increase or decrease in hydrogen concentration. The number of yellow LEDs lit in the probe LED bar graph array can indicate detected hydrogen concentration in four ranges.

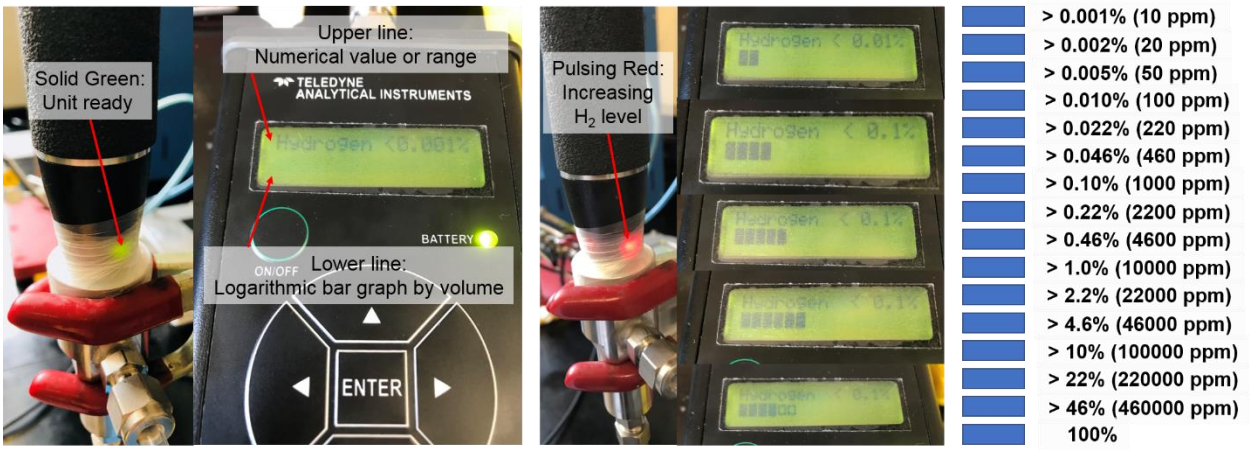

Figure 2-5. Pictures of the hydrogen sensor showing how the instrument detects and reports the hydrogen concentration near the probe tip.

Hydrogen sensing test in $MgCl_2$-KCl and NaCl-KCl

Prior to do the Zr getter experiment, we checked the open current voltage (OCV) of the Zr metal, which was around -1.2 V (vs. Ag/AgCl) (Figure 2-6) which is a good value in NaCl-KCl as well as. $MgCl_2$-KCl since Mg and Na ions have more negative reduction potentials than Zr ions.

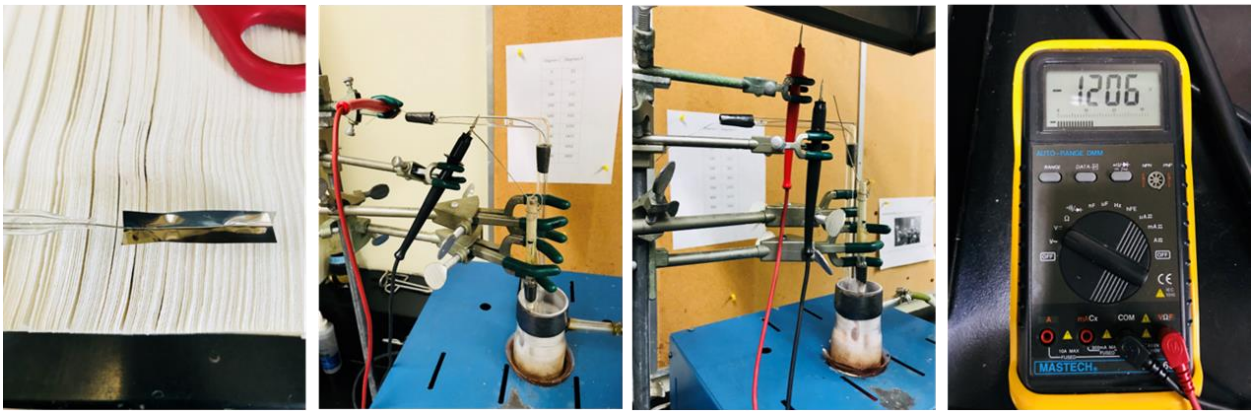

Figure 2-6. OCV of Zr getter versus Ag/AgCl in $MgCl_2$-KCl molten salt.

Hyderogen sensing test of NaCl-KCl

The hydrogen sensing test with Zr getter of two different NaCl-KCl samples was also conducted under the same experimental conditions used for the dehumidifying tests. As shown in **Figure 2-7**, the dehumidigying process was successfully completed for both test #1 and #2. Also, the hydrogen sensing curves showed very similar behavior. However, when we put the Zr getter into the cell after the pretreatment process, the hydrogen concentration was not changed in the test #1 (**Figure 2-7(left)**). In contrast, test #2 showed the hydrogen concentration was slightly increase from 5 to 6 bar for a while, and then droped to the 5 bar (baseline we assumed) (**Figure 2-7(right)**). To further elucidate the effect of the Zr geter on the hydrogen generation, we remeasured the hydrogen concentration (**Figure 2.8**). Additionally, we introduced the wet Argon gas into the molten salts when there was no water to check whether a steady state of H_2 shows up on the H_2 sensor or not. In this experiment, we kept running the humidity sensor to confirm the introduction of the wet Argon. When we put the Zr getter into the molten salts after the dehumidifying process, there

was no change of the hydrogen concentration. Moreover, although we introduced the wet Argon gas for 10 miniutes in the salts, there was nothing to be changed.

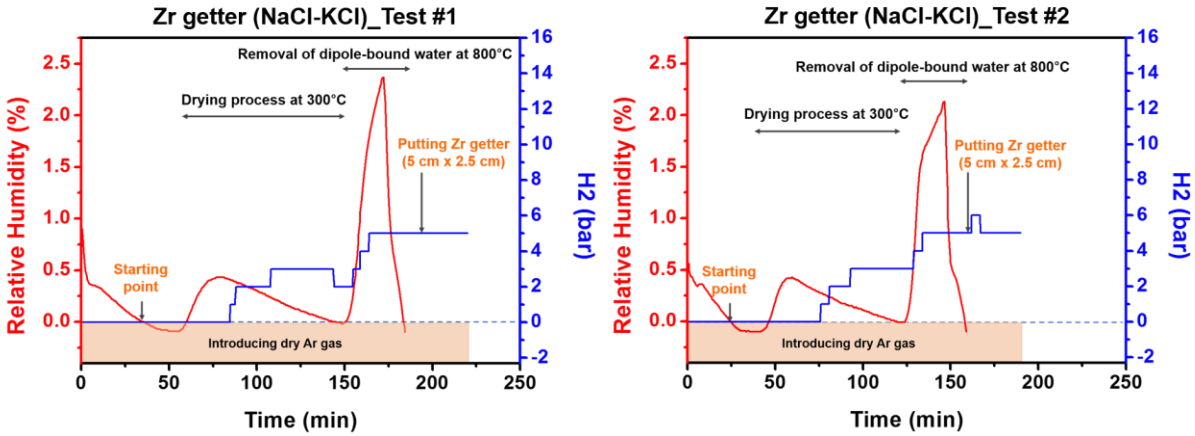

Figure 2.7. H_2O and H_2 versus time of exiting gas during and after treatment process of NaCl-KCl. The drying process was conducted at 300 °C. The pretreatment process were conducted at 800°C. The salt mixture was sparged with dry Argon at 240 sccm.

After that, the dry Argon was circulated to make the steady state for 10 minitues. Then, we reintroduced the wet Argon for 20 minutes, but there was no change as well. However, as the dry Argon gas was being introduced, the hydrogen concentration was increased from 5 (220 ppm) to 6 bar (460 ppm), maintained for about 15 mins, and then droped to 5 bar (220 ppm). To verify this behavior occurred by the wet Argon, we did this process again, and saw the very similar behavior happened

.

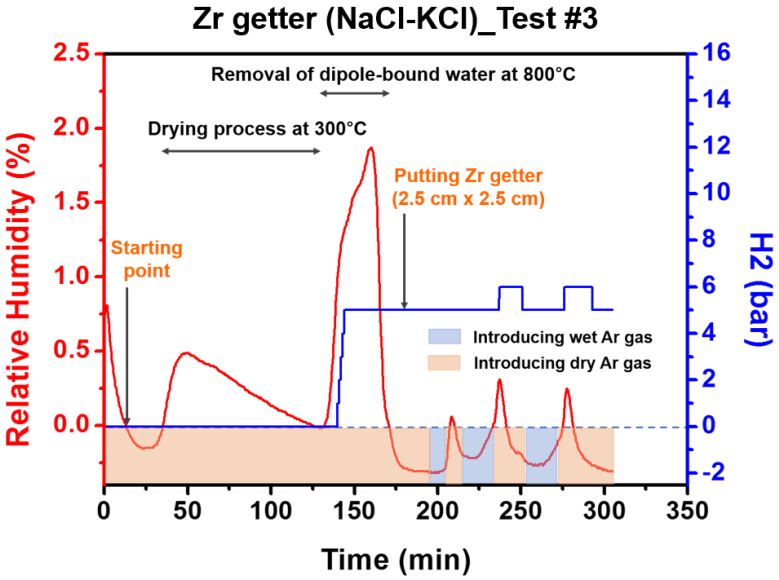

Figure 2-8. H_2O and H_2 versus time of exiting gas during and after treatment process of NaCl-KCl. The drying process was conducted at 300 °C. The pretreatment process were conducted at 800°C. The salt mixture was sparged with dry and wet Argon at 240 sccm.

The reason why the hydrogen concentration was changed during introduing the dry Argon gas, not the wet Argon gas as followed; 1) the water molecule could adhere to the completely dried tubing line so the

moisture could not be effectively carrying to the molten salt. 2) the introducing time was not enough to reach at the molten salts. The humidity sensor seemed to misread the humidity values showing too low under 0%. The RH curve, the water level rapidly inreased when we introduce the dry argon. Based on the above result, we conformed that the hydrogen was generated from reacting Zr metal with H_2O in the molten salt. This implies that the Zr getter could be a promising way to remove oxidants from molten salt.

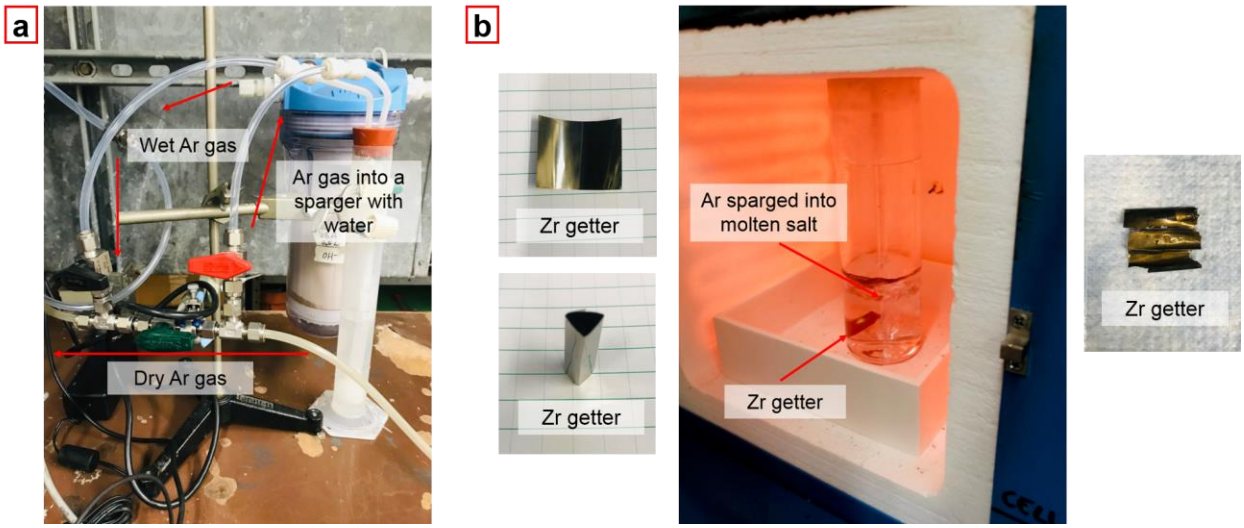

Figure 2-9. a) sparging line to introduce wet Argon gas and b) Zr getter before and after the experiment.

Figure 2-9 a) shows the sparging line. The Zr getter sheet is folded so it can easily put into the cell as shown **Figure 2-9 b).** After the experiment, the Zr getter maintained its own shape well.

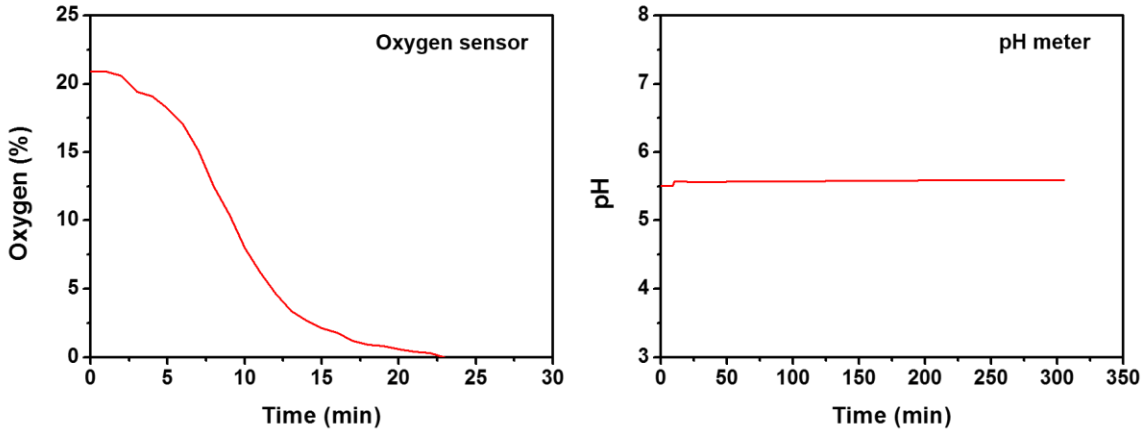

Figure 2-10. Percent of Oxygen exiting gas during and pH value during the treatment of NaCl-KCl.

Percent of oxygen exiting carrier gas during treatment of NaCl-KCl was measured as shown in **Figure 2.18**. This result shows that oxygen molecule can be removed within 25 minutes before starting the dehumidifying process. The pH barely changed over the entire process.

As performed the hydrogen sensing test with Zr getter, it is not clear the reason why the hydrogen concentration increased during the drying process at the relatively low temperature A black colored

residues is found at the bottom of the cell even after washing and may be insoluble Zr metal. A Zr getter experiment was done with a new cell body (**Figure 2.11 b)**). The blue line (**Figure 2.11)**) during the drying process did not changed and indicated that the hydrogen was not generated. Based on the above result, these residues which accumulated in old cells is Zr metal pieces, which generated the hydrogen by reacting when physisorbed water molecule desorbed from solid salt at 120C during the drying process.

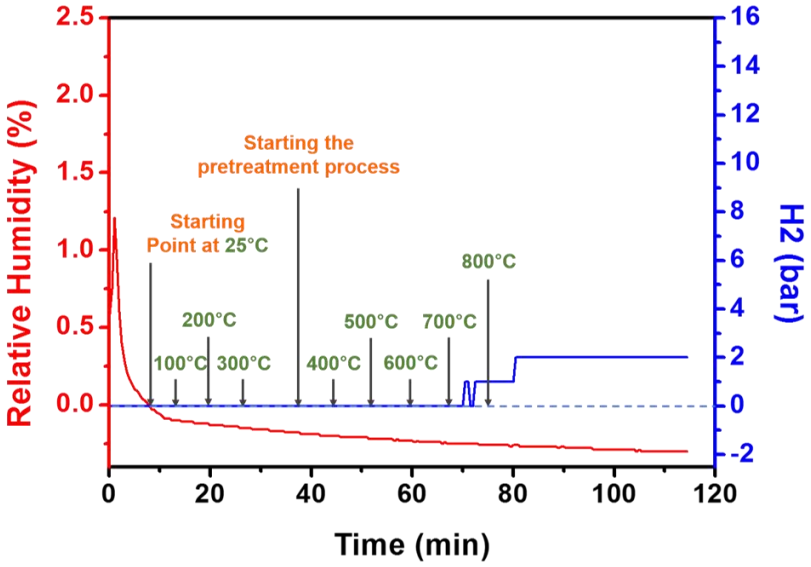

(a)

(b)

Figure 2-11. H_2O and H_2 versus time of exiting gas from the cell filled with alumina oxide balls (2 mm). The drying and pretreatment processes were conducted at 300 for 10 mins and 800°C for 30 mins, respectively. The salt mixture was sparged with dry Argon at 240 sccm.

It was observed that a metal with a high negative reduction potential (refractory Zr and Cr and none refractory Mg) directly in salt solution or shorted to the interior of the pipe metal can reduce proton on protic species, e.g., proton on H^+Cl^- , $MgOH^+$ Cl^- or water; $MgOH^+$ Cl^- is an aggressive non-volatile oxidant when in molten chloride salt. No further work is needed here to show this getter effect in more detail. Clearly, immersed or shorted Zr, Cr and Mg getter metals remove proton no matter what its form is (proton on H^+Cl^- , $MgOH^+$ Cl^- or water) but these getter give no signal for detecting the leaking of oxidant into the molten salt, e.g., when there is a hole in the pipe. *For detecting oxidant leaking the molten salt, an active cathodic protection system with a power supply is needed*. The anode for the power supply should be a refractory metal with highly negative reduction potential, like Cr, or ductile high Cr alloy, like nichrome. The benefit of using Cr is that, as long as the Cr rod is present, the oxidation product is chrome ion and not molecular chlorine (Cl_2) an aggressive oxidant that must be avoided. Task2 on getters is 100% completed; no further work need be done to alleviate the cost overrun of year 1. The effect of getters indirectly continued while working on counter electrodes in tasks 3 and 4 on cathodic protection and the reduction potential of pure metals in molten chloride salt.

Task 3.0. Cathodic protection (CP) of metal in molten chloride salt at 800C

Problem Statement 3 – Cathodic protection (CP) of metal in molten salts. CP stabilizes the metallic state of structural metal by imposing a cathodic potential on the metal surface. CP is done 2 ways: 1) by shorting the metal to be protected (cathode) to a sacrificial anode, or 2) by impressing a negative potential on the metal to be protected (cathode) by a power supply, For 2) a power supply is inserted between the metal (cathode) to be protected and a sacrifical anode. Both work, but the first gives no signal of danger while the second gives a reduction current, which is signal of dangerous corrosive conditions.

And with a power supply, the protective reducing power can be raised as desired by raising the voltage. For metal containers of molten chloride salt, the cathodic protection is impressed on the metal surface on *INSIDE* of metal containing molten salt by making this surface a cathode. A power supply applies an overpotential (η, a potential more negative than the open circuit votage of the metal in anaerobic molten salt). From first principles, it is expected that a η of 100 mV to 200 mV should suffice to maintain the metallic state od the *INSIDE* surface, if there is good potential distribution along the inside surface. Since molten salt is very ionically conductive then the potential distribution is uniform and this persists for many meters. Since the presence of oxidants shift the surface potential to values more positive of anaerobic open circuit, then biasing the metal negative of the open circuit potential in the absence of oxidants give reducing power to keep the metal in the metallic state when oxidant is introduced.

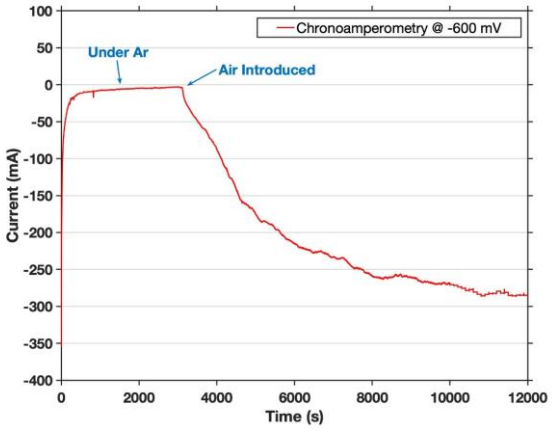

Figure 1-12. Chronoamperometry (i vs t at const E) of H230 coupon in molten NaCl-KCl molten salt. A = 8 cm^2. E set at -600mV vs SSE which is -100 mV versus open circuit (OCV = -500mV vs SSE). T= 800^{o}C. System was held under argon for 1hr followed by air for 2.5 hr.

These above design rules are first steps. The actual cathodic protection regimen uses first principles as a starting point and the actual optimal cathodic protection potential are small perturbations best found quickly by trial and error. This is done by applying cathodic potential for a time, introducing oxidant and analyzing the metal surface for corrosion by weight loss and using electron microscopy (SEM) and energy dispersive spectroscopy (EDS).

Cathodic protection in a pipe is experimentally modeled in a the quartz cell cell. Such a result is shown in **Fig**. **1-12.** Recall, the molten NaCl-KCl salt was equilibrated with Argon at 800^{o}C to create an inert atmosphere, similar to that inside a pipe. The OCV (E_{oc} also called E_{corr}) of the Haynes 230 working electrode (WE) immersed in molten salt in the quartz cell is just like the metal surface inside a pipe containing molten salt. It was found that the E_{oc} of this H230 WE in anaerobic salt is -500 mV. When the potential of this H230 metal is set to -600 mV vs Ag/AgCl reference electrode (RE), that is, overpotential (η) is set -100 mV vs. E_{corr}, this negative (cathodic) overpotential (η) reduces residual oxidants (water, oxygen) from salt solution and keeps the metal surface in the metallic state.

When reduction current on the H230 WE at -600 mV vs goes from -50 mA to 0 mA in anaerobic molten salt, depletion of oxidants is complete near the H230 surface. Then, air blown over the molten salt simulates a leak in the pipe metal. Air generated a large negative current leveling off to -280 mA which is the warning signal of an air leak giving a high concentration of oxidants inside the CSP system. The steady state reduction current is correlated to oxidant concentration in the molten salt using the Cottrell equation, which well models the behavior shown in **Fig**. **1-12**.

Task 3.1 Anode materials for CP and e*x-situ* EDS detection of corrosion of cathode and anode

The surfaces of the H230 WE and H230 CE in the aerated cell have been analyzed using energy dispersive spectroscopy (EDS) after the H230 WE potential was set to -600mV vs SSE to see if setting the H230 WE to a potential of -600mV vs SSE does iin fact cathodically protect the H230 WE relative to the H230 CE.

Choosing a counter electrode (anode) material to place INSIDE a pipe influences how negative the potential of the surface of the metal INSIDE the pipe can be biased during cathodic protection to arrest metal oxidation (corrosion) of the metal surface, that is, maintain the metallic state of the surface INSIDE the pipe. If a getter metal, like Mg or Zr, is used as the anode, then the potential of the WE set by the power supply is the same or more negative than the reduction potential of getter metal. When changing anodes, EDS gives a sensitive measure of composition of an alloy surface. Depletion of metals on the surface tells if any element ionized (corroded).

The EDS cross section was performed on the H230 cathode (WE) and H230 anode (CE) used during the chronamperometry experiment shown in **Fig**. **1-12**. These Haynes 230 alloy samples were analyzed using HITACHI S-4800 SEM/EDS at the University of Arizona Kuiper imaging facility.

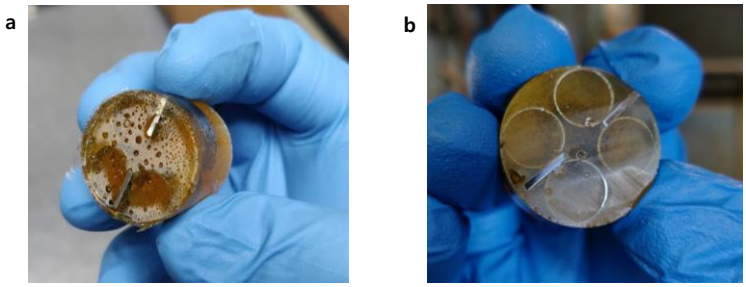

Figure 3-1. Working and Counter electrode samples from the cathodic protection experiment **a)** before final surface finishing and **b)** after final grind with 1200 grinding paper.

The WE metal was cathodically protected for 12 hours while the CE was the sacrificial metal. During this test, both metals are immersed in a 225g of 50 mol%NaCl-50mol%KCl salt at 800°C. The atmosphere initially is dry Argon, then the salt is exposed to air for 12 hours as shown in **Fig**. **1-12** For EDS analysis, the anode and the cathode are removed from the cell and cut in half. Cross sectioned metal samples are mounted in epoxy as shown in **Fig**. **3-2a,** then ground using a Pace NANO 2000T double wheel grinder polisher bench top polisher with water as cutting fluid successively using 320, 600 and then 1200 silicon carbide grinding papers to obtain a smooth metal surface. Before and after salt exposure during CP, the polished sampled were observed by SEM /EDS. Images of the Hayes 230 working and counter electrodes, shown in **Fig. 3-3**.

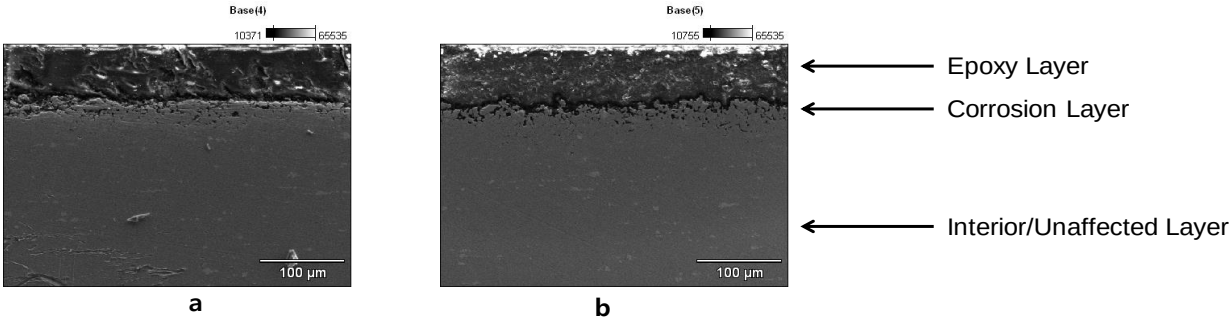

Figure 3-2. SEM of cross section of the a) WORKING Electrode compared to b) COUNTER Electrode

Figure 3-2b shows the cross section of the anode counter electrode surface (labeled corrosion layer in **Fig**. **3b**) looks rougher than the surface of the working electrode. This is evidence that after 12 hours in molten salt in air, the H230 counter electrode suffered more corrosion than the H230 working electrode that was

being held at -600 mV vs SSE. These observations show the WE held at -600 mV is cathodically protected from corrosion while the counter electrode was sacrificed. EDS images can map the spatial distribution of the different elements in the alloy as a very sensitive indication of corrosion. When a metal corrodes, the least noble elements leave the surface first. Therefore, depletion of elements gives a clear indication of their corrosion. Fig. 3-3 shows the EDS mapping of copper, a noble component in the H230 alloy, and chromium, a non-noble component, to see if these metals corroded from the counter electrode.

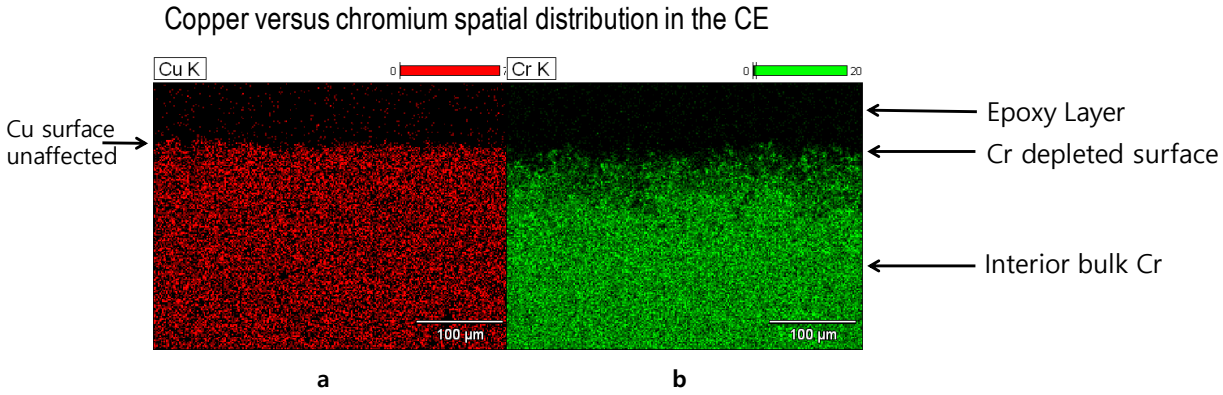

Figure 3-3. EDS of the H230 counter electrode comparing **a)** Cu in alloy, that does not get as affected by oxidants as **b)** Cr in alloy, that oxidized and more depleted from the surface.

Fig. 3-3 shows uniform distribution of the more noble copper through the entire cross section, and the noticeable depletion of the less noble chromiun, from the surface. Thisis a clear indication that the WE is protected and the CE corrodes during CP. **Table 3-1** shows EDS analysis telling the relative stability of the WE and CE evaluated by comparing the Cr content on the surface of the H230 working electrode, under cathodic protection and the H230 CE electrode, the sacrificial anode..

Table 3-1: Chromium peak intensity near the surface of the working and counter electrodes during cathodic protection of the working electrode at -600 mV vs SSE for 12 h in NaCl-KCl in air at 800°C.

WE

14:37:29
Filter Fit Chi-squared value: 1026.532 Errors:+/-1 Sigma
Correction Method: Proza (Phi-Rho-Z)
Acc.Voltage: 15.0 kV Take Off Angle: 34.1 deg

Element	Element Wt.%	Wt.% Error	Atom %	Atom % Error
Cr	36.55	±0.24	13.21	±0.09

CE

14:48:37
Filter Fit Chi-squared value: 1613.657 Errors:+/-1 Sigma
Correction Method: Proza (Phi-Rho-Z)
Acc.Voltage: 15.0 kV Take Off Angle: 34.1 deg

Element	Element Wt.%	Wt.% Error	Atom %	Atom % Error
Cr	26.83	±0.16	12.46	±0.07

Table 3-1 shows there is a noticeable difference between the WE with a stronger Cr content (36.55%) than the CE with a lower chromium content (26.83%), which indicates that more of the Cr in the CE surface was oxidized relative to the WE. Clearly, SEM/EDS analysis shows during corrosion of H230, the first element to oxidize is chromium. A power supply applying CP requires a counter-electrode. A polarizable counter electrode will experience potentials more and more positive of the potential for chloride oxidation to molecular chlorine as more and more cathodic potentials are applied to the cathode. Chlorine is an

aggressive oxidant. Forming chlorine during cathodic protection is counter-productive. To prevent forming chlorine during CP, a non-polarizable anode, like chromium metal is ideal. The anode potential is the chromium reduction potential, roughly -0.7V vs NHE or approximately -0.9 V vs SSE in water, a first guide to the reduction potential in molten salt. Finding the reduction potential of Cr in molten salt is Task 4. The cathode potential supplied by the power supply is equal to or more negative as the potential of the anode, which guarantees the cathode stay metallic. Another good feature of using a getter metal like Cr as the anode is that the chrome anode deposits chrome ions in molten chloride salt solution during CP which further inhibits chrome loss from H230 by shifting the equilibrium as CP proceeds. However, pure chromium is expensive and also brittle. This limits manufacturable dimensions and increases costs. A pure chrome plate manufactured 0.125 x 0.125 x 10 inches costs $465 from Fine Metals Corporation. A pure chrome rod that is 5.0 mm dia. x 100 mm length from Sigma Aldrich costs $2,310. The brittle nature of chrome limits plate thickness and rod diameter to be 0.125 inches, with maximum lengths of 4" (rod) and 24" (plate), and does not allow the manufacture of wire. A project goal is to help find new methods and materials to reduce costs of operation and maintenance in CSP plants. Although using a pure chromium anode might work, but it would difficult and costly, because Cr metal rods are costly and lack needed mechanical proprieties. A Cr rich alloy like nichrome is cheaper and has good mechanical properties. Cathodic protection with pure chromium and nichrome anodes have been done to guide the best anode selection, as described below.

Haynes 230 alloy rods are prepared as described in Task 1. Pure chromium metal, dimensions 0.125in x 0.125in x 10in (99.9%), is purchased from Fine Metals Corporation (Ashland, VA). A test coupon is held in a male joint with Ceramond to make gas-tight seal. To create a continuous electrical connection with the Cr, the potentiostat was connected via a 0.5 mm dia. nickel wire (99.95%, Fisher Scientific) soldered to the exposed Cr above the joint. Cr wire cannot be spot welded. The Cr rod is not sanded due to its brittle nature, but is rinsed with DI water and ethanol before being placed inside the cell. The salt mixture is Na-K-Mg-Cl ternary eutectic (29.4wt%NaCl, 25.8%KCl, 44.7%$MgCl_2$) as described in Task 1. 200g of salt is used to fill a short cell required because Cr is NOT available in long rods. The volume of the solid salt mixture is significantly larger than the volume of the liquid salt, therefore it must be added in increments to the short cell and melted. Initially, 2/3 of the salt is melted inside of the cell at 425˚C with Argon blowing above the salt at 240 sccm. After the salt is fully melted, the cap is briefly removed and the rest of the salt is added. The Ag/AgCl reference electrode, Mg ribbon (when the salt is to be dried with Mg), and the gas-bubbling tube is inserted once all of the salt is melted. Then, the Argon gas is switched from blowing over the salt to sparging into the salt at 240 sccm. For Mg drying, the temperature is 650˚C for 24hr after removing the Mg, the temperature is increased to 800˚C.

Experiment 1, Passive Cathodic Protection: sacrificial anode shorted to cathode

Passive cathodic protection is done by electrically shorting a less noble sacrificial anode, like Cr, to a metal cathode, like H230. Electrodes are placed in salt dried with Mg, and the atmosphere is dry Argon gas. The gas is blowing over the salt while the electrodes are in the cell. The anode corrodes before the cathode. The electrons released from the anode go to the cathode to maintain the metallic state of the cathode.

A pure Cr CE (anode) is shorted to an H230 WE (cathode), and both are connected to an SSE RE. A potentiostat is used to monitor the open circuit potential of the electrodes in time. Two different H230 WE were studied; each immersed for 23 hours and shorted to Cr for 22 hr. Haynes 1 is inserted first. Immediately after the first electrodes are removed, Argon gas is sparged in the salt for 45 min to remove any oxidants. Then, in the same salt, a new Haynes 230 electrode (Haynes 2) was placed, and the same Cr electrode was placed after it had been cleaned with DI and EtOH. There was no visible

salt or impurities on the Cr electrode when it was placed. The new Haynes was cathodically protected for a total of 22 hr and immersed for 23 hr.
Fig. 3-4.shows the OCP with respect to SSE of each H230 WE recorded while H230 is passively protected by a Cr anode for 22 hr

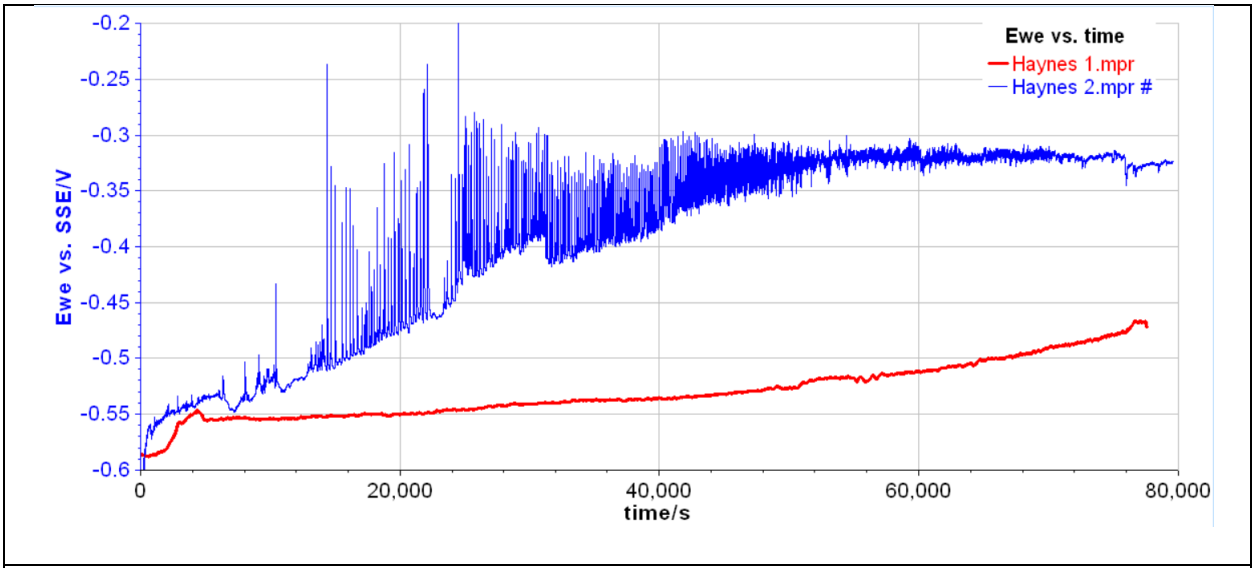

Figure 3-4. The potential of Haynes 230 versus time (over 22 hours) shorted to a Cr CE in molten ternary $MgCl_2$-NaCl-KCl eutectic salt at 800˚C. Salt was dried using Mg under a dry Argon atmosphere at 650ºC. The OCP of Haynes 2 was recorded in the same salt following the removal of Haynes 1 using the same CE, cleaned and weighed between experiments.

The extent of corrosion of the Haynes 230 WE is determined both gravimetrically and electrochemically by small-window cyclic voltammetry and Stern-Geary analysis. Potentiometric scans are conducted once the open circuit potential (OCP) of the system is at equilibrium, defined as when the change in potential is less than 1 mV/hr.
The OCP of Haynes 1 equilibrated at -0.587 V after approximately 15 minutes. A potentiodynamic scan was conducted ±30 mV around OCP, first scanning negative, then positive past OCP. A Stern-Geary plot is generated from this data (Fig. 3-5). Using the equation referenced in Task 1, the CR is calculated from the corrosion current i_{corr} of -1.24 $mAcm^{-2}$ and found to be 534 µm/yr. The CR was calculated for each cycle (n=4), and the values of those were averaged for a final CR of 439 ± 119µm/yr. When compared to the CR calculated for H230 in Mg dried salt under dry Ar in task 1 (145 ±101µm/yr). This difference in CR is outside the standard deviation.
The biggest difference between these experiments is the use of the short cell, which was made and is used because the pure chromium electrodes are short. The salt cannot be sparged efficiently because salt must be added to the cell in increments, the gas-in tube must be removed and replaced to blow gas over the salt, opening the cell to the air and the salt is not located at the center of the oven, but in the upper ¼, which is difficult to make isothermal. These conditions make removing oxidants ineffective and account for the high corrosion rate and discrepancy between this and the system in Task1.

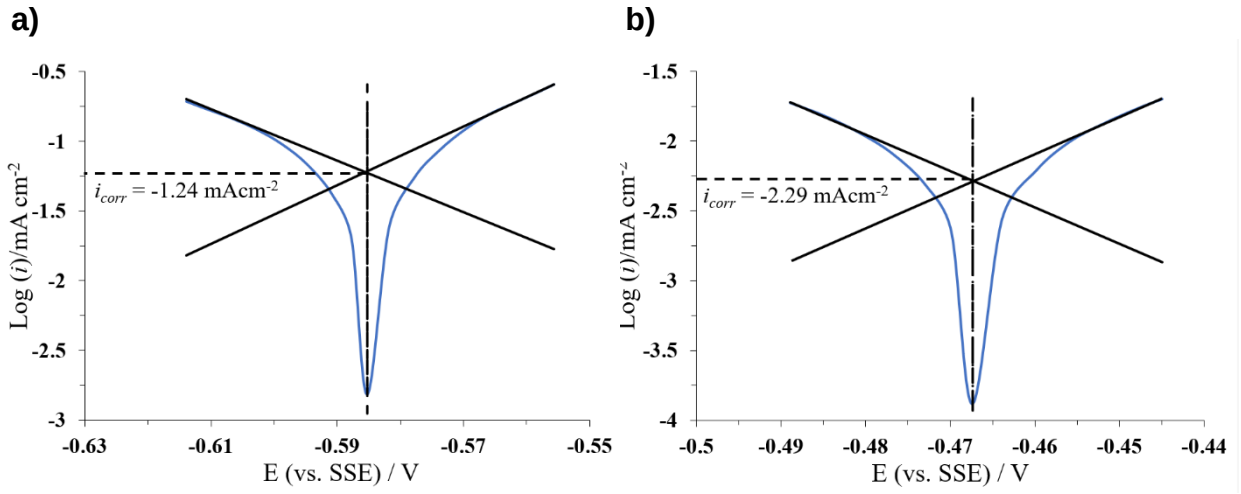

Figure 3-5. Stern-Geary plots of "Haynes 1" WE before **(a)** and after **(b)** passive cathodic protection by a Cr anode in molten ternary $MgCl_2$-NaCl-KCl eutectic salt dried with Mg at 800˚C under a dry Ar atmosphere. The potential was scanned ±30 mV around OCP at a scan rate of 0.4 mV/s. **a)** The corrosion current before cathodic protection i_{corr} is equal to -1.24 mAcm^{-2}, which mathematically equates to a CR of 534 µm/yr. **b)** After 22hr under passive cathodic protection, i_{corr} = -2.29 mAcm^{-2} and CR = 47 µm/yr.

Table 3.1 Gravimetric and Potentiometric analysis of the corrosion of H230 in molten ternary $MgCl_2$-NaCl-KCl eutectic salt dried with Mg at 800˚C under a dry Ar atmosphere under passive cathodic protection by a Cr anode. The initial OCP of Haynes 2 was erratic, and therefore the initial corrosion rate could not be determined.

		Initial OCP vs SSE (V)	OCP After 23 hr (V)	Initial Corrosion rate (µm/yr)	Corrosion rate after 23 hr (µm/yr)	Mass loss (mg)
Haynes 1	H230 WE	-0.587	-0.468	439 ± 119	48 ± 3	56.9
	Cr CE	-0.765	-0.751	n/a	n/a	68
Haynes 2	H230 WE	varied	-0.324	n/a	138 ± 21	54.9
	Cr CE	-0.774	-0.757	n/a	n/a	85.9

This experiment demonstrates successful passive cathodic protection of H230 with a Cr anode. There was a significant decrease in the CR of Haynes 1 by an average of 391 µm/yr. The mass loss of Haynes 2 was not significantly different than that of Haynes 1. The mass loss for Cr however was 17.9 mg more when it was protecting Haynes 2 than Haynes 1, indicating an increase in oxidants over time. The higher OCP and overall noise in the Haynes 2 OCP recording (fig.3-4) is consistent with this conclusion. The H230 mass loss data shows that this small increase in oxidant concentration does not affect the efficacy of passive protection.

Experiment 2: Active CP H230 with nichrome anode during CP with a power supply

Subtask 3.2 Summary: Active cathodic protection induces a current by using a power supply to set the potential of the WE (cathode) more negative than its open circuit potential relative to the RE, sending electrons from the CE (anode) to the surface of the WE to keep it metallic. The extra driving force from the power supply provides even more protection from corrosion than by passive protection. In this experiment, the potential of a H230 WE is set 200 mV negative (cathodic) of its open circuit potential relative to an SSE RE, inducing an electron protective reducing (cathodic) current from an NiCr CE to the WE. The current is monitored as a function of potential, and corrosion is determined gravimetrically and through SEM/EDS imaging. A regular sized cell (not the short cell) is used because ductile nichrome electrodes can be made longer than brittle pure chrome electrodes.

A nichrome anode (NiCr), like pure chromium (Cr), gives a source of chrome ions and electrons for CP, but pure Cr is brittle and expensive, while NiCr alloy is ductile and inexpensive. CP with NiCr is easier to do at a substantially lower cost due to the properties and lower cost of the NiCr anode. The nichrome alloy Ni80Cr20 manufactured with 6.3mm dia. x 100 mm length costs $217 from Sigma Aldrich. Haynes 230 alloy rods are prepared as described in Task 1. NiCr (80/20) alloy wire from Fine Metals Corp (1mm dia., annealed, 99.95%) and Sigma Aldrich (1mm dia, 99.9%). The NiCr is prepared by rinsing the surface with DI water and EtOH.

Initially 236.85g of ternary $MgCl_2$-NaCl-KCl eutectic salt sparged with dry Ar gas is heated to 200˚C, held at that temperature for 2hr, then the temperature is increased to the final experimental temperature of 800˚C at a rate of 220˚C/hr. Determined through trial and error, this method of drying the salt without Mg prevents the sparging tube from getting clogged. After the salt is at 800˚C for 24-36hr, Ar gas is blown over the salt and the H230 WE and NiCr CE are placed in the cell. In most of the experiments, the gas-in tube is removed and is replaced with an “observer” H230 electrode, which is not connected to anything. Since the corrosivity of the salt varies between experiments, this observer electrode gives the baseline of corrosion for H230 in that salt with no cathodic protection.

Once the OCP for H230 in the system is determined, the potentiostat applies a potential to the WE that is 200 mV negative of that OCP for either 24 or 48 hr. Since the salt is not treated with Mg, aggressive oxidants such as MgOHCl and HCl are still present in the salt. The time frame for the cathodic protection experiment is determined by the magnitude of the recorded current. If the current suddenly increases, this is a sign that either the RE is broken, or more commonly the Cr in the NiCr has been mostly consumed and the CE has broken off into the salt at the salt line. The heavy Cr depletion seen in SEM imaging (fig. 13) is consistent with the sharp increase in current density on the H230 WE (fig. 12). Occasionally, this will overload the potentiostat and stop the experiment, leaving a variable amount of time that the H230 WE is under passive rather than active cathodic protection. A total of 5 cathodic protection experiments were performed in untreated salt under dry Ar in the regular cell, and one experiment was performed at 20% RH in the short cell. Table 3.2 is a summary of the gravimetric analysis for each experiment and notes the time which the WE was protected and unprotected.

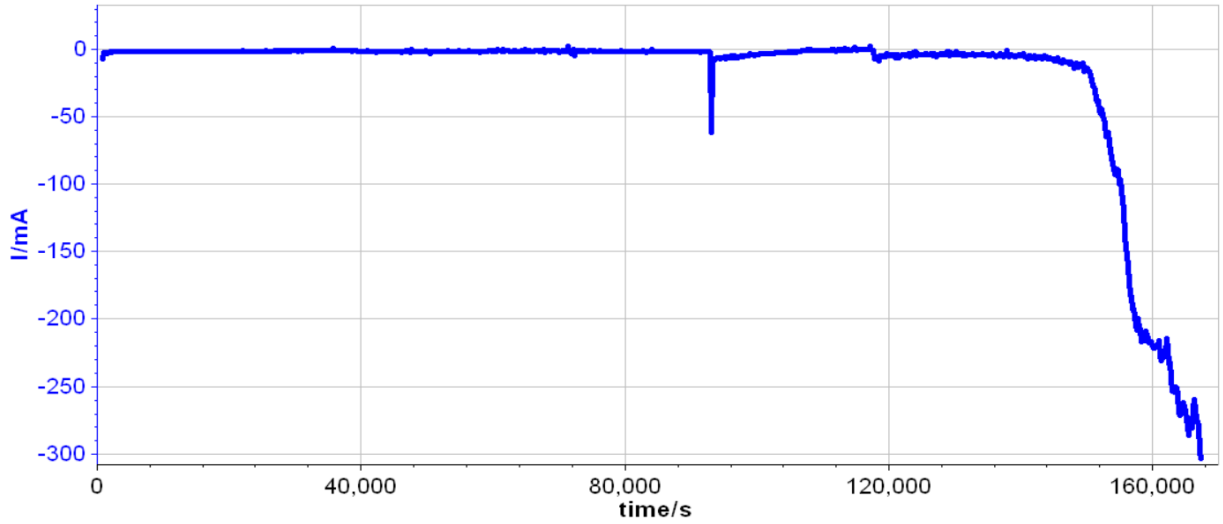

Figure 3-6. The current density on the surface of the H230 WE biased at -0.636 V vs SSE, 200 mV negative of the recorded OCP of -0.436 V, recorded over 48hr using NiCr as the anode.

Table 3.2 Gravimetric analysis for 6 CP experiments with a H230 WE protected by a NiCr anode and an unconnected H230 observer (obs) electrode in ternary salt, untreated (exp 1-5) and at 20% RH (exp 6) at 800˚C. The time H230 was actively protected is notated as t_{CP}, while the time where the electrode was passively protected (active protection failed) is notated as t_{PP}. Experiments 1 and 6 did not use an observer electrode, and the NiCr CE broke off in experiment 3 and had to be replaced, so the mass difference could not be determined. The observer electrode in experiment 2 was kept in the salt 24 hr after (48 hr total) the WE and CE were removed.

Experiment	**1 (dry Ar)**		**2 (dry Ar)**		**3 (dry Ar)**		**4 (dry Ar)**		**5 (dry Ar)**		**6 (20% RH)**	
	t_{PP} (hr)	**t_{CP} (hr)**	**t_{PP}**	**t_{CP}**	**t_{PP}**	**t_{CP}**	**t_{PP}**	**t_{CP}**	**t_{PP}**	**t_{CP}**	**t_{PP}**	**t_{CP}**
	0	48	21.2	2.8	0	48	0	45.5	0	23	9.5	6
	Mass loss (mg)		**Mass loss (mg)**		**Mass loss (mg)**		**Mass loss (mg)**		**Mass loss (mg)**		**Mass loss (mg)**	
H230 WE	49.5		254.2		89.2		100.4		37.6		161.1	
H230 Observer	n/a		383.4 (48 hr)		503.9		437		123.1		n/a	
NiCr CE	278		263.6		n/a		1311.1		846.7		226.6	

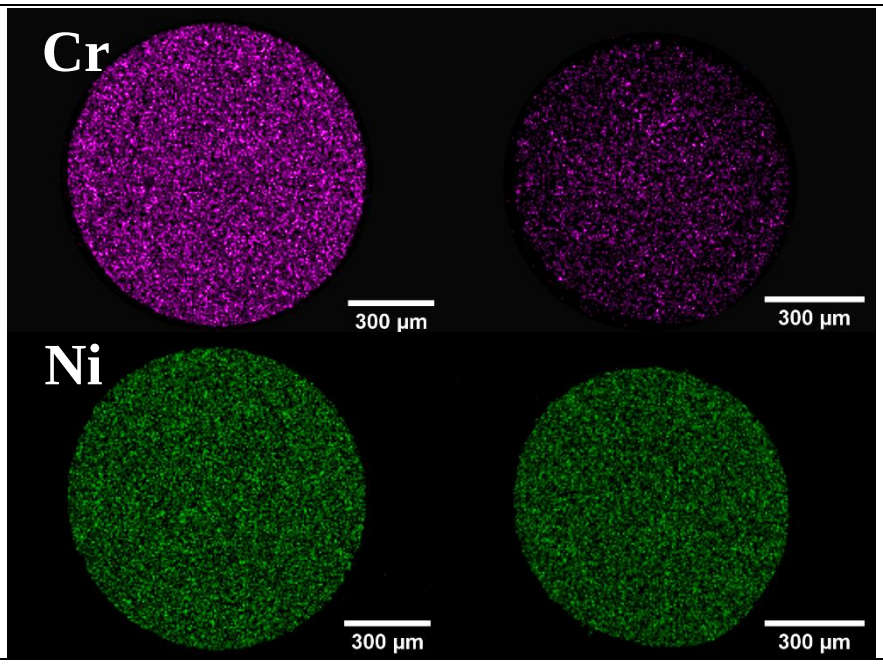

Figure 3-7. SEM/EDS Imaging of NiCr CE before (left) and after (right) cathodic protection of a H230 WE in $MgCl_2$-NaCl-KCl salt under dry Ar for 46 hr. The significant reduction in Cr content throughout the entire wire is consistent with the sharp increase in negative current observed in Fig. 3-6 after 42 hr. There is also a significant reduction in the diameter of the wire, decreasing from 1 mm to an average of 0.8 mm.

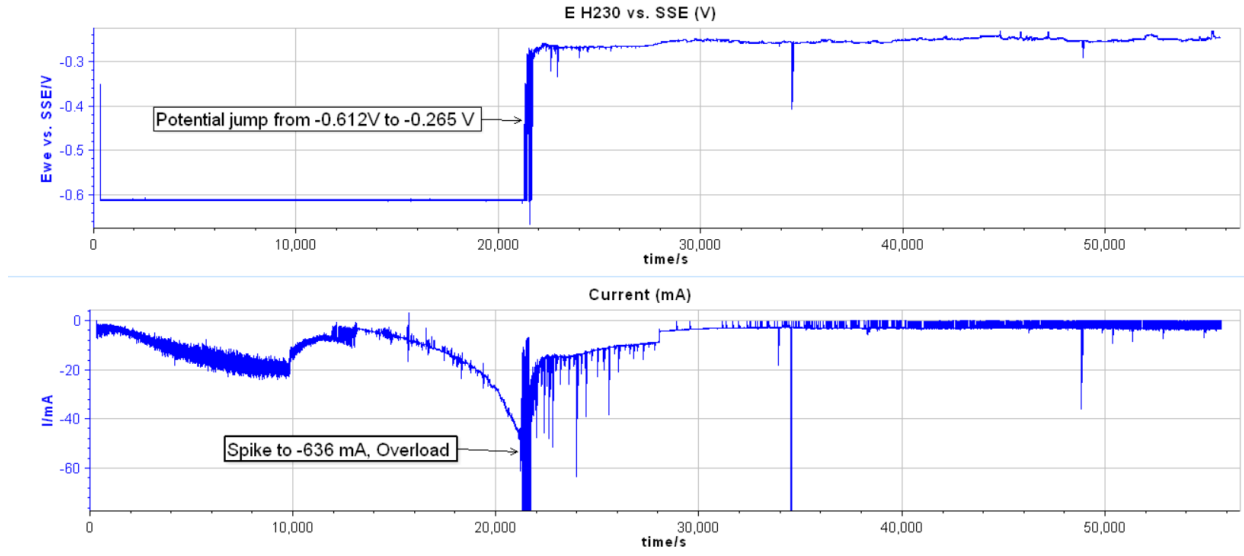

Figure 3-8. Potential (top) and current (bottom) of H230 WE under active cathodic protection with a NiCr CE in 20% RH. After 6 hr, the current spiked, overloading the potentiostat. The subsequently recorded potential fluctuated between -0.265V and -0.25 V vs. SSE, and the current fluctuated between 0 and -3 mA, indicating passive cathodic protection.

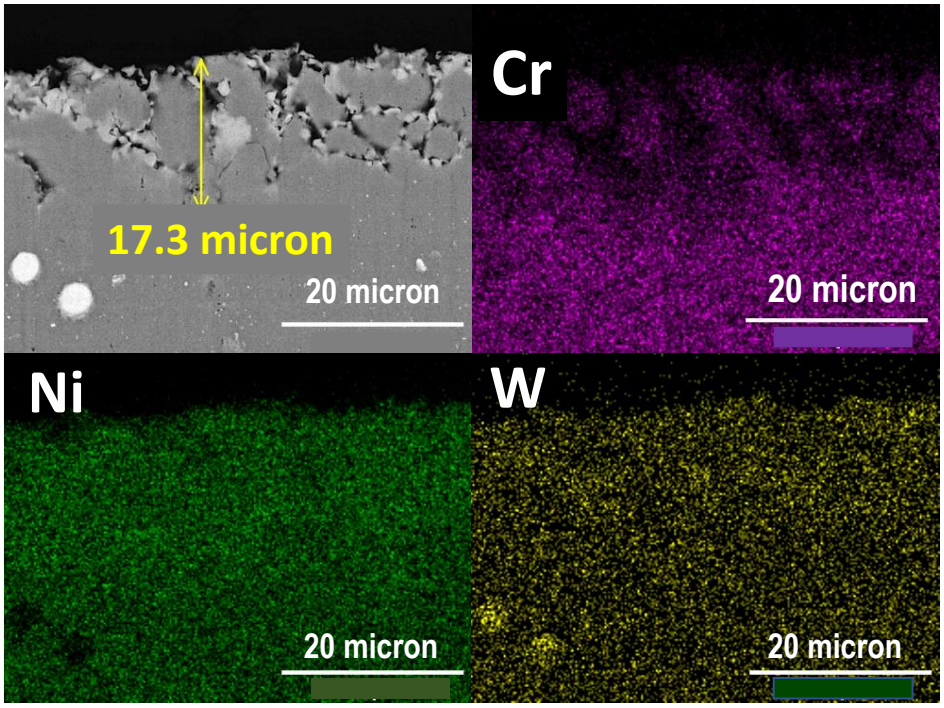

Figure 3-9. SEM/EDS imaging of the "observer" H230 electrode after 23 hr in the ternary salt under dry Ar but not treated with Mg. The corrosion depth is measured by Cr depletion

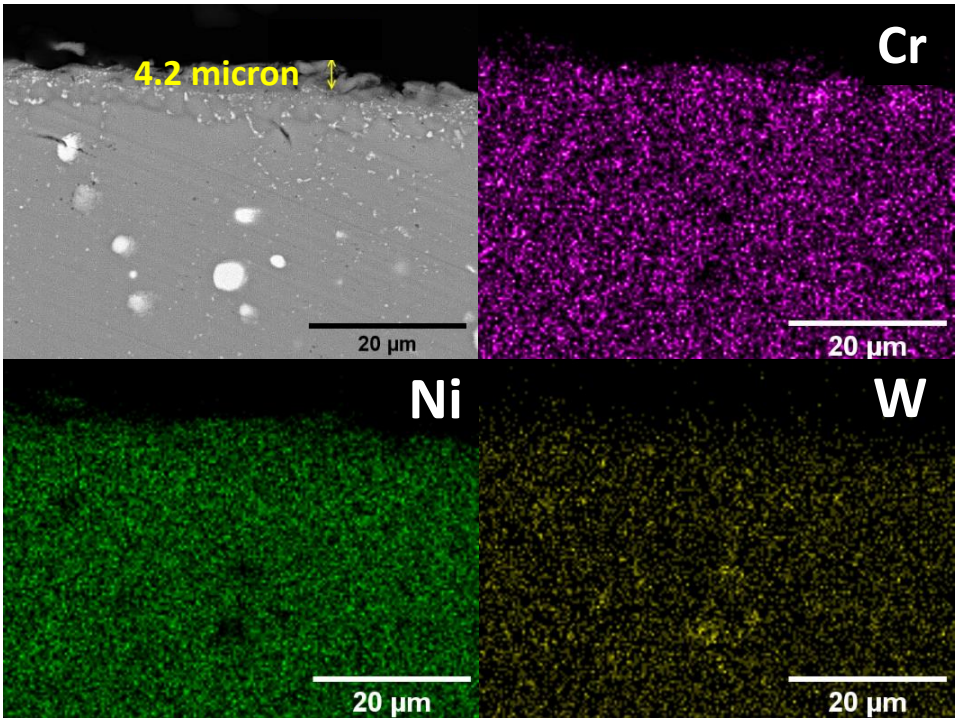

Figure 3-10. SEM/EDS Imaging of H230 under cathodic protection by NiCr for 23 hr. There is no surface corrosion characterized by Cr depletion

The gravimetric analysis (Table 3.2) and SEM/EDS imaging (Figures 3-9 and 3-10) shows significant suppression of corrosion of H230 alloy electrode, when it is in molten salt with oxidants under cathodic protection with a NiCr CE compared to the substantial corrosion of H230 “observer” electrode when it is in molten salt with oxidants and is not protected. *In conclusion, applying a cathodic potential to a metal in molten chloride salt retards metal corrosion in the presence of water when using a Cr rich anode. This concludes Task3.*

Task 4.0 Fundamental quantum chemistry modeling of reduction potentials in salts

Subtask 4.1. Standard Reduction Potential of chromium in molten chloride salt.

Subtask summary: The electrochemical characterization of the reduction potential of chromium and chromium alloys in molten chloride salt has been done 2 ways, by:

i.) chronopotentiometry
ii.) cyclic voltammetry

in anaerobic NaCl-KCl and NaCl-KCl-$MgCl_2$ eutectic molten salt mixtures at 800^{o}C. NiCr has better mechanical properties and is much less expensive than Cr. Electrochemical characterization of chrome and nichrome will determine if nichrome has similar enough electrochemical properties to pure chromium so that NiCr can be used as a reliable long-term anode substitute for Cr.

The cell for studying a chrome electrode is shown in Figure 4-1. This cell must be significantly shorter than the cell used for studying nickel alloy electrode, because cost effective chrome electrodes are not made very long due to the brittle nature of chrome.

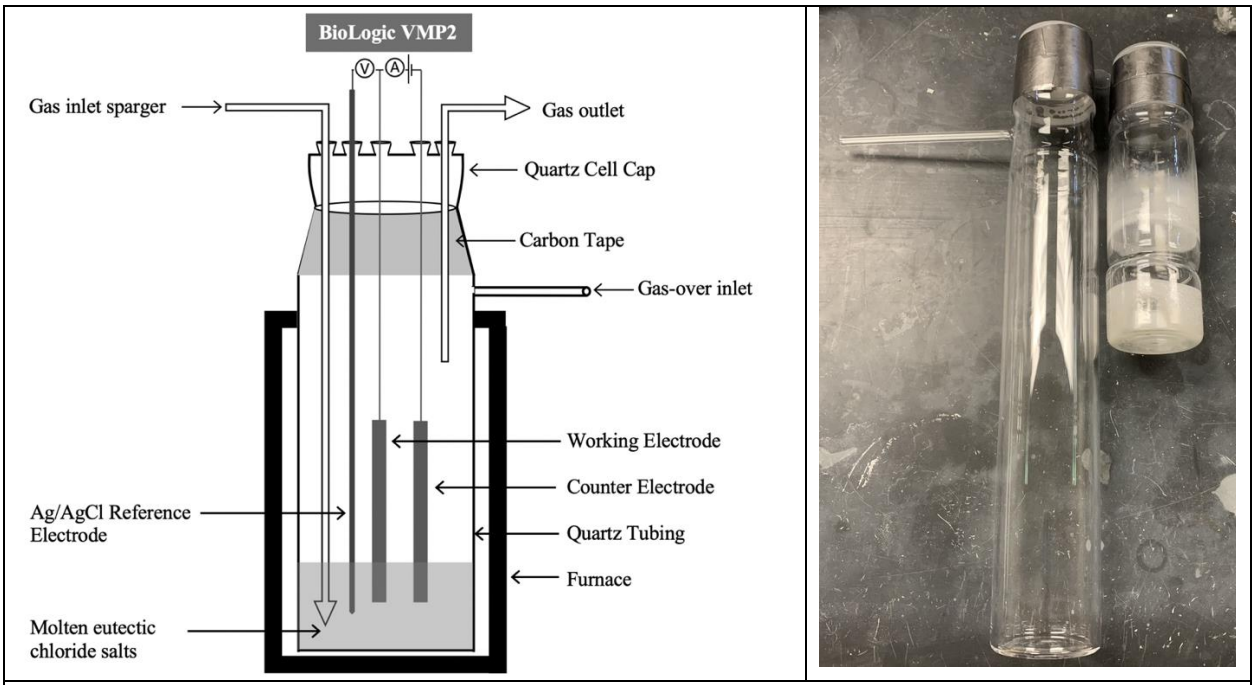

Figure 4-1. A diagram of the cell used in the molten salt studies (left) and a photo comparison of the short cell used in the chrome experiments and the longer cell used in the nickel experiments (right).

Fine Metals Corp, one of the few and best manufacturer of chrome electrodes, cannot create a chrome rod longer than 15cm, because of its brittleness. So a short cell is needed and has been made to test a Cr electrodes. The conventional longer cell is used to test a nichrome anode, since nichrome is ductile and making different lengths is no problem. The same short cell has been used for studies during the cathodic protection experiments of Tasks 3 and the reduction potential experiments of Task 4 when pure chrome is used as an electrode.

In an effort to dry the NaCl/KCl salt, metallic sodium was introduced into the molten salt and removed 24 hours later, mirroring the experiment with solid Mg in the $MgCl_2$/NaCl/KCl salt. The corrosion rate before and after sodium drying was 314μm/yr and 307μm/yr, respectively. The open circuit potential of -0.750 V also did not change. The quartz of the inside cell wall is disfigured after sodium exposure. Apparently, the sodium metal in molten chloride salt reacts with the silica in the quartz cell instead of water.

Mg metal removes strongly bound water from the NaCl/KCl salt without disfiguring the cell. The corrosion rate of H230 falling from 348μm/yr to 56μm/yr, and the open circuit voltage shifting negative, from -0.750 to -1.025V after 24 hours. So Mg is used to remove strongly bound water instead of Na metal in NaCl/KCl salt. All of the Mg metal was consumed, so additional Mg was added. After 24 hours, the open circuit voltage shifted further negative to -1.128V and the corrosion rate dropped to 30 μm/yr. Since this drying introduces Mg, $MgCl_2$/NaCl/KCl salt is used instead of NaCl/KCl salt and Mg metal to remove residual oxidants for reduction potential determination of Cr.

One challenge with chromium is making an electrical connection. Currently, a Ni wire is welded to a chromium alloy metal electrode since these alloys form insulating chrome oxide which break the continuity of the current need by the test electronics (potentiostat and multimeter) to measure electrode properties. Chrome is so brittle metal that attempting to weld a nickel wire to it breaks the Cr rod. Solder is a solution to this problem. Experiments with H230 and nickel wire show that solder and welds both give good connections, and the measured open circuit voltages and corrosion rates of the H230 rods in NaCl/KCl at 800°C are equally stable. Therefore, solder is used to create the electrical connection between the chrome rod and nickel to make electrical connection to the test electronic.

Chromium (Cr): The open circuit potential (OCP) is -0.824V vs SSE for a Cr rod in ternary Mg-K-Na-Cl molten salt at 800°C under and equilibrated with a dry Argon atmosphere. The reduction potential of chrome is obtained by potential measurements and the voltammetry of a Pt electrode in ternary Mg-K-Na-Cl molten salt with dissolved Cr ions at 800°C equilibrated with a dry Argon atmosphere over the salt. The chromium ions come from dissolution of Cr ions from the oxidation of a Cr metal rod being used to find the OCP in Mg-K-Na-Cl molten salt at 800C under Argon. When Cr ions are added to the molten salt, the results are identical. A Cr WE corrodes continuously with no transport limited current, so an inert Pt electrode is used to characterize changes of oxidation state of C in molten salt, such as the Cr+2/Cr+3 couple but also the Cr ion reductions to chrome metal and the oxidation of chrome metal to chrome ions.

Platinum (Pt): The open circuit potential (OCP) is +0.545 V versus SSE when the working electrode (WE) and counter electrode (CE) are Pt in ternary Mg-Na-K-Cl salt dried with Mg metal under Argon in a short cell. After the OCP of Cr was determined there was an unknown concentration of Cr in the salt. It was this Cr that was studied by Pt voltammetry. Many peaks are in the voltammetry of Pt in in molten Mg-Na-K-Cl salt containing Cr ions from dissolved from a Cr metal electrode in the salt at 800°C. The Pt voltammetry potential range is from -1.7 and 0.1 V to -1.5 to -0.5 V. The most negative oxidation peak at -1.24 and reduction at -1.5 are assigned to Mg oxidation and Mg^{+2} reduction, respectively. Setting scan bounds between -1.5 to -0.6V removes the oxidation peak at -0.73 V, but retains a small reduction peak at -1.13V:Re-extending scan bounds to -1.2V and -0.4V restores an oxidation peak at -0.8V. The positive peak current at -0.8 is assigned to the oxidation to chrome ion and the negative peaks found at -1.06 V to the reduction of chrome ion. This related redox couple has a reduction potential of -0.93 volt vs SSE. This is

assigned to the oxidation of chrome metal to divalent chrome. Window opening scan show the effect of the shifting the lower potential limit to more positive potentials, where the currents are much lower (about 10x reduction). Altering scan bounds to -0.3V and 0.6V removes oxidation small peak at-0.22V which may be for oxidation of divalent to trivalent chrome. Chlorine oxidation does not occur on Pt until 0.6V.

Nickel: the initial OCP is at -0.460 V versus SSE (silver/silver-chloride). There are three redox couples in the voltammogram of nickel in molten chloride salt. The redox couples have electrode potentials, *E*, and anodic and cathodic peaks, $E_p^a|E_p^c$ (anodic|cathodic), are found at

- E = - 1.495vs SSE (-1.55|-1.44V),
- E = -0.895 vs SSE (-0.93|-0.86V).
- E = -0.7 vs SSE (-0.73|-0.67V).

where $E = E_{red} = \sim E_{1/2} = (E_p^a + E_p^c)/2$. At more negative potential there is a redox couple at E = 1.495 V vs SSE with oxidatrion|reduction peaks at (-1.44|-1.55V) and with much larger peak current than any of the other redox couples which shows E = 1.495 V is not for Mg whose oxidation peak is at -1.65V: A redox couple is found at E = -0.7 vs SSE with its associated oxidation peak at -0.67 whose accompanying reduction peak is at -0.73V, which are very broad peaks, making the peak values difficult to pinpoint and so approximate. The standard reduction potential of Nickel in a molten chloride salt system equilibrated with ultra-dry argon at 800°C was reported to be -0.825 ±0.006 V vs. SSE by chronopotentiometry as a function of Ni ion concentration. This is a method based on the Nernst equation.

The standard reduction potential of Ni ions in water is -0.25 vs NHE or -0.45 vs SSE, so the standard reduction potential of Ni in molten salt is -0.375 more negative in chloride than water. The 0.375 V more negative reduction E^o in the molten salt is consistent with the stronger complexation of Ni^{2+} with Cl^- ions in the molten salt as compared to complexation of Ni^{2+} with water. It is expected that the reduction potential of nickel ion is more negative (less spontaneous) in molten chloride salt, because it is more difficult to put an electron on a more negatively charge nickel ion associated with negatively charged chloride ions than a more positive charged nickel ion associated with water molecules. The redox couple at E = -0.895 vs SSE (-0.93|-0.86V) is attributed to nickel metal/metal ion redox reaction as it is close to the value of -0.825 ±0.006 V vs. SSE found by a Nernst equation method. However, a redox couple at E = 1.495 V vs SSE with oxidation and reduction peaks at -1.44 and -1.55V vs SSE respectively have much larger peak current than any of the other redox couples, which could be for nickel oxidation. Metal oxidation reactions have large currents. This warrants further investigation but this cannot be done as the program is ended. The student who studied this will nevertheless continue to look into this during the PHD studies and a publication on this is expected.

Conclusions: The main goal of Task 4 was to find the reduction potential of chrome metal. The reduction potential of other metals in molten chloride salt was estimated and these results are summarized below.

Chrome: The open circuit potential (OCP) is -0.824V vs SSE for a Cr rod in ternary Mg-K-Na-Cl molten salt at 800°C under and equilibrated with a dry Argon atmosphere.

A preliminary determination of the reduction potential of chrome at 800°C was done by the voltammetry of platinum working electrode in ternary Mg-K-Na-Cl molten salt containing trace chromium metal ions from the dissolution of chrome ions from a solid chrome bar during the open circuit of chrome in molten salt. The determination of the reduction potential of chrome from the voltammetry of chrome metal in molten salt will be reported in March 11.

Nickel (Ni) has an OCP at -0.460 V versus SSE (silver/silver-chloride) and four redox couples in the voltammogram of nickel in molten chloride salt as shown in Figure 6 below. The redox couples have electrode potentials, E, and anodic and cathodic peaks, $E_p^a|E_p^c$ (anodic|cathodic), found at E = - 1.49 vs SSE (Eanodic|Ecathodic = -1.55|-1.44V), E = -0.895 vs SSE (-0.93|-0.86V) and E = -0.7 vs SSE (-0.73|-0.67V). The redox couple at E = **-0.895 vs SSE** (-0.93|-0.86V) could be nickel oxidation as it is close to

the value of -0.825 ±0.006 V vs. SSE found by a Nernst equation method and reported in Q4. The redox couple at E = -1.495 V vs SSE with oxidation and reduction peaks at -1.44 and -1.55V vs SSE respectively have much larger peak current than any of the other redox couples, which could be for nickel oxidation, since metal oxidation reactions typically have large currents. This warrants further investigation. These experiments conclude task 4.

Overall Conclusions for Tasks 1,3 and 4.

All work is completed except for the voltammetry of Cr and NiCr to be report March 11.
Task1. Oxidants can be detected by OCV and CR of H230 metal in molten salt with various levels of oxidant water.

Task3. Cathodic protection with a power supply gives a reduction current which signal oxidants in the salt and retards corrosion of metal in molten salt containing oxidants.

Task4. A chromium anode has a reduction potential of potential of -0.93 volt vs SSE. Chromium rich alloy is inexpensive and ductile making nichrome easy to handle unlike brittle chromium metal. Results about this will be reported March11.

Task 4.2 Quantum chemistry modeling for elucidating corrosion mechanisms in molten salts

Quantum mechanical modeling gives a rationalization for the the differences in reduction potentials of metal ions in molten chloride salts versus what is known for metal ions in water.

Task 5 Develop corrosion test sections integrated into molten salt flow loop

Problem Statement 5 – Development of corrosion test sections integrated into molten salt flow loop

This task is set to modify the molten salt flow loop at the University of Arizona in order to accommodate the installation and instrumentation for the test of corrosion and the measurement of the effect of the cathodic protection. Dr. Li's team will design the ceramic connections and fittings (customarily manufactured by a company) for the reference electrode, counter electrode, as well as the fixture that holds the metal coupon in the molten salt flow stream. The electrodes and the metal coupon must be electrically insulated from metal pipes using the ceramic fittings. The entire cathodic protection section must be integrated into the molten salt flow loop. Components in the test loop must be able to withstand a temperature as high as 800°C

New features of molten salt corrosion and heat transfer test loop incorporated in Q4

Dr. Perry Li's team has completed all the manufacturing and welding of all parts for the molten salt test loop. Figures 5.1 show respectively the schematic design of the test loop, the photo of the connected pipes for test section, the molten salt pump and tank, as well as the furnace that will house the molten salt tank and control the temperature of the molten salt.

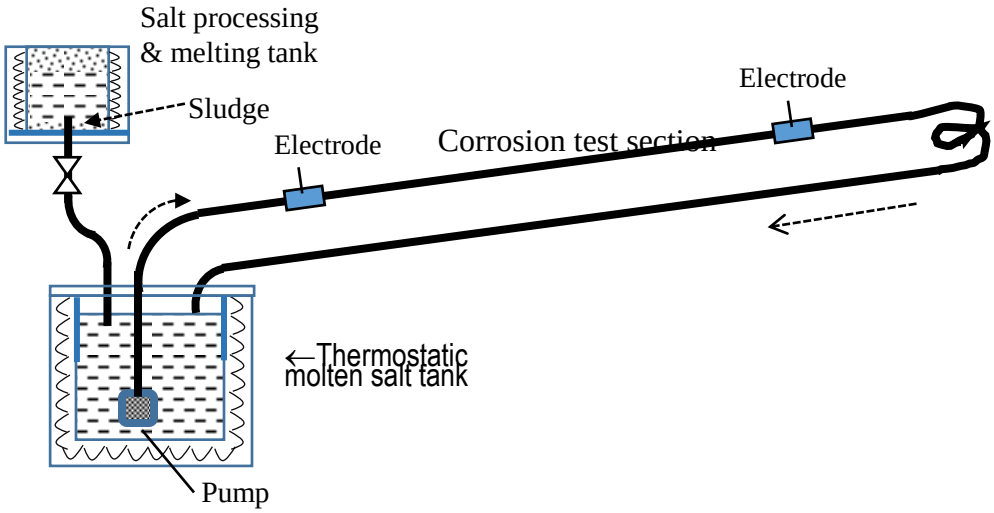

(a) Moten salt loop system layout

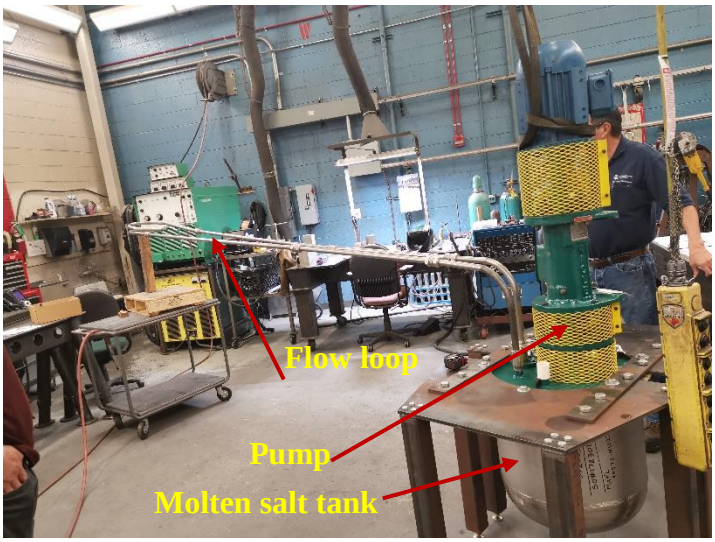

(b) Photo of the test loop and connection to the pump and molten salt tank

(c) Furnace to house salt tank to control salt temperature

Figure 5.1 Test loop featuring corrosion test using electrochemical method

The system was manufactured in the U of Arizona machine shop and checked for preliminary assembly. It will be moved to Dr. Li's research lab for formal installation at around April 5th. Due to the interruption from the outbreak of the corona virus, the installation was suspended. Once the shelter-in-place order is relieved, the team will ship all the components to lab for assembly. Following the formal installation, thermal protection to the system will be applied and instrumentation including flow meter, temperature measurement, corrosion monitoring, and heat transfer test will be accomplished for experimental tests.

Update on the State of the Art: Although cathodic protection is well known and has long been practiced in aqueous systems, in non-aqueous systems and in molten salt CP is virtually unknow. ***The work in this project is new and unprecedented.*** During the past months work in labs has been halted by the state of Arizona in order to arrest the spread of the COVID-19 virus. At this time, several papers have been drafted by the corrosion group at the University of Arizona on metal corrosion and cathodic protection of metal surface inside containers of molten chloride salt. The plan is to submit and publish these papers with the hope that they will guide workers in the field and advance the state of the art where molten chloride salts are used in industry, e.g., in the CSP and nuclear power industries.

Significant Accomplishments and Conclusions:
To date there has been one degree granted, a Master of Science of Chemical Engineering and another, a Ph. D. of Chemical Engineering is expected in the summer after this report. Two manuscript are in preparation to peer-reviewed journals. Two patents are being sought from the work undertaken in the project i) on simplified reference electrodes and ii) applying the cathodic protection to metal in molten salts.
Originally this was planned as a 5 task, 3 year project, starting in May 2019, After Q4, the project was scaled back and the reorganized SOPO was reduced to 3 tasks to end in 3 quarters, that is, after Q7. The main reason for discontinuing the project was the repeated failure of the University to pay the proper cost-share leading the DOE to reorganize the scope and duration of the project.

Inventions, Patents, Publications, and Other Results:
Work on reference electrodes continued during this project. Use of a power supply to monitor and control corrosion was a central focus. This work is being continued after this project in parallel efforts funded by the Sloan Foundation and the City of Tucson, respectively. Patents are submitted partly under this award. Two patents are being sought from the work undertaken in the project i) on simplified reference electrodes and ii) applying the cathodic protection to metal in molten salts. To date there has been one degree granted, a Master of Science of Chemical Engineering and another, a Ph. D. of Chemical Engineering is expected in the summer after this report. Two manuscript are in preparation to peer-reviewed journals. There was one public release of this work and preliminary results to the media as a result of this award.

Path Forward:
There is no plan to continue the specific work for this project although some elements are being continued as students finish their University graduate degrees. One student is continuing to develop reference electrodes under a Sloan scholarship. This reference electrode work is focused on making a durable metal metal-ion reference electrode with no quartz-tube housing, which is to be marketed by a startup company, Caltrode, Inc. Other work supervised by Peiwen Li is to develop and use the molten salt flow loop located in the Mechanical Engineering department at the University of Arizona.

References:
Two papers and 2 patents are under preparation.